

**EXPERIMENTAL STUDY OF LUBE OIL CHARACTERISTICS IN THE PCV
SYSTEM AND EFFECTS ON ENGINE OIL CONSUMPTION**

by

Oscar Lopez

B.S., Mechanical Engineering
Purdue University, 2002

Submitted to the Department of Mechanical Engineering
in Partial Fulfillment of the Requirement for the Degree of

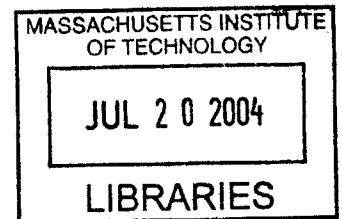
MASTER OF SCIENCE IN MECHANICAL ENGINEERING

at the


MASSACHUSETTS INSTITUTE OF TECHNOLOGY

June 2004

© 2004 Massachusetts Institute of Technology
All Rights Reserved



Signature of Author _____

 _____
Department of Mechanical Engineering
May 7, 2004

Certified by _____

 _____
Victor Wong
Lecturer, Department of Mechanical Engineering
Thesis Supervisor

Accepted by _____

Ain A. Sonin
Chairman, Department Committee on Graduate Studies

BARKER

(This page was intentionally left blank)

EXPERIMENTAL STUDY OF LUBE OIL CHARACTERISTICS IN THE PCV SYSTEM AND EFFECTS ON ENGINE OIL CONSUMPTION

by

Oscar Lopez

Submitted to the Department of Mechanical Engineering
on May 7, 2004 in Partial Fulfillment of the Requirements for the
Degree of Master of Science in Mechanical Engineering

ABSTRACT

Engine oil consumption is an important source of hydrocarbon and particulate emissions in modern automobile engines. Great efforts have been made by automotive manufacturers to minimize the impact of oil consumption on engine emissions. Research engineers in the last decade have been trying to study the sources and driving mechanism of oil consumption. In contrast to oil consumption mechanisms in the piston-ring-liner system of the engine, the Positive Crankcase Ventilation (PCV) blowby-oil consumption mechanism has not yet been fully characterized. Studies have shown that the blowby contribution to oil consumption could be significant under certain conditions.

In this study, an experimental approach was taken in order to study the sources and characteristics of oil in the PCV blowby gases at different speeds and loads. An extensive diagnostic system was successfully integrated in a production spark ignition engine, to measure total oil consumption, blowby oil consumption and flow and in-cylinder variables, such as inter-ring pressures, oil film thickness and liner temperatures.

Results showed an increase in blowby oil consumption with load and speed. Blowby flow was mainly dependent on the load of the engine. Oil concentration in the blowby varied with engine operating conditions. A strong relationship was observed between oil consumption and sump oil level, showing that the oil in the crankcase is an important source of oil in the blowby.

Moreover, extensive experiments were conducted to determine the blowby flow's oil characteristics, by varying the liner temperatures and analyzing the mass distribution of different oil particle size. It was found that the average oil droplet size decreased as the load and speed were increased.

This work is an important step in understanding blowby oil consumption in efforts to minimize oil consumption in spark ignition engines.

Thesis Supervisors:

Victor W. Wong
Lecturer, Department of Mechanical Engineering

(This page was intentionally left blank)

ACKNOWLEDGEMENTS

I would like to thank Victor Wong for the opportunity given to me and his support and guidance provided throughout my project and stay at MIT. I also would like to thank Tian Tian for the inputs made to the project and all the technical discussion, with whom this project have been going forward. My sincere thanks to Ertan Yilmaz, whom have show me all about the experimental setup, and for all the discussion that we have had and that have help my project.

I would like to thank PSA Peugeot Citroën and the members of the Consortium on Lubrication in Internal Combustion Engines at MIT (current members include Dana Corporation, Mahle GmbH, Renault SA, PSA Peugeot Citroën, and Volvo AB) for sponsoring this research. I would like to thank Dr. Sébastien Messé at PSA Peugeot Citroën for his support and help in this project. I would like to thank Rémi Rabuté and Randy Lunsford at Dana for his support and valuable technical input and help. I would also like to thank Fredrik Stromstedt, Bengt Olson at Volvo, Dr. Rolf-Gerhard Fiedler and Dr. Eduardo Tomanik at Mahle for their interest and support. I would like to express special thanks to Lubrizol Corporation for formulating and providing the special lubricants for this project.

I gratefully acknowledge the support of the Sloan Automotive Laboratory staff. Thane Dewitt and Raymond deserve special credit for their technical assistance. I would also like to thank Alexis Rozantes for her help and pleasant attitude. Special thanks also to Leslie Reagan for her support and help.

I would also like to thank the following list of graduate students and visiting engineers in the Sloan Automotive Laboratory for their help and for making my research in the laboratory enjoyable: Liang Liu, Morgan Andreae, Jinchul Hong, Grant Smedley, Jeff Matthews, Yong Li, Tiffany Groode, Jim Cowart, Adam Vokac, Fiona McClure, Mohammad Rassuli, Vincent Constanzo, Brian Hallgren, Ioannis Kitsopanidis, Joseph Acar, Jeremy Llaniguez, Yuetao Zhang, Kevin Lang, Gerardo Jose Cordova Lao, Halim Santoso, and Yeunwoo Cho.

Outside the Sloan Automotive Laboratory, I would like to thank Juan Hernandez, Jose Santivanez, Daniel Scholl, Jose Miranda, Javier L. Gorriz, Maria Jesus Anitua, Erkuden Lopez, Ibone Lopez and Karen Tarud for their friendship, help, and support. You all are my family. I would especially like to thank Sofy Tarud for her support, care, and understanding. She has been a constant source of love and encouragement to me, and if it was not for her, I would not get through the MIT experience. Maite Zaitut.

I would like to express my special thanks to all members of my family. This thesis would not have been completed without their unconditional support. In particular, I am very grateful to my grandmothers Paz San Martin and Eloisa Petra Gorriz, grandfather Dionisio Lopez, mother, father, and sisters for their continuous encouragement and support. Os quiero familia.

Cambridge, June 2004

(This page was intentionally left blank)

TABLE OF CONTENTS

ABSTRACT	3
ACKNOWLEDGEMENTS	5
CHAPTER 1: INTRODUCTION	15
1.1 Motivation.....	15
1.2 Project Background.....	17
1.2 Project Scope	18
CHAPTER 2: EXPERIMENTAL SETUP	21
2.1 Experimental Objectives.....	21
2.2 Test Engine: Production Spark Ignition Engine	22
2.3 Measurement techniques.....	23
2.3.1 Total Output Measurements.....	23
2.3.1.1 Engine Oil Consumption.....	23
2.3.1.1.1 High Sulfur Oil	24
2.3.1.1.2 Low Sulfur Fuel	25
2.3.1.2 Oil Consumption Measurements Setup	26
2.3.1.3 Engine Blowby Oil Consumption.....	30
2.3.1.3.1 Difference Method.....	30
2.3.1.3.2 Direct Method	31
2.3.1.3.3 Gravimetric Method.....	32
2.3.1.4 Blowby.....	34
2.3.1.5 Oil Consumption Formulas	37
2.3.2 In-cylinder Measurements	38
2.3.2.1 Laser Induced Fluorescence System (LIF) System	40

2.3.2.2 Cylinder and Land Pressure Traces	45
2.3.2.3 Liner Temperatures	48
2.4 Experimental Conditions	49
2.4.1 Ring-pack Design	51
CHAPTER 3: ENGINE BLOWBY OIL CONSUMPTION AND OIL SOURCES ..	53
3.1. PCV System blowby Oil consumption	53
3.2 Factor Influencing Positive Crankcase Ventilation Blowby Oil Consumption	54
3.3 PCV Blowby Measurements	56
3.3.1 Steady State Blowby Oil Consumption	56
Figure 3-5 PCV blowby oil consumption map in grams per hour	58
3.3.1.1 Different Diagnostic Measurement Result Comparison	58
3.3.2 Steady State Total Oil Consumption	59
3.3.3 Blowby	60
3.3.4 Oil Loading in Blowby Gas Flow	64
3.3.5 Blowby Oil Consumption Relative Contribution	65
3.4 PCV System blowby Oil sources	66
3.4.1 Oil Source Investigation Approach	67
3.4.2 Oil Source Measurements	68
3.4.2.1 Ring-pack Oil Entrainment	71
3.4.2.2 Crankcase Oil Entrainment	72
3.4.3 Lubrication Condition in Interring Pack for Different Oil Levels	74
CHAPTER 4: PCV SYSTEM BLOWBY LUBE CHARACTERISTICS	77
4.1 Blowby Oil Particle Size Distribution	77
4.1.1 Oil Separators	79
4.1.2 Particle Size Mass Distribution Measurements	80

4.2 Effect of Cylinder Liner Temperature	83
4.2.1 Different Cylinder Liner Temperature Measurements	84
4.2.1.1 Liner Temperature Effect on Blowby Flow	86
4.2.1.2 Liner Temperature Effect on the Oil Concentration	86
4.2.2 Liner Temperature Effect on the Oil Evaporation	88
CHAPTER 5: CONCLUSIONS	91
NOMENCLATURE.....	95
REFERENCES.....	97
APPENDIX.....	101
Appendix A: Sample of Results Acquired and Calculations	101
Appendix B: Common Reference Numbers	109
Appendix C: Experimental Configurations	110
Appendix D: Other Significant Blowby Results and Plots.....	112

LIST OF FIGURES

Figure 1-1 Oil entrainment in the blowby flow from the piston-ring-liner system and the engine crankcase	16
Figure 1-2 Positive Crankcase Ventilation (PCV) system and the direct sampling line ..	18
Figure 2-1 Baseline oil sulfur content with distillation	25
Figure 2-2 Schematic of oil consumption measurement system	26
Figure 2-3 Antek® sulfur detector [29]	28
Figure 2-4 Antek® R6000 SE sulfur detector in the test cell	28
Figure 2-5 PCV valve and blowby flow characteristics	31
Figure 2-6 Setup of gravimetric method.....	33
Figure 2-7 Gravimetric method component setup in the SI engine	34
Figure 2-8 Flow meter picture with volume damping tank	36
Figure 2-9 Crankcase volume changes as a function of crank angle.....	36
Figure 2-10 Measurement locations of in-cylinder variables	39
Figure 2-11 Measurement probes in the engine 3 rd cylinder	39
Figure 2-12 Schematic of LIF system setup	41
Figure 2-13 Axial position of LIF probes and of different piston regions with crank angle [1].....	42
Figure 2-14 Arrangement of LIF housing sleeve and probe assembly [1]	43
Figure 2-15 Piston scratch marks for LIF calibration [1]	44
Figure 2-16 Surface profile of piston skirt and scratch marks at anti-thrust side [1]	44
Figure 2-17 Example of LIF traces and ring piston locations	45
Figure 2-18 Axial locations of the pressure transducers [1]	46
Figure 2-19 Pressure transducer housing assembly.....	47
Figure 2-20 Example of the lands pressure trace.....	48
Figure 2-21 Relationship between the coolant and lower liner temperature	49
Figure 2-22 Controlled torque and the engine torque at 100% as a function of speed.....	50
Figure 2-23 Investigated steady state engine-operating conditions	51
Figure 2-24 Piston and baseline ring-pack geometry	52
Figure 3-1 Factors on the blowby oil consumption	53

Figure 3-2 Oil film thickness for different loads and speeds.....	55
Figure 3-3 Load effect on particle size distribution in the blowby flow at 2500 rpm [1]	57
Figure 3-4 PCV blowby oil consumption map.....	57
Figure 3-5 PCV blowby oil consumption map in grams per hour.....	58
Figure 3-6 Comparison between the three diagnostic methods.....	59
Figure 3-7 Total steady state consumption.....	60
Figure 3-8 Cylinder pressure traces for 3500 rpm and different loads.....	61
Figure 3-9 Interring pressure traces for 3500 rpm and two different loads.....	62
Figure 3-10 PCV blowby flow map.....	63
Figure 3-11 Blowby flow map in per cycle basis.....	64
Figure 3-12 PCV blowby oil loading for different engine operating conditions.....	65
Figure 3-13 PCV blowby Oil Consumption relative contribution map.....	66
Figure 3-14 PCV blowby consumption at 3500 rpm as a function of oil level and load..	69
Figure 3-15 PCV blowby consumption at 100% load as a function of oil level and engine speed.....	70
Figure 3-16 PCV blowby oil loading at 3500 rpm as a function of oil level and load.....	73
Figure 3-17 PCV blowby oil loading at 100% load as a function of oil level and speed.	73
Figure 3-18 Total oil consumption for 100% load as a function of oil level and engine speed.....	74
Figure 3-19 Oil Film Thickness (OFT) distribution at different oil levels for 3500 rpm and 75% Load.....	75
Figure 3-20 Top crown land average oil film thickness for 2500 rpm.....	76
Figure 3-21 Second land average oil film thickness for 2500 rpm.....	76
Figure 4-1 Typical droplet size distribution and separation efficiency [5].....	78
Figure 4-2 Illustration of several inertial separators [5].....	79
Figure 4-3 Oil consumption for the two different pore size paper filters.....	81
Figure 4-4 Percent oil mass of total PCV blowby oil for different engine operating conditions.....	82
Figure 4-5 Total engine oil consumption for different liner temperatures.....	85
Figure 4-6 Temperature effect on oil consumption for 2500 rpm.....	85
Figure 4-7 Temperature effect on blowby flow for 2500 rpm.....	86

Figure 4-8 Temperature effect on oil loading for 2500 rpm.....	88
Figure 4-9 Temperature effect on oil consumption for 3500 rpm	89
Figure 4-10 Oil consumption percent change from the coldest coolant outlet temperature [T _{coolant} =56 °C] to the higher coolant temperature [T _{coolant} =91 °C].....	90

LIST OF TABLES

Table 2-1 Test engine characteristics.....	22
Table 2-2 Relevant baseline oil specifications.....	25
Table 2-3 Gravimetric experimental components.....	33
Table 2-4 Filter Specifications.....	33
Table 2-5 Blowby meter specifications	35
Table 2-6 Specification of LIF setup	40
Table 2-7 Specification for the LIF probe assembly components	43
Table 3-1 Sump oil level characteristics and oil stick schematic	67

(This page was intentionally left blank)

CHAPTER 1: Introduction

1.1 Motivation

In an effort to reduce automotive engine emissions and extend the costumers oil change intervals, there have been a lot of studies that aim at reducing engine oil consumption. Engineers have identified the power cylinder as one of the main contributors to the engine oil consumption. Many engineers have investigated the different types of oil transport in the power cylinder that affect the oil consumption in internal combustion engines. Some previous studies have investigated the main oil consumption mechanisms such as inertia and oil evaporation [1][2][3][4]. However, little effort has been done to thoroughly study the blowby oil consumption mechanism. The only studies on crankcase ventilation systems focused on the contribution of the crankcase blowby gases to oil consumption and the performance of oil separators [1][4][5][6][7].

Recent studies have shown that the blowby oil consumption through the Positive Crankcase Ventilation (PCV) system can be significant for various engine-operating conditions [8][9]. However, these studies lack the information about the source and characteristics of the oil in the blowby gas that flows back to the intake. This knowledge becomes more important as engineers lower engine total oil consumption, and the relative contribution of blowby oil consumption increases. As modern automotive engines get more compact and clearances in the engine get tighter, there is more contact between the moving parts and the lubricating oil. The smaller clearances promote oil droplet breakup into smaller particle sizes, which are harder to filter with the current oil separators.

The PCV system in the spark ignition internal combustion engines circulates to the intake the gases from the combustion chamber that flow past the piston rings and lands into the crankcase. These gases in the crankcase are then pulled through the PCV line by the intake manifold vacuum. The high-speed gases that flow through the piston rings atomize the oil in the liner into small oil liquid particles that are entrained into the flow [6]. The high piston-ring-liner temperatures also evaporate the oil species with lowest partial pressures. The piston reciprocating movement produces high gas velocities that

also entrain oil and flow past the PCV system after mixing with the blowby gases [10][11]. On the other hand, this system compensates for periodic volume changes caused by the kinematics of the crank mechanism via an orifice or by a PCV valve. Therefore there are two main sources that carry oil in liquid and vapor form to the crankcase ventilation system. The schematic for this two oil entrainment mechanism are shown in Figure 1-1.

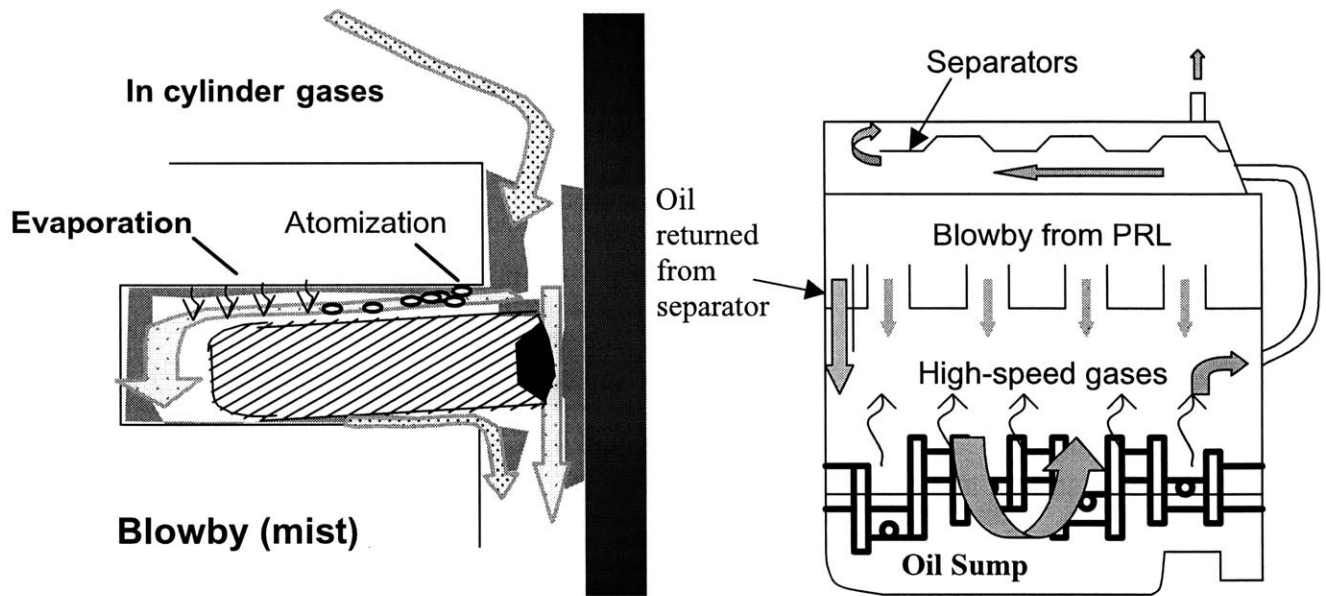


Figure 1-1 Oil entrainment in the blowby flow from the piston-ring-liner system and the engine crankcase

As automotive engines get more powerful and small, they also run at higher operating temperatures, which increase their oil evaporation [2]. However, the increased temperature augments the engine parts thermal expansion, thus modifying the clearances between the engine parts and affecting some of the oil properties. Experiments were run to see the effect of increased liner temperatures in PCV blowby oil consumption. The increase in engine speeds and loads also affect the oil entrainment in the blowby gases by changing the oil droplet sizes as well as the flow magnitude and paths [7]. This has an impact in the PCV system oil consumption, since for actual separators efficiency drops for small size droplets and different lower pressure drops [5].

In this paper, a study was carried out to measure, analyze and characterized the PCV blowby oil consumption sources and their contribution to total oil consumption at steady state conditions.

1.2 Project Background

This project aims at futhering the knowledge about the blowby oil transport phenomenon. Previous experimental studies carried out by Ertan Yilmaz in the Sloan Automotive Lab have investigated thoroughly various oil transport mechanisms in the piston-ring-liner system for a production spark ignition engine [1]. That study showed the different oil transport mechanism the relative contribution of the different oil transport modes such as the inertia or mechanical throw off, evaporation or the blowby flow. The Engine Lubrication Consortium of MIT has sponsored this and the previous studies in engine oil consumption [1][12][20]. The consortium looks into the different oil transport mechanisms that occur in the power cylinder experimentally and analytically, and it develops simulation tools for the oil consumption study for the member companies.

In this study, the PCV blowby oil consumption was characterized for different operating conditions, and some of the oil characteristics were measured along with several particle size distribution measurements. In addition, total oil consumption was measured which showed that blowby oil consumption was not one of the major oil consumption mechanisms for the four-cylinder spark ignition engine. Nevertheless, for turbocharged or compression ignition engines, where the blowby flow rates might be much larger, the contribution of blowby oil consumption could be much bigger [4][7]. However, as engineers strive to minimize the oil consumption driven by the major oil transport mechanism, the relative contribution from the blowby increases. Moreover, automotive manufacturers are also concerned about the critical engine conditions where the oil starts to foam and consumed via the PCV system. These concerns of the automotive industry have motivated this investigation to understand the oil characteristics through the crankcase by studying different PCV blowby oil transport characteristics. Figure 1-2 shows the external PCV system of the SI production engine along with direct sampling line.

The experimental setup, which includes the PSA production spark ignition engine, was setup previously in the Sloan Automotive Lab [1]. In addition to the previous setup, a direct blowby sampling line and a gravimetric filter have been added. The blowby oil consumption contribution has been obtained accurately by performing the experiments using three different oil consumption diagnostic methods: a difference method, direct method and a gravimetric method. The experimental apparatus is described in more detail in Chapter 2 of the thesis.

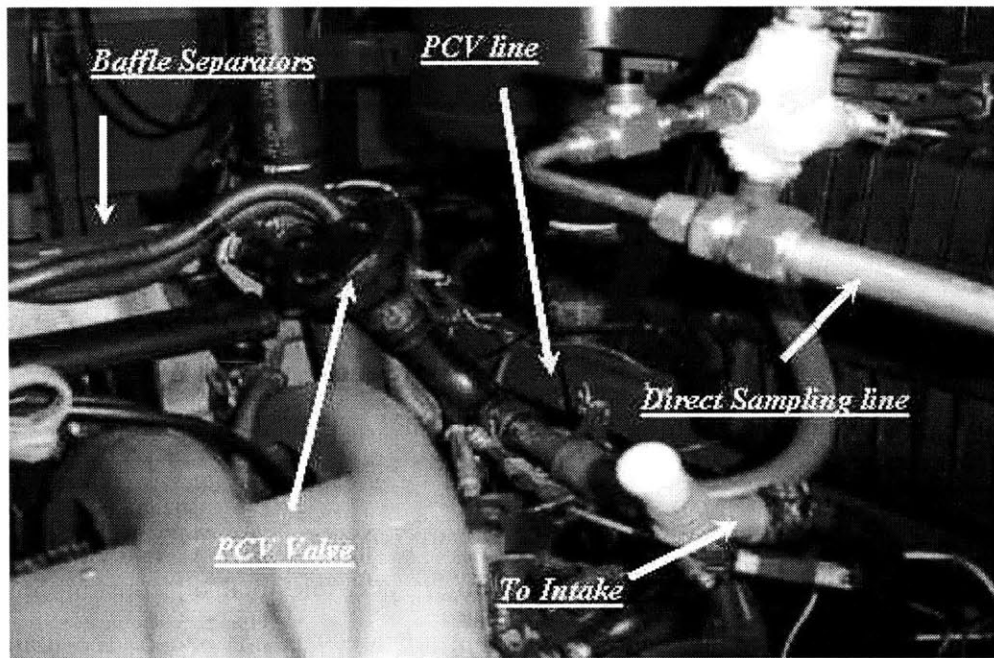


Figure 1-2 Positive Crankcase Ventilation (PCV) system and the direct sampling line

The objective is to answer the unknown question about the source and oil characteristics of the blowby flow, which affect the total engine oil consumption.

1.2 Project Scope

One of the major questions regarding the engine's PCV blowby oil consumption is the source of oil in the flow. Two major oil sources are believed to contribute to total oil consumption: the piston-ring-liner system and the oil sump (See Figure 1-1). In order to quantify the oil contribution from each of the sources one of them needs to be isolated.

Although running the engine with a dry sump was considered, technical difficulties did not make it feasible. However, the production engine was run at different oil sump levels inside the operational engine limits in an effort to isolate the contribution of oil entrainment in the crankcase. The engine's lubrication system relies on oil jet. However, due to safety reason the lowest level for the sump was inside the limit. Chapter 3 in the thesis explains the different oil source contributions for various engine-operating conditions.

In addition, the investigation also looked into the oil characteristics in the blowby flow. The characteristics of the oil in the blowby are an important issue for automotive manufacturers. Modern spark ignition engines use oil separators in order to remove the oil from the flow. However, most of these separators have a limited capacity to remove most of the smallest oil particles from the blowby flow. Therefore the efficiency of these separators is of great importance when trying to reduce the blowby oil consumption contribution [4][5].

Experiments were run for different engine thermal conditions to see the impact of oil evaporation on the blowby oil consumption. Results for these experiments along with the analysis are shown in Chapter 4 of the thesis. Furthermore, a gravimetric measurement system implemented in the engine's PCV system was used to collect the oil from the blowby flow with different pore size filters. These experiments have shown some of the effects on the characteristics of the oil particles entrained in the blowby flow. This study of the oil particle characteristics is also discussed in detail in Chapter 4 of the thesis.

Therefore, the main objectives of the project are summarized in the following points:

- 1- Check the three different diagnostic systems for blowby oil consumption
 - a. Difference Method
 - b. Direct Method
 - c. Gravimetric Method
- 2- Map the engine oil consumption for different loads and speed
 - a. Blowby
 - b. Total
 - c. Relative contribution of the blowby

- 3- Study the oil source in the blowby
 - a. Different oil level experiments
 - b. Difference in total oil consumption
 - c. Lubricating condition
- 4- Investigate the oil characteristics in the blowby flow
 - a. Liner temperature effect on oil consumption
 - b. Oil particle size mass distribution

CHAPTER 2: Experimental Setup

2.1 Experimental Objectives

For the experimental investigations it is critical to control the parameters that are most likely to affect the oil consumption and its sources. Therefore it is critical to choose, develop and implement suitable experimental techniques. In this section the experimental objectives and the technical approach to meet these objectives are discussed.

Oil transport in the piston-ring-liner system is governed by the ring-liner lubrication condition, piston and ring dynamics and gas flow. All the driving forces vary with different engine operating conditions. All parameters and especially the thermal expansion of the component geometries vary with the operating conditions, thus affecting the gas flow process in the piston-ring-liner system. In addition, the thermal conditions on the cylinder are believed to affect the oil evaporation process. All these parameters affect the oil transport process in the piston-ring pack, and thus the oil consumption sources. Therefore in order to thoroughly study oil consumption and the blowby oil consumption source it is vital to obtain simultaneous measurements of oil consumption and in-cylinder parameters affecting the oil transport sources.

Accordingly, an experimental setup with the capability to measure oil consumption along with blowby and in-cylinder variables that govern the oil transport and consumption mechanisms is needed for the study of blowby oil consumption.

The experimental objectives are summarized as follows:

- 1- Present fast and accurate measurements of total engine oil consumption
 - a. Measurement of total engine consumption
 - b. Measurement of blowby oil consumption with three different diagnostic methods
- 2- Present accurate blowby measurements
- 3- Present measurements of in-cylinder parameters that affect engine oil transport and consumption
 - a. Measurements of oil film thickness
 - b. Measurements of cylinder and inter-ring pressures

- c. Measurements of the liner thermal conditions that affect oil evaporation

2.2 Test Engine: Production Spark Ignition Engine

The test engine was a four-cylinder spark ignition engine. The engine characteristics are shown in Table 2-1.

Engine Type	Port Injected Spark Ignition Engine
Number of Cylinders	4
Displacement	2.01 liter
Bore	86.25 mm
Stroke	86.00 mm
Maximum Power	97.4 kW @ 5500 rpm
Maximum Torque	180 Nm @ 4200 rpm
Compression Ratio	10.4:1

Table 2-1 Test engine characteristics

The following engine was chosen for use in the experimental study because the 4-cylinder spark ignition engine is a very representative automotive engine currently used in the automotive industry. It gives the possibility to study the oil transport phenomena with an engine that is widely used by automotive manufactures, thus giving us meaningful results that can be compared with other automotive literature.

The test engine was modified for the implementation of different experimental techniques and to control different engine operating condition [1]. The cylinder head was modified to fit a pressure transducer in the third and fourth cylinders. Moreover, the engine's block and liner for the third cylinder were machined to allow inter ring pressure and liner temperature measurements, as well as for optical access to the piston-liner interface for oil film thickness measurements.

In order to control the engine's thermal conditions, the coolant temperature was controlled [1]. The engine coolant from an external coolant tank was circulated through

the engine block. To regulate the coolant temperature to the desired temperature, the flow of water city in a heat exchanger was controlled with a valve.

2.3 Measurement techniques

An extensive diagnostic system was implemented on the test engine to measure oil consumption, blowby, in-cylinder parameters, cylinder and land pressure, and liner temperatures. In this section the oil consumption experimental techniques are further discussed.

2.3.1 Total Output Measurements

Engine total output measurements are the parameters such as the oil consumption, blowby flow or air to fuel ratio that are measured before or after they go through the engine system. The total output measurements from the test engine are the oil consumption, the intake airflow, blowby flow, and the air to fuel ratio.

2.3.1.1 Engine Oil Consumption

Nowadays, modern passenger car engine oil consumption rates have reached quite low numbers, of the order of 10 g/h. Due to this small consumption, the measurement of oil consumption has been one of the major challenges for automotive engineers. Traditional methods, such as weight and drain, and continuous weight require several hours of operation. This length of time might introduce measurement errors due to potential interferences with other engine physical mechanisms. For example, engine oil consumption can be negative with these techniques due to the fuel dilution in the lubricating oil [7][16].

One alternative to these traditional methods is the sulfur tracer technique. This technique requires the use of high sulfur content oil and a low sulfur content fuel. It monitors the sulfur concentration in the exhaust/blowby gases to determine engine oil consumption. Researchers in the automotive industry have successfully demonstrated the capabilities of the sulfur trace technique for the oil consumption measurements

[1][2][3][4][5]. One of the techniques most widely used to obtain the blowby oil consumption is by taking the difference between the total oil consumption output with and without the blowby line connected. More on this technique and other measurement methods will be discussed in Section 2.3.1.2.

2.3.1.1.1 High Sulfur Oil

The high sulfur oil is a vital component of the measurement technique, since the oil consumption measurements rely in the sampling of sulfur in the exhaust or the blowby. The overall concentration of sulfur in oil needs to be around 1.5% [wt.] in order to have reliable measurements throughout the engine operating range [1]. The oil evaporation process is selective, and major contribution comes from the species at the light end. Thus, a consistent sulfur concentration in the oil is required throughout the oil distillation curve. This is to assure that the consumed oil in vapor or liquid form has the same sulfur concentration as in the original oil. Lubrizol Corp. formulated the special high sulfur content baseline oil with the desired properties. Figure 2-1 shows the sulfur content of each distillate (ASTM D 4294) versus the distillation (ASTM D 5236) of the baseline oil [1]. Table 2.2 shows some of the most relevant properties of the oil such as the volatility and viscosity. Fresh high sulfur oil needs to be run for about one to two hours to break-in before running any experiments. The oil has a settling period where most of the hydrocarbon species that are in the light end of the distillation curve are evaporated. The measurements might turn out higher than steady state oil consumption masking the true steady state results.

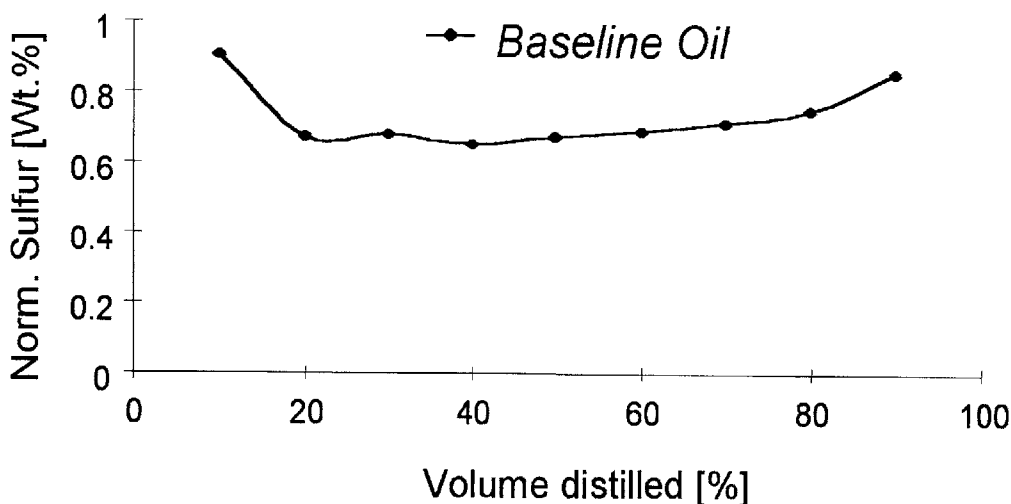


Figure 2-1 Baseline oil sulfur content with distillation

Baseline Oil (Mineral)		ASTM D
SAE Viscosity Grade	SAE Viscosity	10W-30
Sulfur [wt. %]	1.51	1552
Volatility: GCD % off @ 371° C	11.6	
Noack	16.8	5800
Kinematic Viscosity @ 100°C	10.77	445
HTHS viscosity [cP]	3.04	4683

Table 2-2 Relevant baseline oil specifications

2.3.1.1.2 Low Sulfur Fuel

In order to have accurate measurements of the oil consumption, it is necessary to minimize other sulfur sources. Since the air has very little sulfur (< 10 ppb), the only way that the result could be altered would be with the interference of sulfur in gasoline. For gravimetric experiments, fuel can be absorbed by the oil in addition to the gasoline combusted in the chamber, masking the actual sulfur level of the samples. Nevertheless, the distillation curve of the fuel shows that it evaporates much faster than the oil, almost

not impacting the gravimetric runs. When running the blowby oil consumption measurements, there is not any measurement equipment that can read the fuel level in the flow. Thus it has been neglected due to its small contribution. To minimize its impact, a low sulfur fuel was used with a sulfur level below 2 ppm [wt.]

2.3.1.2 Oil Consumption Measurements Setup

The oil consumption measurement setup is shown in Figure 2-2.

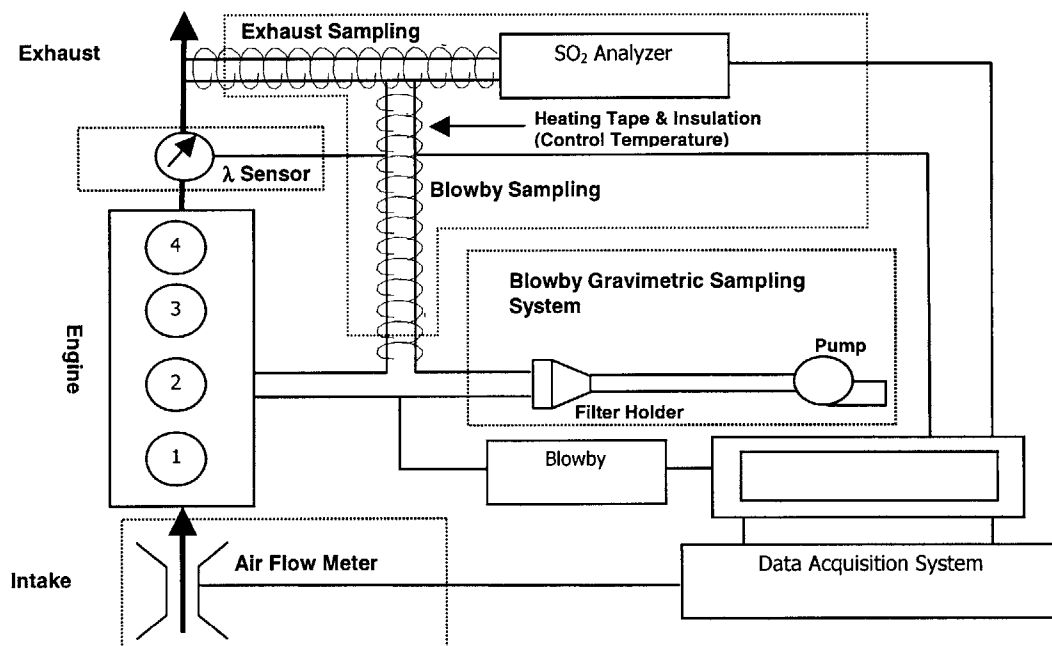


Figure 2-2 Schematic of oil consumption measurement system

The system is composed of the exhaust sample system (exhaust/blowby), the lambda (λ) sensor, the air flow meter, the gravimetric particle filter and the data acquisition system. One of the most critical elements is the exhaust/blowby sampling system. Representative samples from the exhaust and Positive Crankcase Ventilation (PCV) line are withdrawn and directed to the sulfur analyzer. The sampling line for the blowby and exhaust contains stainless steel tubing (Grade 314) to ensure resistance against sulfur dioxide (SO₂) corrosion [1]. The transport of the hot exhaust gas stream, which contains particulates, might lead to deposition on cold walls. This process, also known as

thermophoresis, could cause plugging of the sampling line. Unburned hydrocarbons or particulates from the exhaust may also condense because the temperature drops. Therefore it is critical to maintain the sampling lines at a high temperature in order to prevent such phenomena from happening. In order to avoid these phenomena it is necessary to control the temperature in the sampling line to 300°C.

An Antek[®] Sulfur-Analyzer (Model R6000 SE) was used to detect the sulfur concentration in the exhaust gas sample [17]. Figure 2-3 illustrates the components of the analyzer in detail and Figure 2-4 shows a view of the analyzer in the test cell. The analyzer is designed as a flow-through analyzer. The sample must be conditioned before entering the sulfur detection part of the analyzer. The sample gas is withdrawn by a bellows pump and directed into a furnace for oxidation. A controlled flow rate of the pyrolysed gas is sent to a second furnace through a fixed restriction transfer tube. Before entering the second furnace, the sample is mixed with additional oxygen to oxidize unburned hydrocarbons, particulates and sulfur compounds contained in the sample. Condensation of water in the cooled detection part of the analyzer could lead to sulfur dioxide absorption and alter the oil consumption measurements. Therefore, after the second furnace, two permeable membrane dryers remove the water in the sample gas before it enters the detector. In the detector, the conditioned sample exhaust gas (oxidized and dried) is mixed with Ozone (O₃) and exposed to ultraviolet radiation in the fluorescence chamber. The UV light brings the sulfur dioxide in the sample to an excited state, which results in a fluorescence emission. A photo multiplier tube detects the fluorescence emission intensity, which has a linear relationship with the sulfur dioxide concentration in the sample gas.

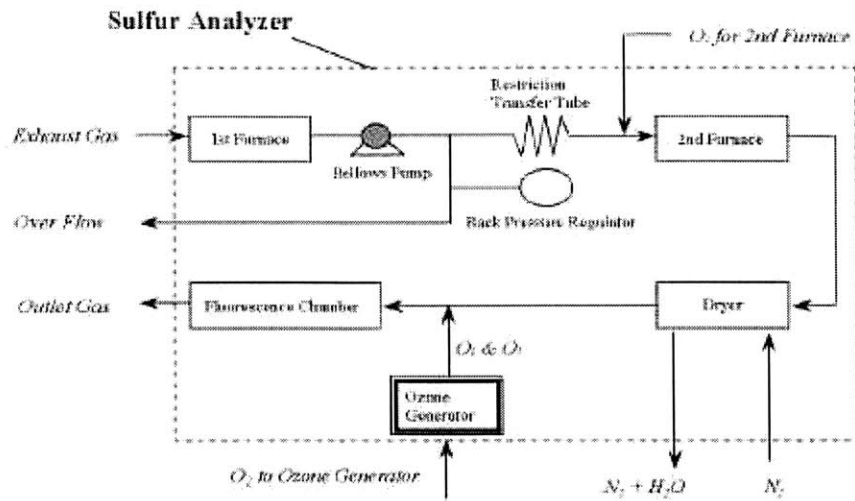


Figure 2-3 Antek® sulfur detector [29]

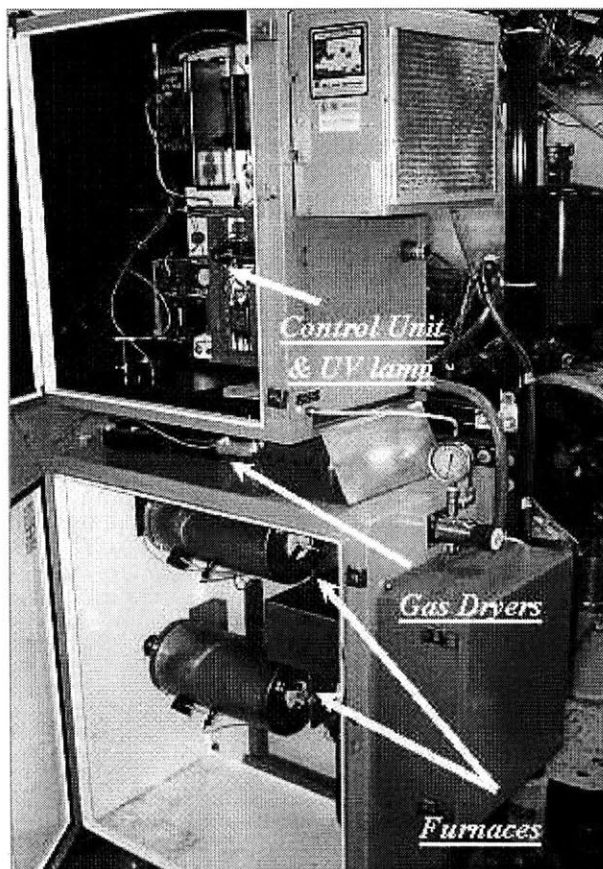


Figure 2-4 Antek® R6000 SE sulfur detector in the test cell

Then the total oil consumption can be determined by measuring the sulfur content in the exhaust, the airflow rate and the fuel flow rate. The airflow was measured with a laminar flow meter and the fuel flow rate might be determined by measuring the air/fuel ratio relative to the stoichiometric ratio in the exhaust. This air/fuel ratio was measured with a λ -sensor, which is installed near the exhaust sampling location. In order to obtain the blowby oil consumption through the PCV by sampling it from the exhaust, the engine was run with the PCV line connected to the intake and disconnected. The contribution from the blowby transport was found by taking the difference between the two configurations and by measuring the blowby flow. This is explained in more detail in section 2.3.1.3.1.

However, the direct blowby measurement case was determined by measuring the sulfur content in the blowby, and the blowby flow. The flow was measured with the Von Karman-vortex shedding flow meter before and while the flow was sampled. The temperature was also controlled in order to calculate the density of the blowby gas (always close to air density). The content of sulfur in the fuel was neglected, since the fuel amount in the blowby gases cannot be measured with the current setup. However, the low sulfur fuel did not have a big impact on the sulfur dioxide measurements in the analyzer. This method is further discussed in section 2.3.1.3.2.

The gravimetric diagnostic system determines the oil consumption by weighting the collection of oil in a particle filter and by obtaining the blowby flow magnitude. The sample flow was drawn with a pump and regulated by a flow meter to be constant. The filters were weighted in a scale accurate to the 0.1 mg before and after the collection of oil, thus determining the amount of oil trapped in the filter (Oil in gas form is not trapped). This diagnostic method is further discussed in section 2.3.1.3.3.

A Lab VIEW based data acquisition program was used to simultaneously take raw data, calculate oil consumption rate, and display it along relevant engine parameters. This lets the test conductor validate the actual data and intervene if necessary. The only data that could not be controlled online is the gravimetric particle collection, since the filters were measured before and after experimentation.

2.3.1.3 Engine Blowby Oil Consumption

In addition to the total oil consumption of the engine, blowby oil consumption was also measured by using the three diagnostic methods described above. In this section, the three different techniques are described more in detail.

2.3.1.3.1 Difference Method

The difference method consists on the measurement of the sulfur concentration from the exhaust by connecting and disconnecting the PCV line while running the engine (See Appendix A). The total oil consumption measurements (Shown in equation 2.1) are assumed to be the sum of all the consumption sources mention in section 1.1.

$$\dot{m}_{OC,w/PCV} = \dot{m}_{evcap} + \dot{m}_{inertia} + \dot{m}_{blowby} \quad (2.1)$$

By disconnecting the Positive Crankcase Ventilation (PCV) blowby line, the assumption made is that the total output measurement lacks the blowby oil consumption source as shown in equation (2.2).

$$\dot{m}_{OC,w/outPCV} = \dot{m}_{evcap} + \dot{m}_{inertia} \quad (2.2)$$

This way, by taking the difference between equations (2.1) and (2.2), the blowby oil consumption can be calculated.

$$\dot{m}_{blowby} = \dot{m}_{OC,w/PCV} - \dot{m}_{OC,w/outPCV} \quad (2.3)$$

In this case, the engine's PCV line, when disconnected, was drawn to the atmosphere thus changing the conditions under which its valve would normally operate. There was less flow through the valve when the PCV line was disconnected due to the weaker vacuum downstream the valve, as shown in Figure 2-5, for which the PCV flow would be the closest to the blowby volume axis [18][19]. However, the blowby production for the

highest load, close to the axis, increased and thus the valve flow characteristics restricted the PCV blowby flow. The pressure in the intake was lower than atmospheric due to the throttle losses increasing the vacuum. More results about the different engine operations will be shown in Section 3.3.

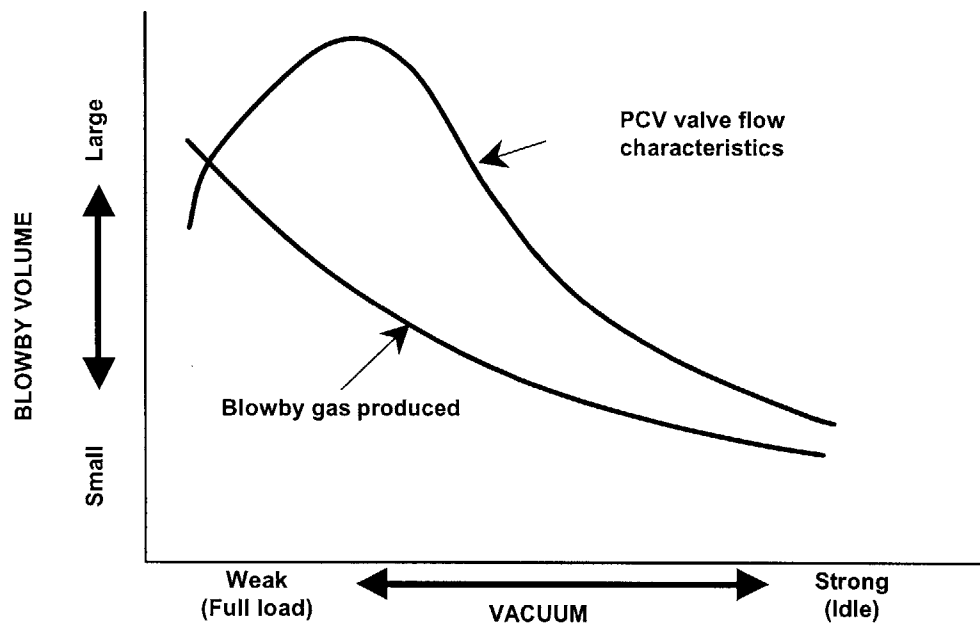


Figure 2-5 PCV valve and blowby flow characteristics

2.3.1.3.2 Direct Method

The direct method consists of taking the measurement directly from the PCV line. As in the total output measurements, this diagnostic method also monitors the sulfur concentration of the blowby gas to determine the blowby oil consumption (See Appendix A).

This measurements approach samples from the PCV line directly. The sampling was done downstream the PCV valve, which is used to regulate the PCV flow to match that of the blowby gas flow in order no to have any pressure losses in the crankcase. The experiments were run when the PCV line is connected or disconnected to the intake and exhausted to the atmosphere. In the contrary to the first method, there was not switching

between the two engine configurations, but rather the experiments were run either when it was disconnected or connected.

The main difference of this method with the differential one was that the sulfur concentration on the blowby gas is much higher due to the higher oil concentration in the blowby flow compared to the exhaust. The resolution of this diagnostic method proved to be higher, mainly because the blowby oil consumption component is not a major one in the total oil consumption and especially at low loads where the differential method has much more trouble to read the blowby contribution from two large oil consumption numbers.

2.3.1.3.3 Gravimetric Method

The gravimetric method was setup to compare and check the results with the other two diagnostic methods and to investigate the oil particle size distribution in the flow. It relies on the collection of oil in a glass fiber and PTFE polymer paper, which is weighted in a precision scale before and after running experiments. Although fuel absorbed by the oil is also collected [8][11][16], the fuel evaporation rate is much faster than that of oil. Therefore the weighing after the experiment was done about five to ten minutes later in order to minimize its impact. This method consists of sampling a fixed flow from the PCV line for a fixed period of time. Researcher in the aerosol-sampling field have already demonstrated and validated similar type of sampling systems [6][10]. However, due to the high cost and lead-time of these systems, a simpler system based on the same method has been built in-house. The schematic of the setup is shown in Figure 2-6. The main components of the diagnostic method are shown in Table 2-3 and the different filter types used in Table 2-4.

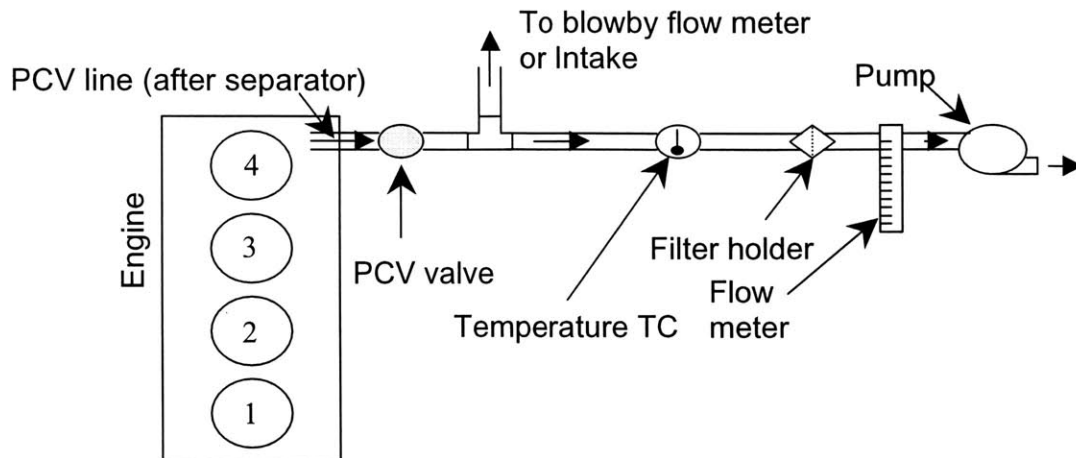


Figure 2-6 Setup of gravimetric method

Filter Holder	47 mm Ø Aluminum Holder
Flow Meter	Rotameter with glass ball
Pump	Positive Displacement
Tubing	Stainless Steel Tubing ½ “

Table 2-3 Gravimetric experimental components

Type	Pore Size (µm)	Thickness	Retention Efficiency (ASTM D2987)
Emfab	0.3	7 mils (198 µm)	99.99%
Zeflour	0.5	7 mils (198 µm)	99.99%

Table 2-4 Filter Specifications

Furthermore, this experimental method gives the possibility of using different pore size filters, thus letting a more detail blowby oil characteristics study of the particle size mass distribution. For the experiments the sampling feed line was not heated because the monitoring of the aerosol temperature showed that it was around 30 °C [10]. This temperature was close to the atmospheric and little condensation of the oil was expected; unlike with the differential method setup which samples from the hot exhaust. On the

other hand, the results for gravimetric method were generally slightly lower than the previous diagnostic methods since it did not collect evaporated oil. Figure 2-7 shows a picture of the setup in the test cell.

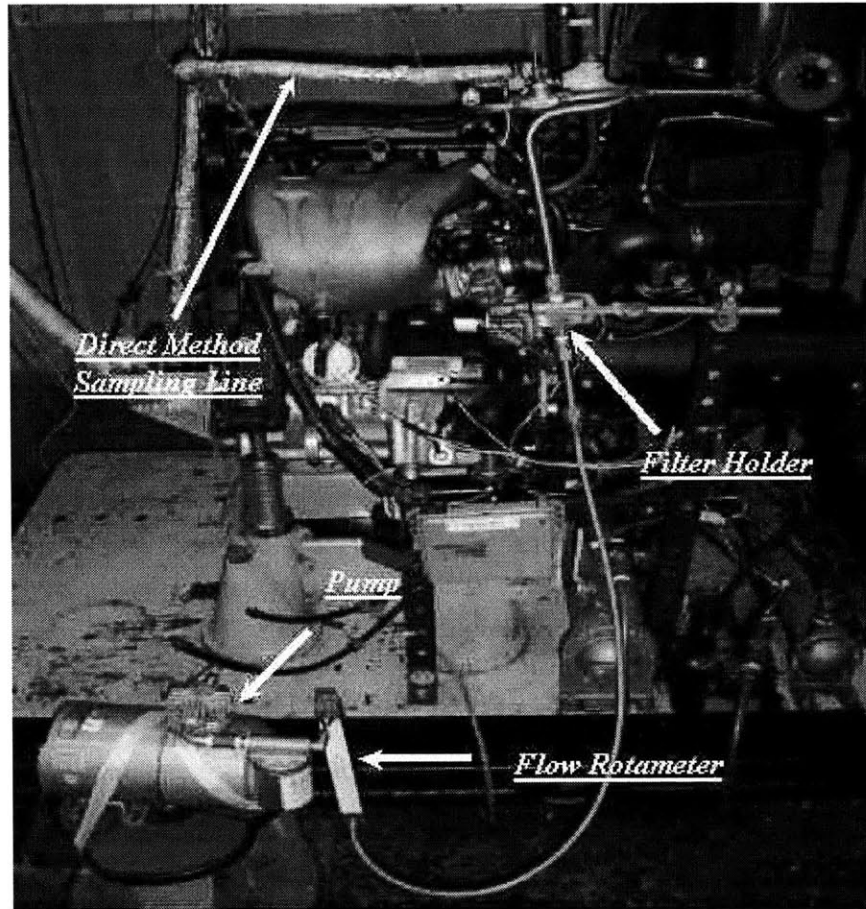


Figure 2-7 Gravimetric method component setup in the SI engine

2.3.1.4 Blowby

Blowby is the leakage of the combustion gases to the crankcase because of the increase pressure in the combustion chamber. It is composed of the burned combustion gases, unburned mixture and the lubricating oil that absorbs while it flows through the ring-pack. Blowby gases are mixed with high-speed gases created by the reciprocating movement of the engine components. Then, the blowby gases are circulated back to the intake manifold by the Positive Crankcase Ventilation (PCV) system to prevent the

emission of pollutants to the atmosphere. Blowby at a given speed and load is controlled primarily by the greatest flow resistance in the flow path between the combustion chamber and the crankcase, which is normally the smallest of the compression ring gap area. However, there is also possibility of flow through the ring groove if there is ring lift off or fluttering.

In order to accurately describe the blowby oil transport phenomena, it is necessary to measure the blowby flow rate into the crankcase. Because of this, an accurate flow meter was installed that was based on the Von Karman-vortex shedding principle [1]. Detail of the blowby flow meter are summarize in Table 2-5.

Principle	Von Karman-vortex shedding
Range	4-100 [l/min]
Accuracy	<1% of reading

Table 2-5 Blowby meter specifications

The flow meter was installed after the PCV valve, which is used to maintain the pressure in the crankcase around atmospheric. As discussed in section 1.1, the reciprocating movements of the engine moving parts can also affect the oil consumption. This reciprocating movement creates high-speed gases that affect the oil entrainment and the pulsating behavior of the blowby flow. Figure 2-8 show the flow meter and some of the components that are in the test cell.

Therefore, the blowby is a pulsating flow, with periods where it is reversed. The flow pulsations are mainly caused by the volume changes in the crankcase due to the kinematics of the crank mechanism as shown in Figure 2-9 [1]. However, the average flow rate is out of the crankcase and what was measured. The PCV valve helps maintain the pressure in the crankcase by only letting the blowby flow when the pressure is above the predetermine one.

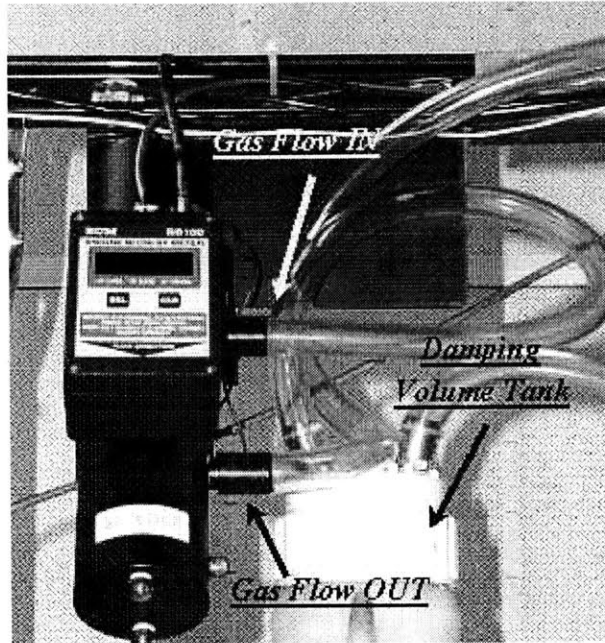


Figure 2-8 Flow meter picture with volume damping tank

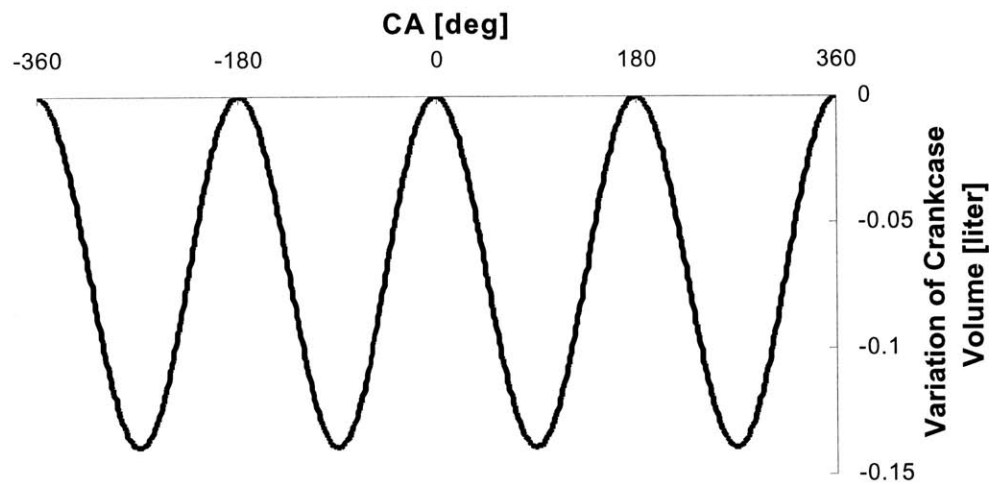


Figure 2-9 Crankcase volume changes as a function of crank angle

Moreover, since the blowby meter is optimized to measure flows in only one direction, if installed in the blowby path, it would give different flow rates than actual due to flow reversal. Therefore, a damping system was installed upstream the flow meter in order to minimize the flow fluctuations. This consisted of two large damping tanks connected in parallel attached before the flow meter [1][18].

2.3.1.5 Oil Consumption Formulas

The formula to calculate oil consumption from the exhaust had been derived at MIT (See Appendix A) using the sulfur dioxide concentration in the exhaust, the airflow rate, the air/fuel ratio, and the mass fractions of sulfur in oil and fuel [1].

For the direct diagnostic method a different formula has also been derived using the sulfur concentration in the blowby, the blowby flow and the mass fraction of sulfur in the oil. In this section the basic assumptions and relations of the blowby oil consumption formula will be described:

Calculating the blowby mass flow rate can approximate the consumed sulfur mass in the blowby gas. The contribution from the fuel in the blowby is hard to approximate, since the fraction of fuel in the blowby has not been measured, and due to the low contribution, it has been neglected

$$\dot{m}_{blowby} = \dot{Q}_{blowby} \cdot \rho_{blowby} \quad (2.4)$$

Where

$$\rho_{blowby} = \frac{P_{atm}}{\left(\frac{R}{M_{blowby}} \right) \cdot T_{blowby}} \quad (2.5)$$

For simplifying purposes it is known that $M_{blowby} \approx M_{air}$, and R is the universal gas constant.

The mass fraction of sulfur in the blowby can be written as

$$\xi_{SO_2,blowby} = \psi_{SO_2,blowby} \cdot \left(\frac{M_s}{M_{blowby}} \right) \quad (2.6)$$

Where $\psi_{s,blowby}$ is the dry sulfur concentration in blowby in wt. %. Then by substituting this in the blowby oil consumption formula

$$\dot{m}_{OC,blowby} = \frac{\dot{m}_{blowby} \cdot \xi_{SO_2,blowby}}{\xi_{s,oil}} \quad (2.7)$$

The current capabilities of the setup do not have the possibility to measure the moles of water and wet blowby. However, further analysis of variation of the water fraction moles showed that there was no much of impact on the final results, and thus it was neglected.

For the gravimetric diagnostic method, it is simple to obtain the oil consumption rate with the sampled flow, the blowby flow, and the measured weight of collected oil:

$$m_{OC,blowby} = \left(\frac{\left(\frac{m_{collected}}{t_{sample}} \right)}{Q_{sample}} \right) \cdot Q_{blowby} \quad (2.8)$$

Where the Q_{sample} is fixed at 2.09 l/min, and t_{sample} is the duration of time of the experiment. The time of wa varied depending on the engine operating condition, for which the oil loading varies.

2.3.2 In-cylinder Measurements

The engine block has been modified in the third cylinder in order to implement in-cylinder measurements [1]. Piezoelectric pressure transducers positioned along the liner provided inter ring pressures. The one-point Laser Induced Fluorescent (LIF) system has been fitted to the engine to gain information about the oil film thickness distribution, with four windows positioned along two different axes in the liner. Thermocouples were also installed in the top and bottom position of the liner to measure liner temperatures. The positioning of these measurements has been chosen for the ease of the test conductor to

access them for experimentation and maintenance. Figure 2-10 shows more on detail the positioning of these measurement probes installed in the third cylinder. Figure 2-11 shows the installed actual measurement probes in the engine

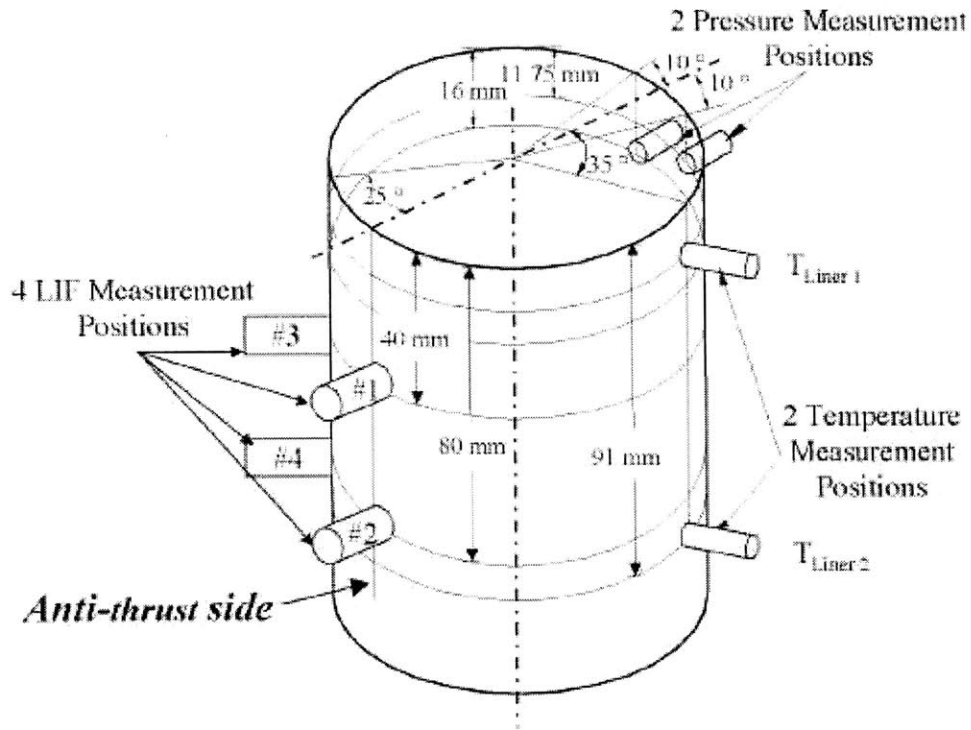


Figure 2-10 Measurement locations of in-cylinder variables

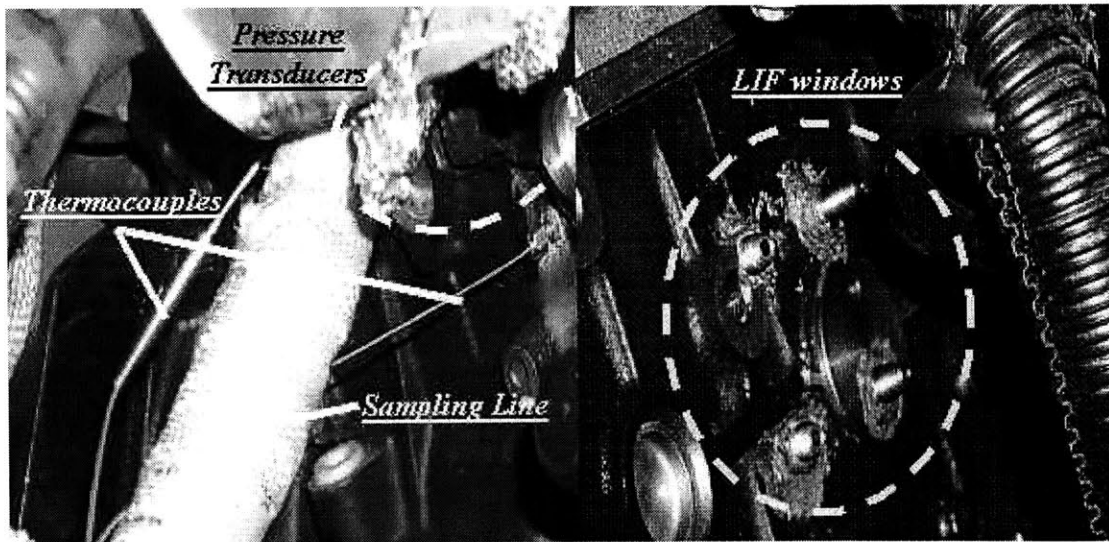


Figure 2-11 Measurement probes in the engine 3rd cylinder

2.3.2.1 Laser Induced Fluorescence System (LIF) System

The Laser Induced Fluorescence (LIF) diagnostic system was used to quantify the oil film thickness between the piston rings and liner and the oil accumulation on the piston lands during operation. The LIF system developed in the Sloan Automotive Lab has shown its capabilities in previous studies [1][2][3][12][20]. For the LIF studies, the oil is doped with a fluorescence dye to increase the natural fluorescence of the oil in order to enable more accurate measurements of film thickness.

The LIF system is composed of a 442 nm 14mW Helium-Cadmium laser (Model LiConix 4214N), focusing optics and optical filters, fiber optics and a photomultiplier [15]. A schematic of the LIF system is shown in Figure 2-12. The laser beam, produced by a Helium-Cadmium laser (441.6 nm), is directed through a bifurcated fiber optics cable into the LIF focusing probe. In the probe, a conventional lens system focuses the laser light onto the lubricating oil film on the piston and ring surface. The dye molecules dissolved in the oil are excited by the laser light and undergo a fluorescence process. The fluoresced light is picked up by the bifurcated fiber optics and directed through an optical filter (495nm) - to block any reflected laser light - to the photomultiplier tube. In order to have accurate measurements, the laser output to the engine from the fiber optics should be about 3 to 4 mW. The output is very sensible to the condition of the fiber optics and proper alignment of the laser beam, so great care should be paid when adjusting. Table 2-6 shows the principal specifications of the laser.

Laser	He-Cd
Power	14 [mW]
Excitation wavelength	442 [nm]
Dye	Coumarin 523
Fluorescence wavelength	495 [nm]
Window Transmission	90 [%]

Table 2-6 Specification of LIF setup

For the actual application, the oil has been doped with the fluorescence dye Coumarin 523 with a concentration of 1.0×10^{-4} mol/liter [1][12]. This oil dye is used to increase the natural fluorescence of the oil molecules and get more accurate results.

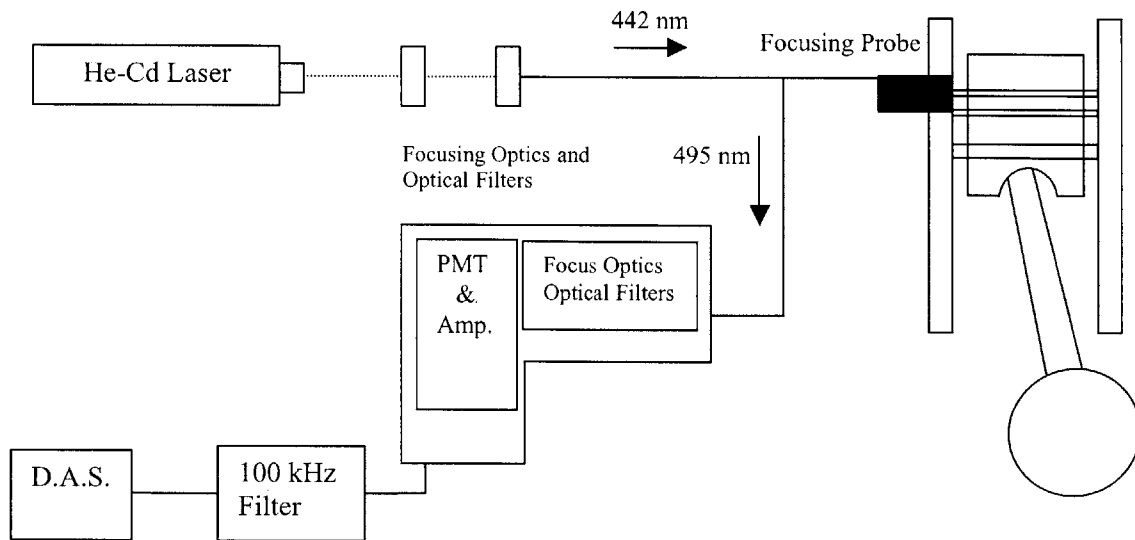


Figure 2-12 Schematic of LIF system setup

The application of the LIF system requires several modifications to the engine block, liner, and piston. First, detail axial and circumferential locations were determined for the optical access to the combustion chamber. The locations needed to be chosen to get optical access for the three lands in the piston-ring-liner system and the piston skirt. Two different windows were located along the anti-thrust side, 40 mm and 80 mm from the top of the liner [1][13]. Figure 2-13 shows the instantaneous location of the land for the compression and expansion stroke.

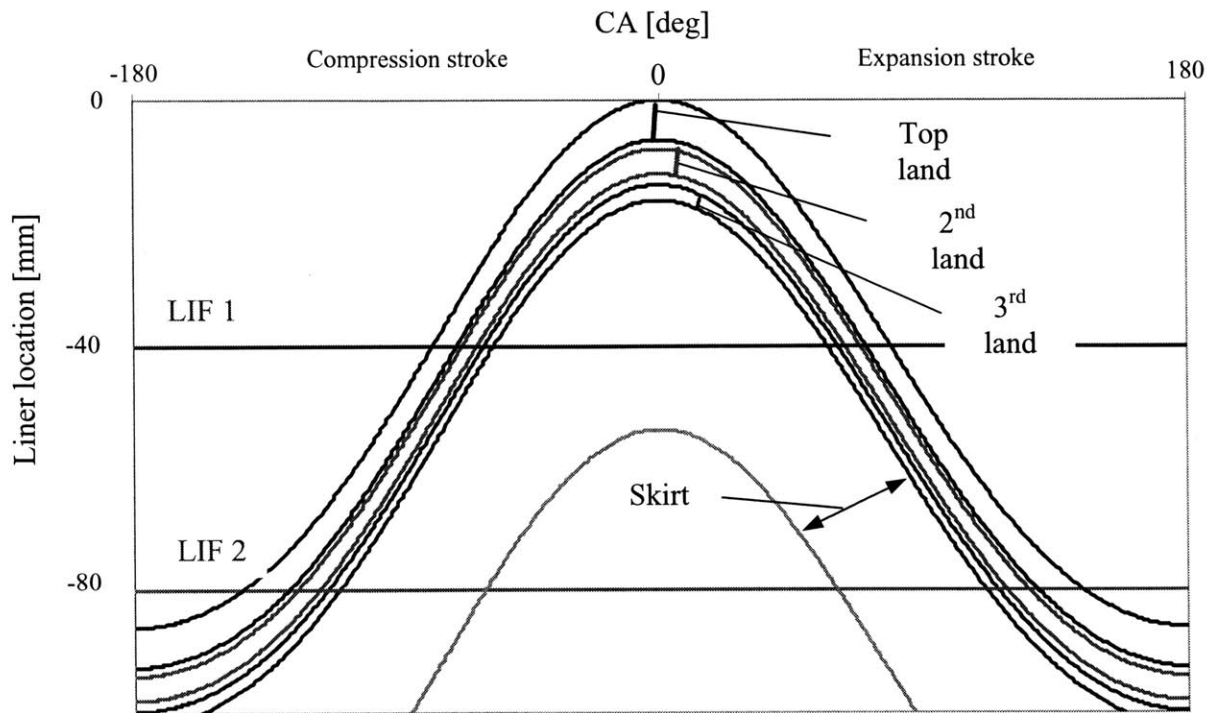


Figure 2-13 Axial position of LIF probes and of different piston regions with crank angle [1]

After the LIF measurement locations were determined, the stock engine block and cylinder liners were machined for the installation of the windows. The machining and assembly of the windows was done previously in the Sloan Automotive Lab. The windows were assembled in a probe, which can be taken out from the engine window mount for cleaning [1]. The window probes were installed inside a housing sleeve, which also can be taken out from the engine for cleaning and maintenance. After installation on the engine, RTV was applied at the inside and outside ends in order to seal the windows from the coolant jacket in the engine.

The focusing probe consists of a probe housing, two optical lenses, and two spacer rings to separate the lenses and to hold them inside the probe housing. The probe is designed to position it inside the housing sleeve. A schematic of the housing sleeve and focusing probe arrangement is shown Figure 2-14. These windows facilitated the cleaning and maintenance of the optics inside the engine. Table 2-7 shows the characteristics of the windows and spacers.

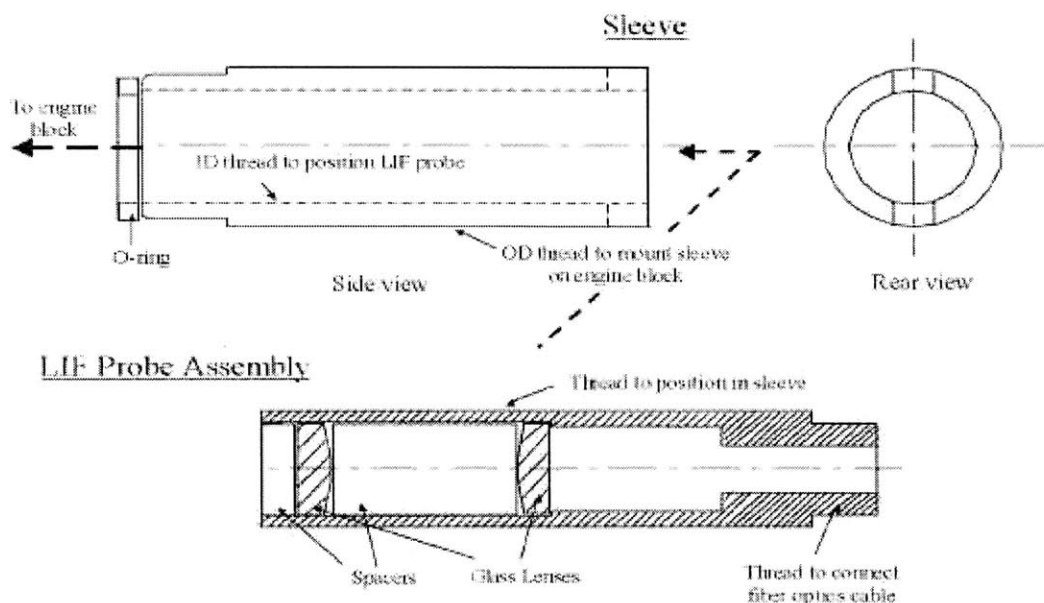


Figure 2-14 Arrangement of LIF housing sleeve and probe assembly [1]

Spacers	Dimension/Properties
Long	.472±.003 in
Short	.09±.002 in
Lenses (both are the same)	6.3 mm Diam. and 12.7mm F.L.

Table 2-7 Specification for the LIF probe assembly components

The oil film thickness was obtained by post processing the output light intensity signal. In order to correlate this output intensity signal, there are several methods that can be used and that have been used in the Sloan Laboratory before [1][12]. However the method used for the experiments was based on the depth of several tool marks in the piston. Several scratch marks of different depths (20-40 μm) were done in the piston as shown in Figure 2-15, along the laser sight path. Talysurf measurements of these marks were used to determine the coefficient to convert the output voltage to microns of oil film thickness [1][2][12].

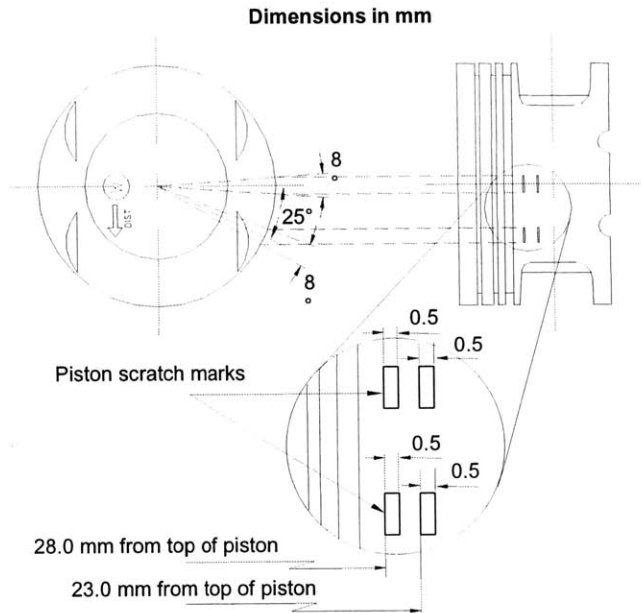


Figure 2-15 Piston scratch marks for LIF calibration [1]

Great effort was directed to achieve a relatively flat groove surface by machining each scratch mark with a new tool. Before reassembling the engine, the piston surface profile was measured with a stylus instrument (Form Talysurf), since the detailed scratch mark depths directly affect the calibration coefficient [1]. Figure 2-16 shows the micro-geometric profile measurements of the piston with the scratch marks at the antitrust side.

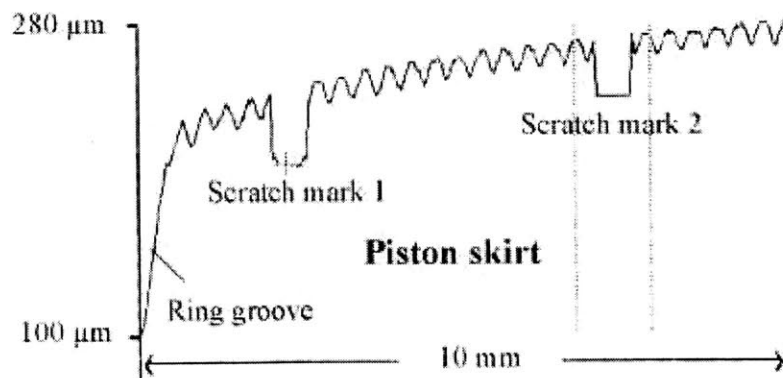


Figure 2-16 Surface profile of piston skirt and scratch marks at anti-thrust side [1]

The LIF calibration was performed with the calibration coefficients obtained during the compression stroke. Figure 2-17 shows a sample LIF traces acquired during steady state engine operation at different times. Each shown trace was averaged over ten consecutive cycles. It has to be taken into account that the measurements were influenced

with the time of data acquisition. For the steady state operation of the engine, the oil film thickness (OFT) varies with time due to the ring rotation that changes the oil transport in the liner [20][21][26][27]. This phenomenon has been characterized by the experiments done on the single cylinder PSA research engine with the 2-D Laser Induced Fluorescence technique in the Sloan Automotive Lab. The ring rotation might align the ring gaps changing the blowby flow and oil supply characteristics, due to the differences in the blowby gas dragging. Moreover, the blowby gas dragging affects the oil film distribution and oil transport characteristics at the same time.

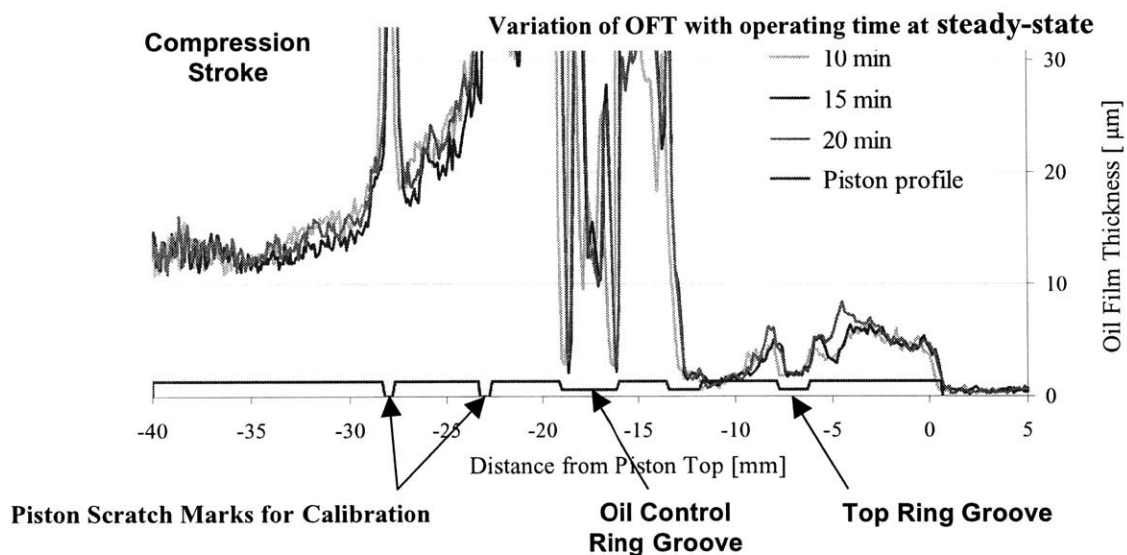


Figure 2-17 Example of LIF traces and ring piston locations

2.3.2.2 Cylinder and Land Pressure Traces

The test engine's head was machined to house two pressure transducers in order to obtain the cylinder pressure trace for two cylinders. The pressure measurements were taken with water-cooled piezoelectric transducers.

In addition, two other pressure transducers were mounted into one side of the engine to get the land pressure traces of the third cylinder. The location of these transducers is shown in more detail in Figure 2-18. These axial locations ensured the measurement of inter-ring pressures for the longest possible crank angle period. This setup was done previously in the Sloan Automotive Lab [1]. One transducer was located just above the top dead center (TDC) position of the scraper ring in order to measure second land

pressures during the period of piston reversal between the compression and expansion strokes. The second transducer was positioned lower on the liner. The distance between both transducers was slightly larger than the width of the piston's second land. This arrangement allowed the measurement of the second land pressure for the periods just before and after the upper transducer upper on the liner was exposed to the second land [1]. Figure 2-18 illustrates the axial positions of both pressure transducers on the liner, and the instantaneous position of different piston regions as a function of crank angle during late compression and early exhaust strokes. The instantaneous positions of the piston regions during the exhaust and intake strokes were identical to the compression and expansion strokes, respectively.

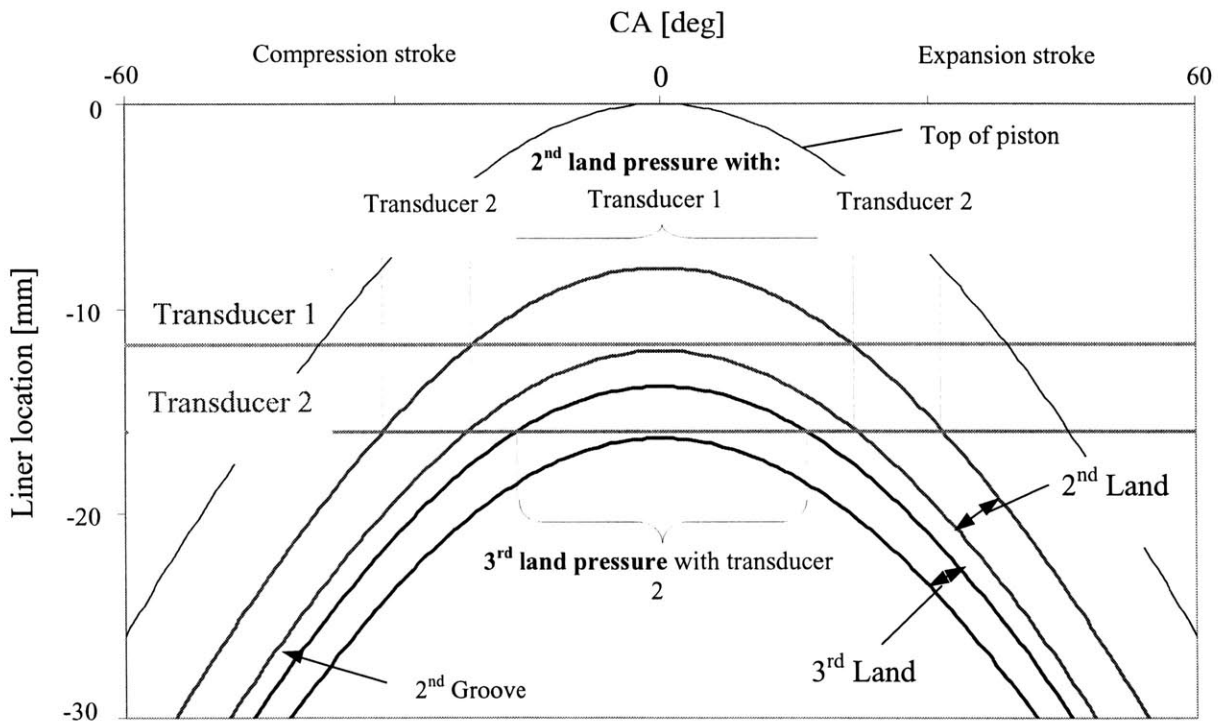


Figure 2-18 Axial locations of the pressure transducers [1]

The transducers were mounted into a housing in order to hold them and seal the cylinder from the engine's coolant leakage [1] as shown in Figure 2-19. On the other hand, the mounting of the pressure transducer could affect the pressure traces by

changing the volume of the cylinder. However, it did not have much effect on the results, since there only was a maximum variation of just about 3% increase in volume.

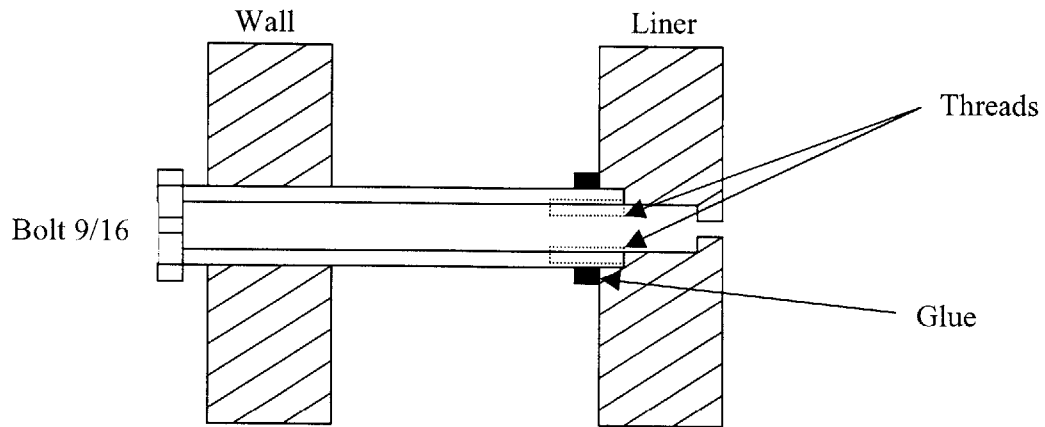


Figure 2-19 Pressure transducer housing assembly

Figure 2-20 shows a sample of the pressure traces averaged over 30 cycles. The 2nd land pressure trace is the combination of the land pressure measured with the lower and the upper pressure transducers, when the 2nd land goes through the two location as shown in Figure 2-18. It is true for the 3rd land pressure trace as well. Figure 2-20 shows the sample of the second and third land pressure measurements with the two liner pressure transducers for the late compression and early expansion strokes at steady state operation for 100% load and 2500 rpm.

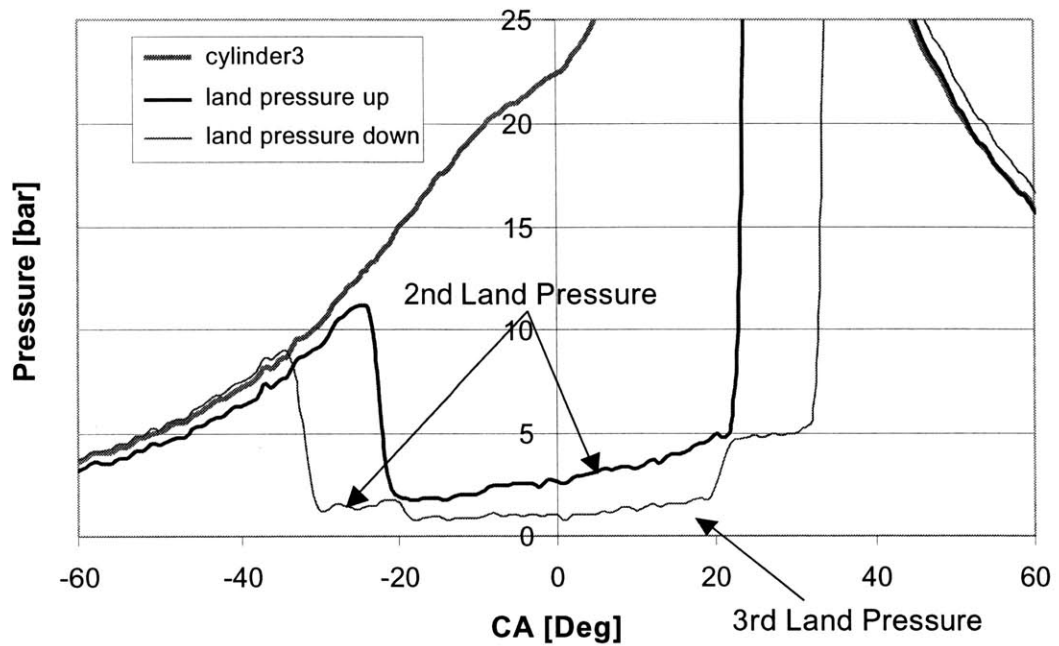


Figure 2-20 Example of the lands pressure trace

2.3.2.3 Liner Temperatures

Cylinder liner temperatures influence the oil evaporation and the oil consumption in consequence. On the other hand, the different temperatures can impact the thermal expansion of the engine components and properties of the oil such as the viscosity. However, the liner temperatures change with engine operating condition and liner location. For example, top liner temperatures are much hotter than the lower one because they are closer to the combustion chamber, having greater heat transfer with the combustion heat. The heat dissipates by the conduction of the engine components, the engine lubricant and the coolant in the engine.

Therefore, the engine liner and block were machined and two fine tip transition joint thermocouples were installed at the liner to measure local temperatures. The ports on the liner were blind holes and the measurements locations were at the top dead center position of the scraper ring and the bottom dead center of the top ring as shown in Figure 2-10 [1].

In order to control the engine's thermal conditions and thus control the evaporation of oil, the coolant temperature was controlled [1]. The engine coolant from an external

coolant tank was circulated through the engine block. To regulate the coolant temperature to the desired temperature, the flow of water city in a heat exchanger was controlled with a valve. Figure 2-21 shows the relationship between the coolant and lower liner temperature.

The plotted figure shows the linear relationship between the lower liner temperature and the coolant outlet temperature that includes all the loads at a given speed. The top liner temperature had greater influence from the combustion temperatures that changed more dramatically with load. Therefore, top liner temperature did not show such a linear relationship of increase thermal loading with the increase in coolant temperature. This relationship was more convenient to compare the different engine conditions, since it showed how the liner increases in temperature with the coolant outlet temperature.

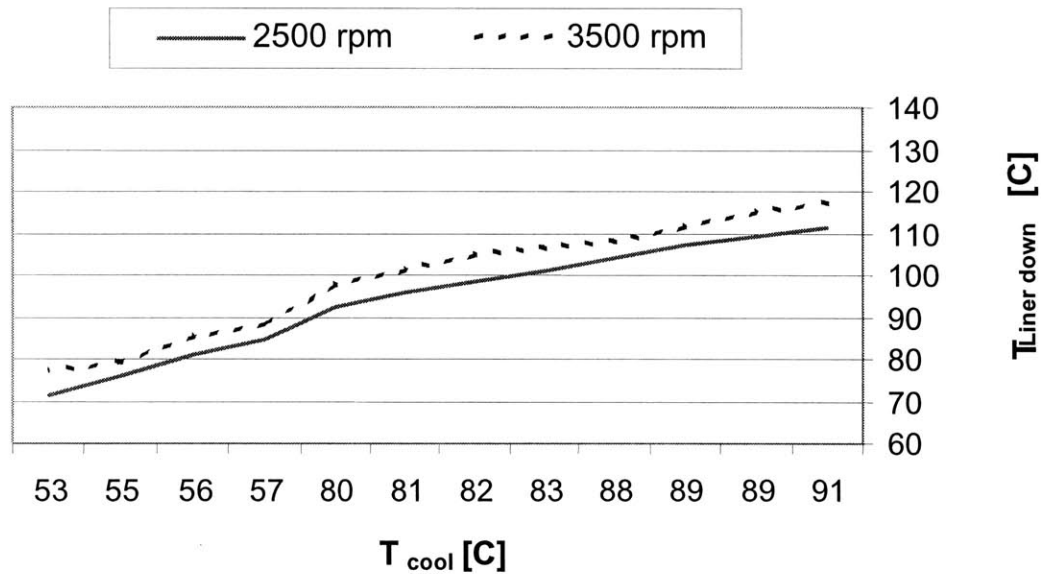


Figure 2-21 Relationship between the coolant and lower liner temperature

2.4 Experimental Conditions

The objective of the study was to investigate the blowby oil consumption and its major oil sources at a wide range of operating conditions, such as speed, load or liner temperature. The tests for the study were run at a range of speeds between 2500 rpm and 4000 rpm. The loads tested ranged between 150 N-m and 37.5 N-m, which are represented in the figures as 100 % and 25 % loads respectively. Although the engine

loads are also related to nominally the throttle position of the intake, the torque was the controlled parameter since there is an intake pressure variation from day to day and season to season. The maximum torque was selected to be 150 N-m because it was just below the engine wide open throttle (WOT) torque curve as shown in Figure 2-22. If the throttle position were controlled, the torque curve would vary, changing the engine conditions, affecting greatly the blowby. The relationship between the load and blowby flow will be further discussed in Chapter 3.

Steady state oil consumption, blowby and in-cylinder variables were measured to obtain information about their response to changing load and speed. The oil consumption and blowby maps were tested for four different loads (150, 112.5, 75 and 37.5 N-m) at four different speeds (2500, 3000, 3500 and 4000 rpm).

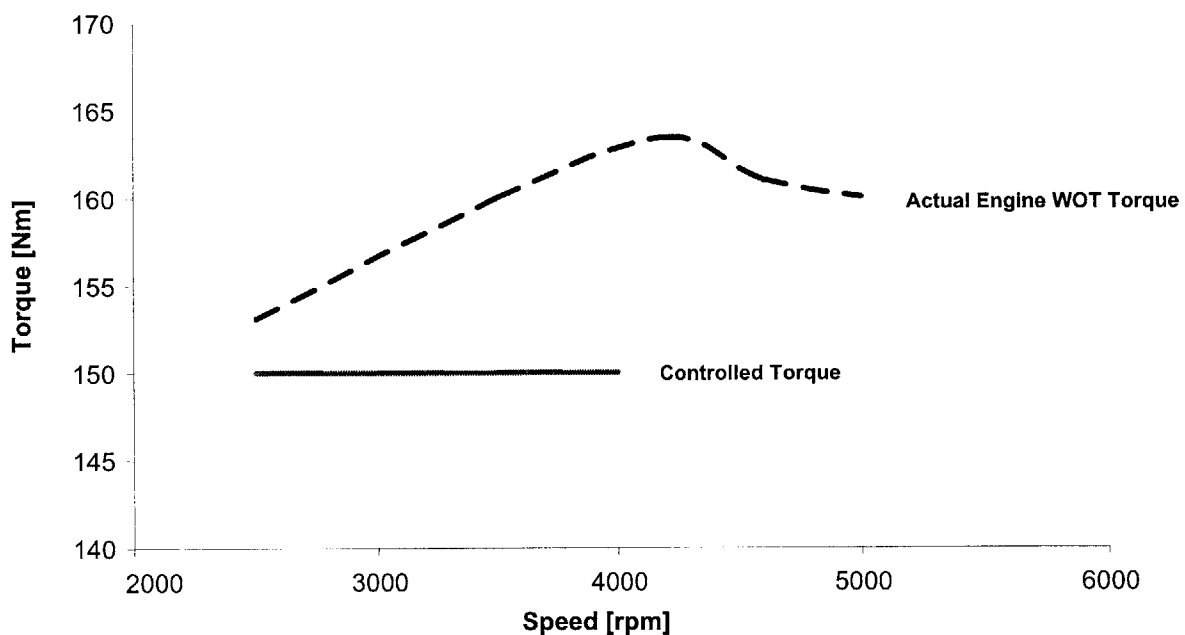


Figure 2-22 Controlled torque and the engine torque at 100% as a function of speed

In cylinder variable were also measured at all the investigated conditions and used for further oil consumption analysis. Figure 2-23 shows the operating conditions of the test engine, along with the test points that were run for different thermal condition than the standard ($T_{coolant} = 81.5 \pm 1.5 \text{ } ^\circ\text{C}$). It has to be noted that the test points that were run at different thermal states also were run at the standard thermal conditions. The figure plots

the torque versus the speed, rather than the intake manifold pressure. It has to be mentioned again that the pressure varies from season to season mainly due to the change in the environment conditions, although it varies less than 1% from day to day.

All the oil consumption diagnostic methods (See Section 2.3.1) have been run for all the test points shown in Figure 2-23, and for both the total and blowby oil consumption measurements.

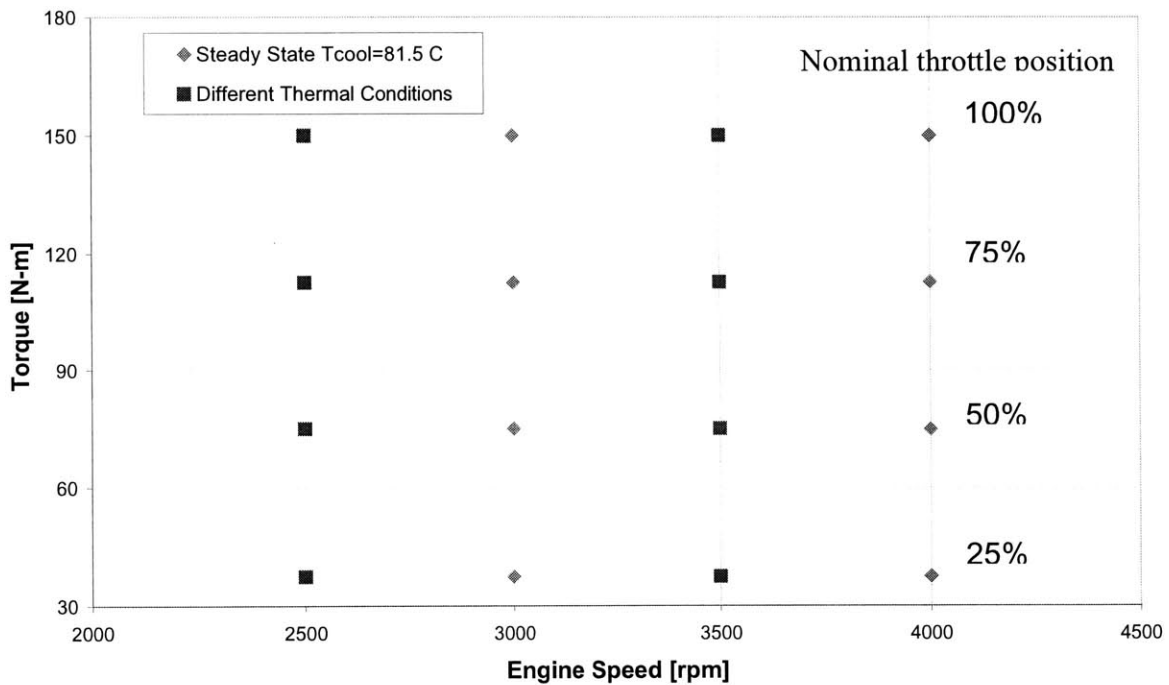


Figure 2-23 Investigated steady state engine-operating conditions

2.4.1 Ring-pack Design

The baseline ring-pack used for the investigation consisted of a rectangular top ring with a barrel faced running surface, a taper faced Napier ring and a U-flex oil control ring, which is divided in about 50 ring segments with gaps between them [1]. Figure 2-24 shows the details of the baseline piston-ring-pack design.

The top ring gap has a gap size of 0.24 mm, which primary function is to seal the combustion chamber. In order to minimize the blowby gas flow, this gap size would need to be the smallest possible (See Appendix C). The second ring dampens the pressure drop across the first ring by sealing the inter-ring pressure increase in the second land

chamfer and delaying the pressure release into the third land chamber. The Napier faced ring, also has the function of scraping the excess oil left in the liner while in the down stroke. The oil control ring function is to control the oil supply to the liner, thus limiting the oil consumption of the engine. They also act as check valve to prevent reverse blowby flow towards the combustion chamber. This function is also carried by the second ring, for which design are purposely done to reduced the reverse flow while simultaneously increasing the down flow.

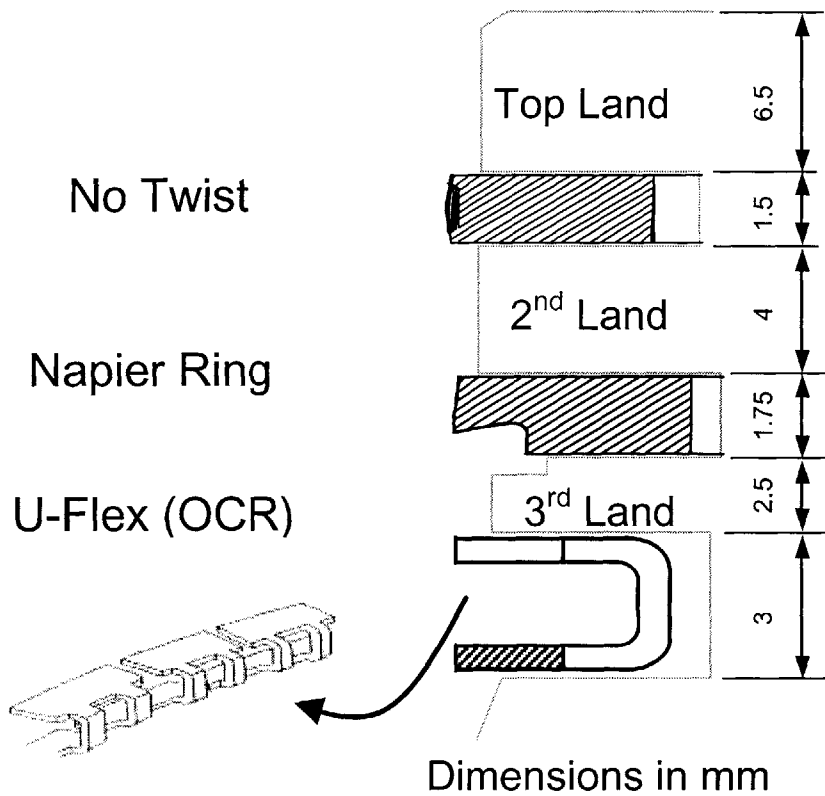


Figure 2-24 Piston and baseline ring-pack geometry

CHAPTER 3: Engine Blowby Oil Consumption and Oil Sources

3.1. PCV System blowby Oil consumption

The Positive Crankcase Ventilation (PCV) system in automotive engines ensures that the harmful gases coming from the combustion chamber and passing through the ring pack do not escape to the environment. These blowby gases entrain oil by particle atomization and evaporation when flowing through the piston ring pack and the crankcase. The blowby gases are composed of the combustion gases, fine oil droplets with some hydrocarbons, water and fugitive dust particles [4][9][16][23]. Since these blowby gases are circulated back to the intake, they represent a mode of oil transport that affects the lube consumption. In addition, it is a source of emissions of hydrocarbons and particulate matter, and of residue buildup that can increase the maintenance cost of critical engine components.

The PCV blowby oil consumption is described as a function of three parameters as shown in Figure 3-1: oil loading, blowby flow, and the separator efficiency. Although the separator is not an integral part of the physical modeling of the blowby flow, it takes a crucial part in the blowby oil consumption. Actual designs already remove a large part of the larger droplets, believed to come from the crankcase.

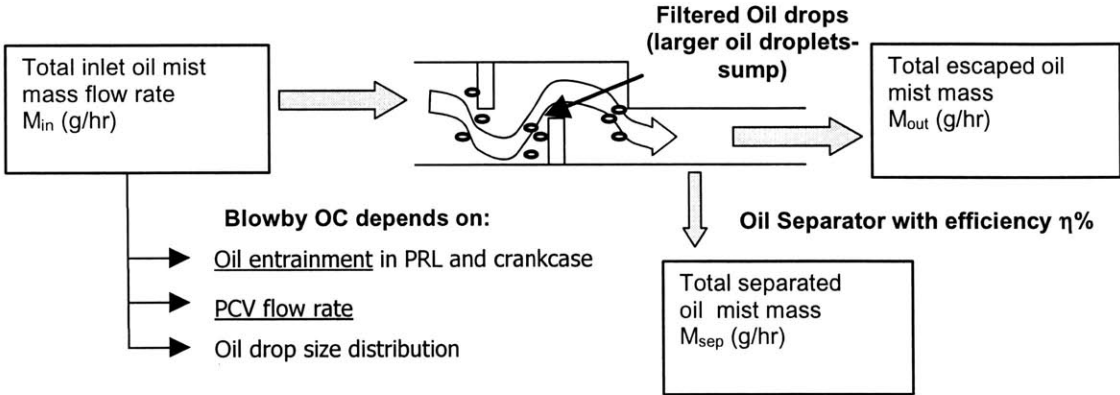


Figure 3-1 Factors on the blowby oil consumption

3.2 Factor Influencing Positive Crankcase Ventilation Blowby Oil Consumption

The oil transport in the piston-ring-liner systems is governed by different driving forces, such as gas flow, ring motion and liner lubrication, which vary with the engine operating conditions. For example, the blowby gas flow increased by a factor of four between the lowest load and full load, due to the variation of the cylinder pressure. The intake pressure increases from about 400 mbar to about 930 mbar for the highest load case, where the throttle is at wide open (WOT). The peak cylinder pressure varies from around 20 bars during the lowest load to about 50 bars at the highest load case. Furthermore, the local pressures in the different regions of the piston-ring pack affect the behavior of the ring dynamics, which affect the gas flow [1]. The gas flow can either flow through the gap or the ring groove if fluttering occurs, which is characterized as vibration of the top ring in the piston groove. This condition that enhances reverse gas flow towards the combustion chamber could occur in the following critical conditions: the inertial force of the ring is pointing towards the crankcase, the cylinder pressure is lower than the second land pressure and the relative of the angle between the top ring and its groove is positive.

In addition, the liner lubrication condition also affects the blowby oil consumption. It is also important to know the oil distribution along the liner, since the oil consumption is limited mainly by the oil accumulation in the second and third lands [1]. The oil distribution along the liner and the flow characteristics through the ring pack controls the atomization and oil entrainment in the blowby flow. In the same manner, the gas flow affects the lubrication, by the gas dragging action that influences the oil film distribution [26]. Figure 3-2 shows the oil film thickness relationship for 3500 rpm between load and speed. When the load is increased, the blowby flow is increased as explained in Section 3.3.3, which drags more oil, thus reducing the oil film thickness. Oil flow to the top land with the reverse gas flow depends on the second land pressure and oil distribution on the second land. PCV blowby oil consumption relative importance is minimized for these cases, since most of the oil transport goes through the combustion chamber.

Engine speed also affects the oil transport characteristics. It affects the interring pressure distribution and thus affects the gas flow between different regions in the piston assembly. Engine speed also increases the inertia of the reciprocating parts in the engine, enhancing mechanical throw off to the combustion chamber. In addition, the PCV blowby is also affected by the speed of the reciprocating movement of the engine components that create high-speed gases in the crankcase. It also influences the splashing of the oil in the sump, creating oil droplets that can be carried by the blowby and high-speed gases in the crankcase if the aerodynamic drag force is greater than inertia of the droplets.

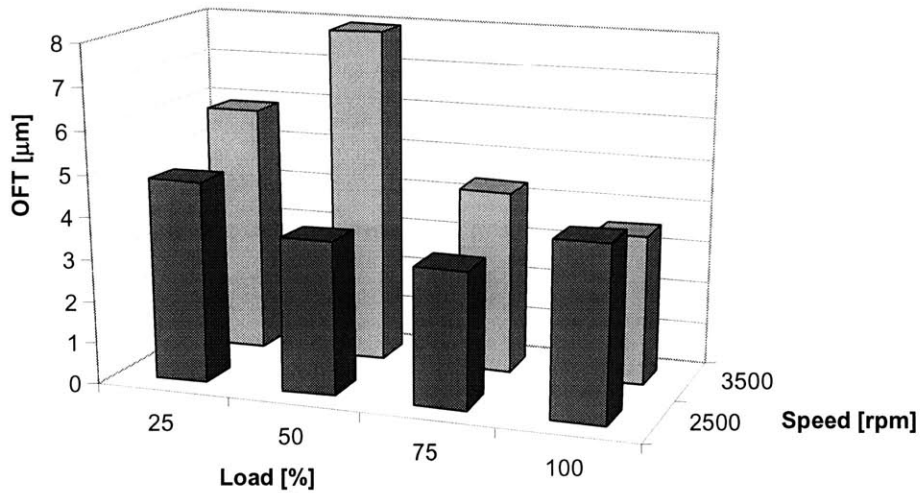


Figure 3-2 Oil film thickness for different loads and speeds

Moreover, operating conditions also influence the thermal loading of the engine components, which affect the oil evaporation, oil viscosity and gas flow paths due to the thermal expansion of the different components. All of these changes in the oil and the component behavior affect the oil transport and oil distribution along the liner.

Therefore, all the oil consumption sources are also expected to change with engine operating condition including the blowby oil consumption. A very detail study of the different oil consumption sources was done previously by Ertan Yilmaz in the Sloan Automotive Lab [1]. However, the blowby oil consumption has not yet been carefully characterized. There is still a lack of understanding of the oil source for the oil

consumption through the PCV system, along with some of the characteristics of the oil entrained in the gas flow.

3.3 PCV Blowby Measurements

Steady state condition measurements were taken for different operating engine conditions. The engine was run at a standard coolant temperature condition ($T_{\text{coolant}} = 81.5 \pm 1.5 \text{ }^\circ\text{C}$). The results are discussed more in detail in the following section

3.3.1 Steady State Blowby Oil Consumption

The steady state PCV blowby oil consumption measurements were made first to gain information about the oil consumption pattern with changing speed and load. The conditions for which the blowby oil consumption was measured are shown in Section 2.4 of the thesis. The baseline oil consumption map versus speed and load is shown in Figure 3-4. The map shows the trend for PCV blowby oil consumption for a maximum oil sump level and standard thermal operating conditions for an outlet coolant temperature of $81.5 \pm 1.5 \text{ }^\circ\text{C}$. The oil consumption is presented in per cycle basis, which can compare the oil consumption results for any speed. This representation implies that there is less time for oil transport as the speed increases. Because of this, although the consumption for 4000 rpm is lower in per cycle basis, it is higher for an absolute unit such as g/h as shown in Figure 3-5, since there are more cycles per time for the higher speeds.

The blowby consumption map showed some important characteristics and patterns. For instance, the measurements showed a strong dependence with load. The increase in load increased the pressure differential between the combustion chamber and the crankcase leading to an increased blowby flow through the ring-pack and the PCV system. Besides the flow velocity increase, the higher speed gases promoted oil film atomization into small size oil particles [7]. Previous results from Ertan Yilmaz showed this relationship as shown in Figure 3-3. There was also an increase in the liner and oil temperature with load that increased oil evaporation.

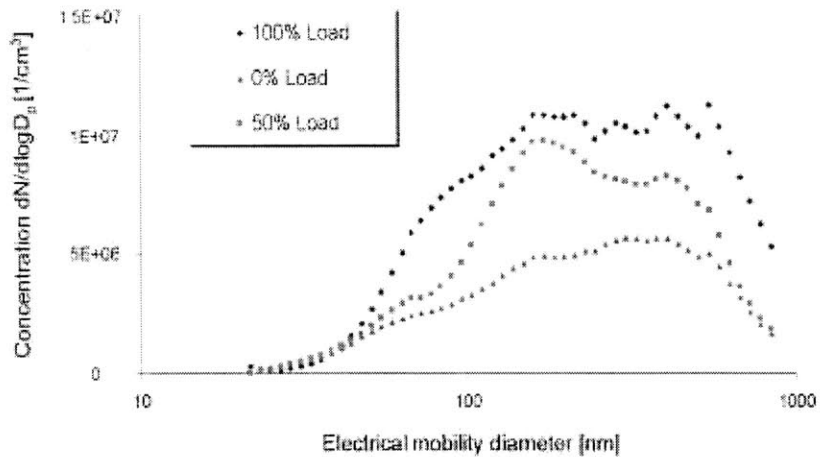


Figure 3-3 Load effect on particle size distribution in the blowby flow at 2500 rpm [1]

On the other hand, there was a strong dependence in blowby oil consumption with speed. Increasing the engine's moving parts speed increased the high-speed gas velocities on the crankcase. Furthermore, there was an effect in the oil droplet size formation with speed, which affected the separation efficiency of the separator [5][7][22], which is further discussed in chapter 4.1.1. Besides, the increase in the stirring of the oil by the engine moving parts enhanced the oil entrainment in the PCV blowby flow. Furthermore, there was also a boost in the thermal loading of the engine, which increased the evaporation and thus the oil loading of the flow.

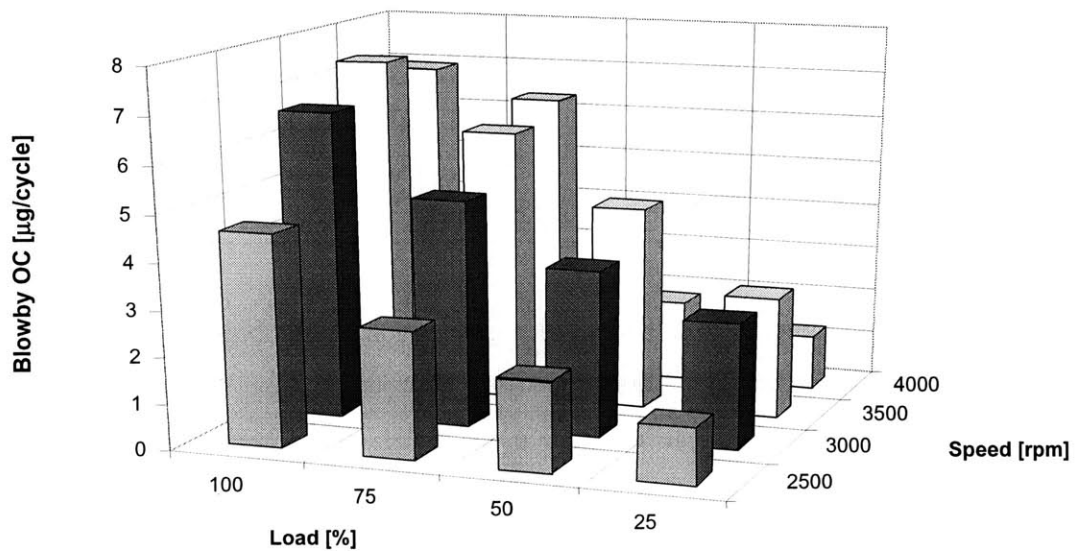


Figure 3-4 PCV blowby oil consumption map

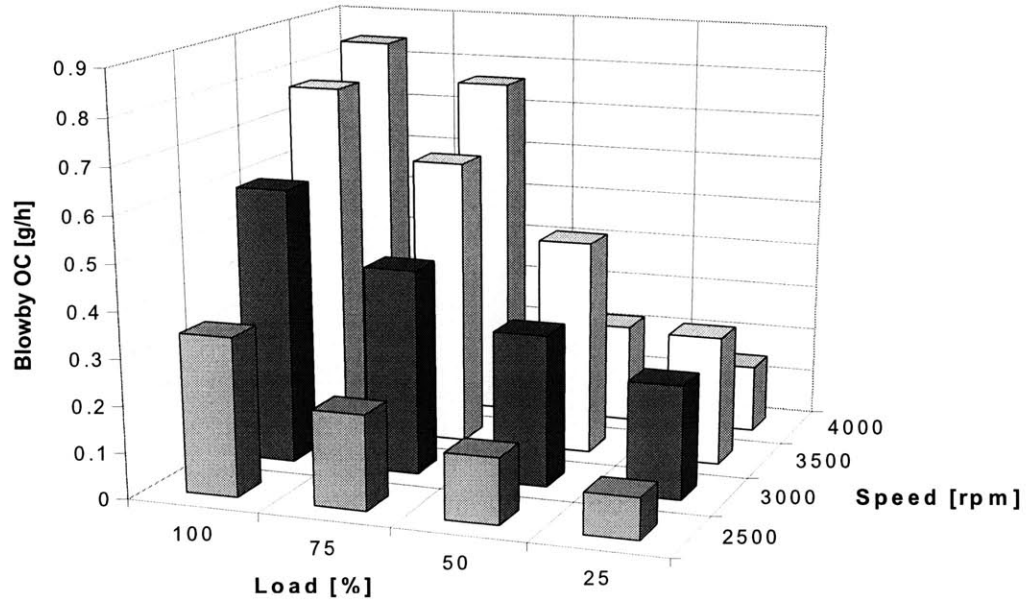


Figure 3-5 PCV blowby oil consumption map in grams per hour

3.3.1.1 Different Diagnostic Measurement Result Comparison

As discussed in Section 2.3 of the thesis, several methods were used to take the measurements of the blowby oil consumption. Figure 3-4 shows the results for oil consumption with the direct method, and the other two methods that showed very similar results. This method was chosen to display the results, because it proved to be the most reliable and the easier to use of the three.

First, the gravimetric method did not collect the oil-evaporated form. Although some condensation could happen while sampling, the blowby gas temperature was already at room temperature ($T_{\text{ambient}} \approx 30^{\circ}\text{C}$) and little condensation was expected. Second, as discussed in Section 2.3.1.3.1 the difference method run between two different engine-operating conditions, which influenced the results for the highest load case especially, giving larger contribution to blowby oil consumption than obtained with the direct method [1][5]. Figure 3-6 shows the comparison between the three different methods for 3500 rpm and different loads. It has to be noted that for the lowest load, the difference method poor resolution gave us a negative contribution of the PCV blowby oil consumption. It is very hard to read the difference between the large oil consumption numbers obtained at the two different engine configurations. However, results trend seem to be similar and about of the same order of magnitude.

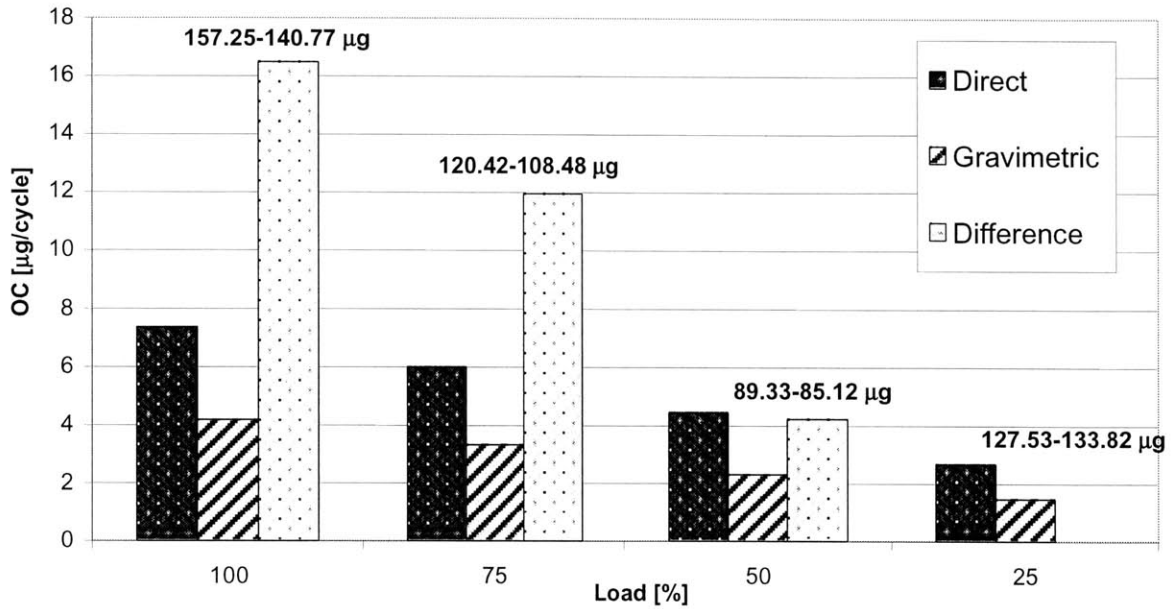


Figure 3-6 Comparison between the three diagnostic methods

3.3.2 Steady State Total Oil Consumption

In addition, total steady state oil consumption measurements were taken to gain information about the total oil consumption pattern and the relative contribution of the PCV blowby oil consumption. These measurements also were taken in previous studies [1][2][3][4][5][8], which showed about the same results obtained in this investigation. Figure 3-7 clearly shows the load and speed dependence in the total oil consumption, which is typical for internal combustion engines as stated in Section 3.2.

Oil consumption became more significant at high speed and loads. However, there was an exception to the general trend at 3500 and 4000 rpm, where the oil consumption increased as the load was decreased from 50% to 25 % for both speeds. The different mechanism of oil transport and relative contribution were studied in great detail in previous studies [1]

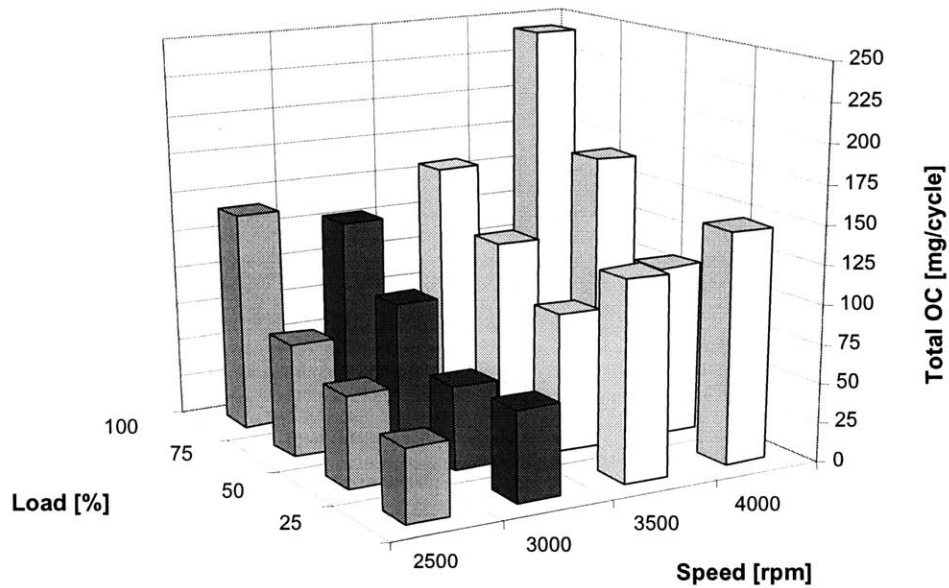


Figure 3-7 Total steady state consumption

3.3.3 Blowby

Engine operation conditions changes the blowby flow magnitude and possible flow paths through the ring-pack. Thus blowby is strongly dependent in the leakage paths. If there are no major instabilities in the rings, then the blowby flow is structured as follows. As the cylinder pressure raise during the compression stroke and combustion, the gases in the combustion chamber are believed to leak to the second land through the top ring gap. On the second land, the gases are believed to flow circumferentially going from the top ring gap to second ring gap [1][20][21]. As the pressure increases due to the finite volume in the second land, a pressure gradient evolves between the second and third lands. This way gases flow to the third land through the second ring gap. On the third land and with a U-flex oil control ring, blowby gases mainly flow in the axial direction. This is assumed because the U-flex oil control ring may assume a wavy shape after installation, which results in additional gaps between the ring and groove surfaces. Nevertheless, it is also important to know that during the intake stroke, late expansion and exhaust strokes blowby gases may flow back from the second land to the cylinder, due to negative pressure gradient between the combustion chamber and second land.

The speed of the leakage of the gases mainly depends in the cylinder pressures and interring pressures of the lands. The pressure directly influences the flow magnitude. Figure 3-8 shows the cylinder pressures of the different piston lands at 3500 rpm. The increase in cylinder pressure induces the increase in blowby flow as shown in Figure 3-10. The increase pressure forced the blowby gases to leak through the different piston lands at much higher rates.

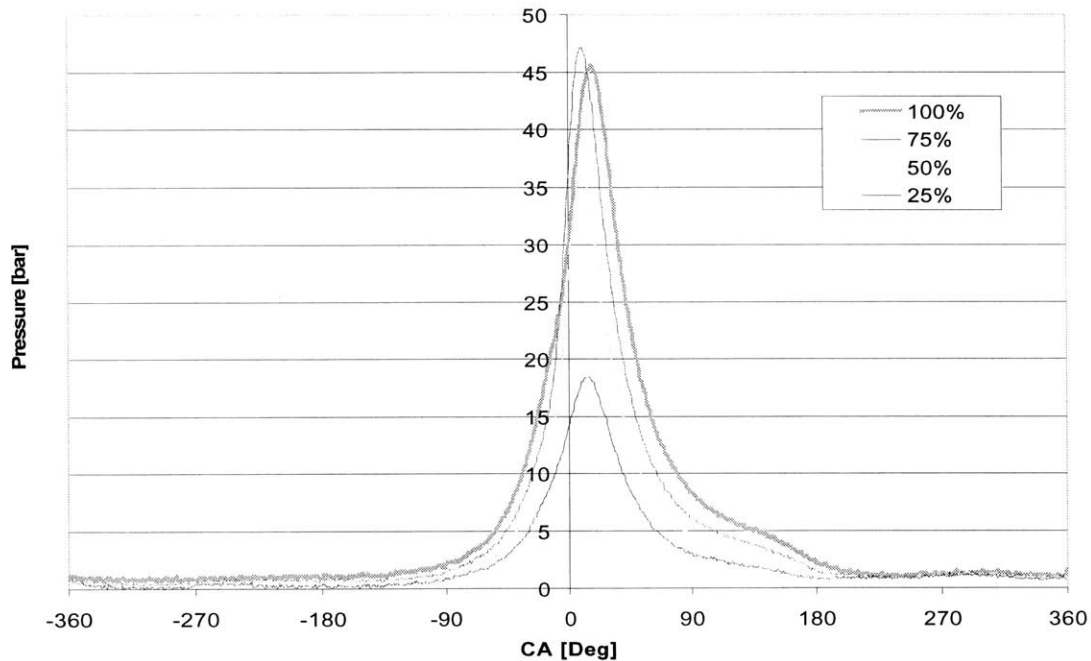


Figure 3-8 Cylinder pressure traces for 3500 rpm and different loads

Even though the pressure was quite similar for the highest load cases, the 100 and 75% cases, the difference between them was that the highest load case pressure increase before in the stroke (earlier crank angle degree). Thus, this difference reconciled that more of the gases at the 100% case will flow through the piston lands. The pressure for 75% case rose more suddenly and would not drive that much flow through the power cylinder, hence having a lower magnitude blowby.

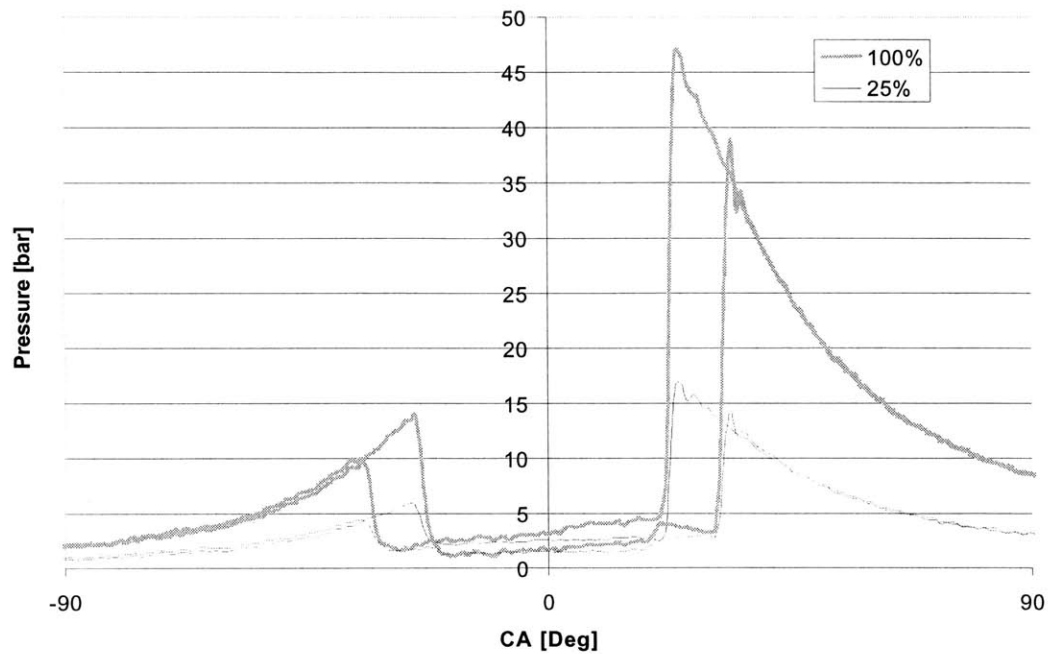


Figure 3-9 Interring pressure traces for 3500 rpm and two different loads

The interring pressure for the different piston lands also displayed differences with load as shown in Figure 3-9. The increase in pressure for the highest load, forced more gases through the first ring gap, thus increasing the second land pressure due to the finite volume. Even though the second land dampened the pressure drop with the third land, there was also a slight increase in the third land pressure. All of these pressure increases are proportionally related to the increase in the blowby flow through the different lands. Since the crankcase pressure did not change that much due to the engine ventilation system, the pressure differential between the combustion chamber and the crankcase increased, leading to the blowby flow increase.

Figure 3-10 shows the blowby flow in liters per minute for different speeds and loads. This representation showed a strong dependence in load, although it almost remained constant for increase engine speed. The increase in cylinder pressure created a greater pressure gradient between the combustion chamber and crankcase as stated above, which enhances the blowby gas flow through the ring pack.

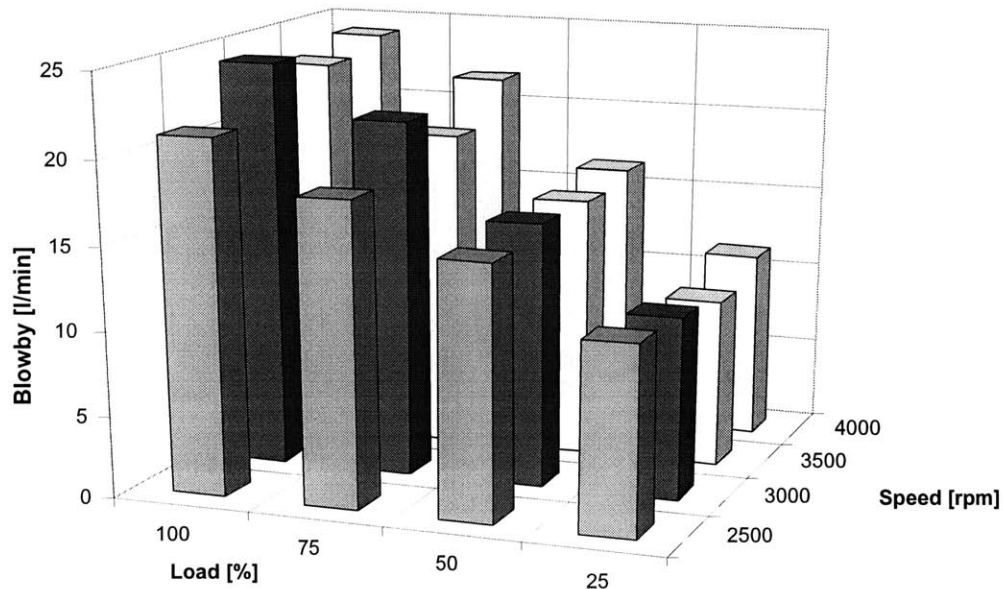


Figure 3-10 PCV blowby flow map

Since all the driving forces that are believed to control oil transport within the piston ring-pack, including the blowby gas flow, repeat periodically every cycle and thus should scale with speed. In order to evaluate the impact of the blowby gas flow in the oil transport, the blowby flow per cycle basis was calculated and shown in Figure 3-11. The results also showed a clear dependence with load. On the contrary, there was a clear dependence with speed at a constant load. This trend is explained as follows. As the engine speed increases, blowby gases have less available time to flow through the land and past the PCV system in one cycle. Therefore the amount of gases leaking through the ring-pack and the blowby through the PCV system each cycle consequently decreases with engine speed.

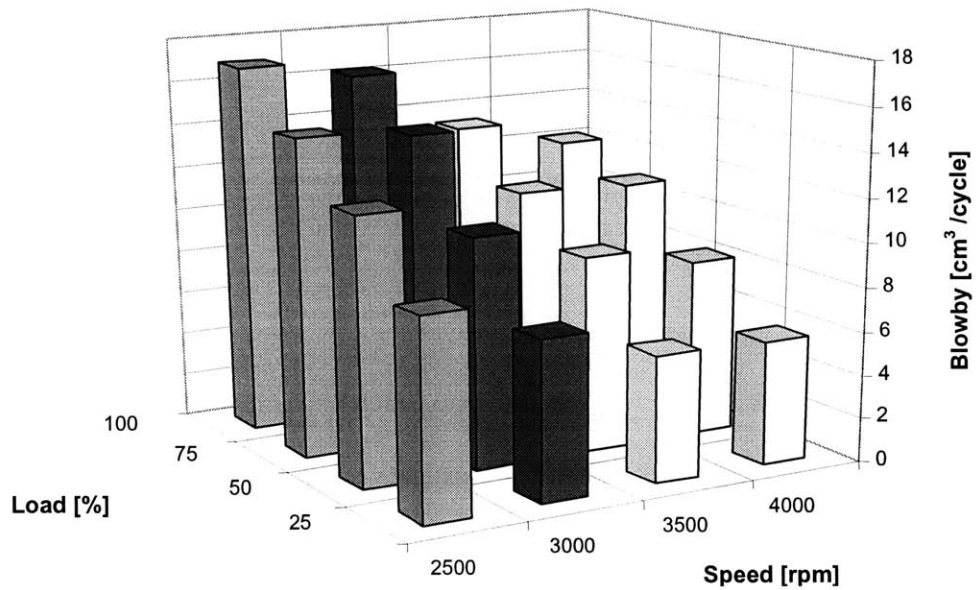


Figure 3-11 Blowby flow map in per cycle basis

3.3.4 Oil Loading in Blowby Gas Flow

Of great interest for the blowby oil consumption is the oil loading of the flow, defined as the mass amount of oil per volume in the flow. The oil loading gives important information about the oil carried in the blowby, and can let us identify the conditions for which the flow absorbs more oil, in either vapor or liquid form. Nevertheless, the result obtained does not reflect the oil already separated in the engine separator. This analysis sets up the basis of comparison between the oil entrained in the crankcase and ring-pack, which is discussed further in Section 3.4.2.

Figure 3-12 illustrates the result for oil loading at the standard thermal conditions and high oil level. The results showed the dependence of the blowby oil content for different loads and speeds. It was clear that the oil loading increases with engine speed, although the increase with load was less abrupt. Even at 3000 rpm the trend was not that clear. As described before, the amount in the blowby depends on the oil entrainment in the ring-pack and crankcase, and on the oil separator performance. The higher component temperatures are likely to increase evaporation, and the higher flow velocities increase the oil film atomization. The higher gas flow driven in the crankcase and the fast moving parts also may enhance the droplet breakup processes in the crankcase as stated in 3.3.1.

Nevertheless, oil loading varied from condition to condition depending on the dominating driving mechanism. Its minimization would lead to much lower oil consumptions through the PCV system.

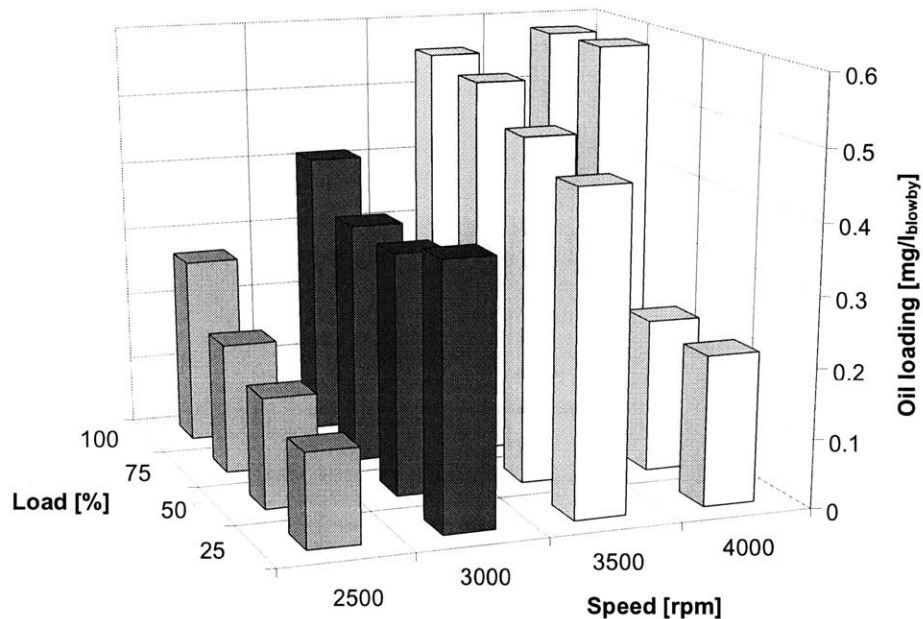


Figure 3-12 PCV blowby oil loading for different engine operating conditions

3.3.5 Blowby Oil Consumption Relative Contribution

In addition to the PCV blowby oil consumption measurements, the total engine oil consumption was also measured from the exhaust. The exhaust sampling measures all the type of oil transport modes that occur in the engine at the same time. This way, the relative contribution of PCV blowby to total oil consumption can be obtained as shown in Figure 3-13.

This map was obtained by the experimental measurements taken from the PCV line with the direct diagnostic method. For the highest load conditions this figure was larger with the differential method [1][4][8] (See section 3.1.1.). However, the relative contribution obtained with the direct sampling method was comparable to other results in literature [1][4][8][9] for other than the 100 % load.

The relative contribution varied with the speed and load since other oil transport modes (evaporation, inertia, and reverse blowby) became more important at different

operating thermal conditions, loads and speeds [1]. However, an increasing trend was quite consistent for all the speeds when increasing the load from 25 to 50% and from 50 to 75%, mainly due to the higher blowby flow rates. Therefore, blowby oil consumption contribution obtained from the experiments was around 2-7% at the investigated conditions.

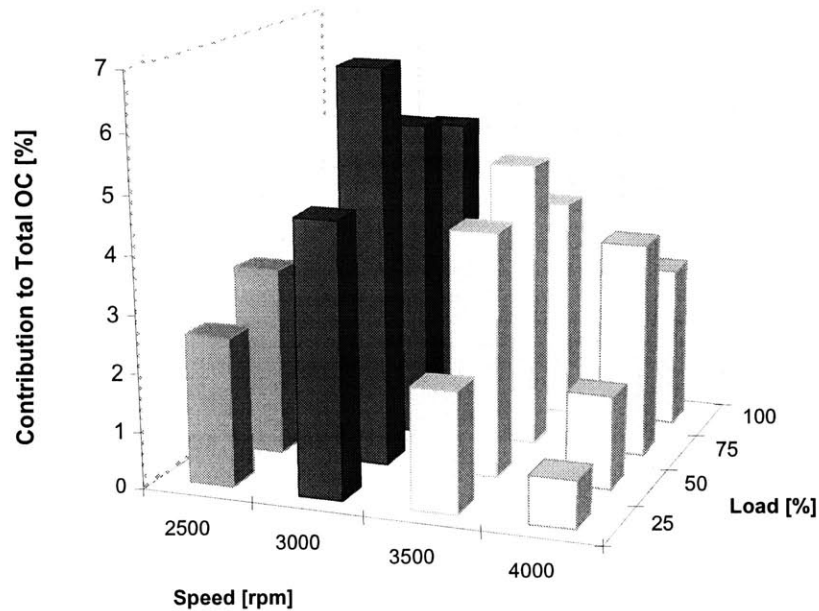


Figure 3-13 PCV blowby Oil Consumption relative contribution map

3.4 PCV System blowby Oil sources

Most of the oil consumed in the spark ignition engines comes from the power cylinder. The PCV blowby is one of the mechanisms for oil transport in the power cylinder and contributes to oil consumption. The oil can be absorbed either by the atomization of few micrometers or through evaporation of the low boiling lubricant oil species under the effect of high gas temperatures in the power cylinder. However, some of the oil evaporated in the power cylinder can be condensed due to the relatively lower temperature of the crankcase. Oil can also be entrained in the crankcase either by atomization of the oil droplets stirred by the moving parts and entrained in the high velocity gases, and through evaporation of the low boiling oil species under high gas temperatures [1][2]. Thus there are two main sources of oil entrainment in the blowby

gas flow: the power cylinder and the crankcase. As the automotive industry struggles to reduce the contribution of the power cylinder in total and blowby oil consumption, it is important to quantify the amount that comes from each source.

3.4.1 Oil Source Investigation Approach

The blowby gases that flow through the ring pack reach the crankcase and interact with the oil in it. The moving engine parts and the high-speed gas temperature promote oil entrainment. As the oil level in the crankcase is lower, it is believed that most of the oil entrained from the sump can be isolated in the blowby flow that goes through the PCV system.

The production engine needs to be run inside an upper and a lower oil level limit in order to ensure safe lubrication conditions. The engine used a pressurized and oil splash lubrication system and due to safety reasons it was decided to run between the limits stated before. The engine was run at these two limits as well as in an intermediate one as shown in Table 3-1, in order to quantify the power cylinder oil contribution. The expectation was that the oil consumption from the PCV blowby would be reduced. Also, it has to be noted that the experiments were run with the stock separator for the production engine [4][7][14]. The separator removes most of the larger particles and that are believed to come from the crankcase [8][14] (See Section 4.1). Therefore most of the contribution from the sump was already minimize for this experimental engine.

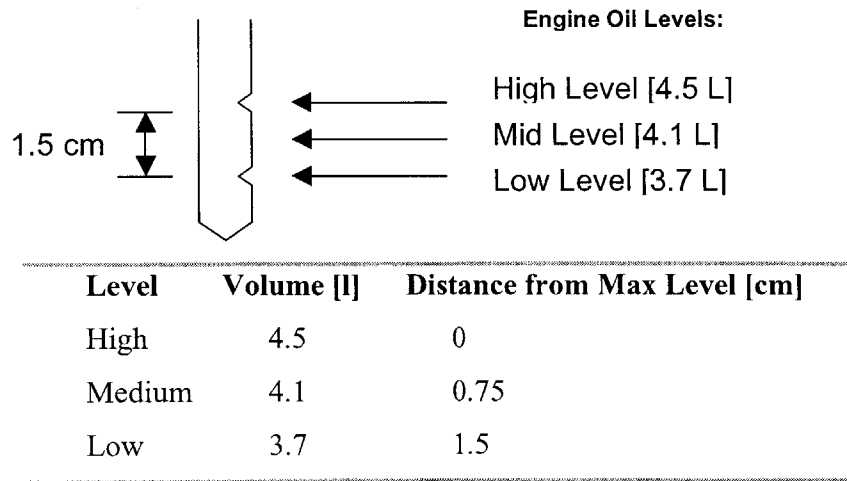


Table 3-1 Sump oil level characteristics and oil stick schematic

The engine was run for the same conditions as for the steady state oil consumption map showed in Section 3.3.1 for comparison of the results. An issue to take into account is that even though the engine oil sump is lowered, the engine lubrication needs to be the same so that engine oil transport methods do not change. Since the engine blowby gas flow through the ring-pack affects the oil distribution in the engine, which in turn also affects the other oil consumption mechanism, LIF oil film thickness experiments were carried to check the oil distribution in the piston land.

3.4.2 Oil Source Measurements

The engine was run for different oil levels and different engine conditions, to obtain information about the trends of oil consumption with the oil level. Figure 3-14 shows the oil consumption for 3500 rpm as a function of oil level and load. There was a strong relationship between the engine oil level and the PCV blowby oil consumption. This reduction is believed to come from the isolation of the oil entrainment in the engine crankcase. The interaction between the crankshaft and the oil in the sump was believed to minimize, as there was less splashing between the moving parts and the oil in the sump. Therefore, the oil level was the limiting factor in the oil entrainment in the blowby gas flow through the crankcase.

The effect of load in blowby oil consumption was reduced to the point, where the increase in load did not increase the oil consumption. The increase of the load increased the thermal loading in the liner, leading to higher oil evaporation. Moreover, the blowby flow increased with the load, usually showing larger oil consumption due to enhanced atomization such as in the high level operation. Nevertheless, there was a strong correlation between the oil level and the PCV blowby consumption that leads one to believe that a large portion of the oil comes from the sump. In addition, high velocity gases created by the reciprocating movement of the engine part might not entrain as much as oil as in the high level oil due to the lower amount of oil in the sump.

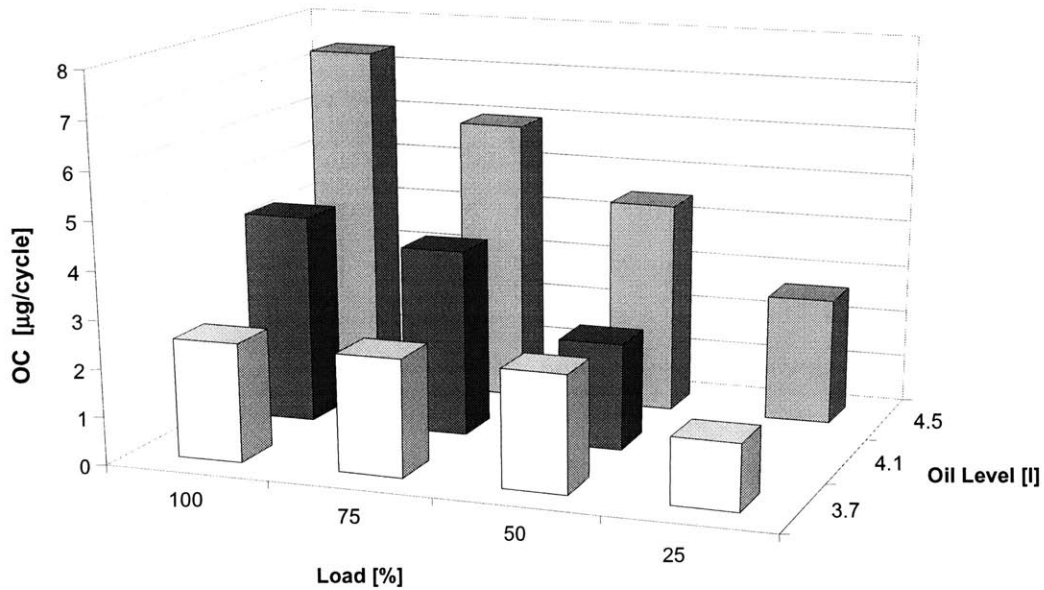


Figure 3-14 PCV blowby consumption at 3500 rpm as a function of oil level and load

Modern automotive engine have oil separator in the PCV system that remove most of the larger oil droplets. These oil droplets are believed to come from the oil crankcase. Smaller droplets come from the power cylinder, where the high-speed gases that flow between the small gaps in the rings and groove promote the atomization of the oil film. Even though most of the impact from the crankcase is isolated with the separators, experiments have shown that there is still a relatively important source of oil that comes from the sump.

Figure 3-14 shows how the oil consumption at 3500 rpm and low oil level reached an oil consumption limit of about 2 µg/cycle. This amount was believed to come from the power cylinder, and seemed to remain constant with the increase load. For the lower oil level, at the higher liner temperature, the blowby flow did not entrain much more oil limiting the oil consumption. Oil was also condensed and separated from the flow in the crankcase because of the relatively lower temperatures.

The percentage difference in oil consumption between the high oil level and low level for all the investigated conditions ranged between 50-70%. This great reduction in blowby oil consumption came from the lowering of the oil level in the crankcase. It suggested that half or less than half of the oil consumption in the PCV system came from the power cylinder in the spark ignition engine.

The entrainment of oil from the crankcase was believed to increase with speed, as the moving parts in the crankcase stirred the oil in the sump more violently. For the high oil level operation this was true as shown in Figure 3-15 for the 100% load case, for which the blowby oil consumption was greater. As the oil level was decreased, this phenomenon tended to vanish, having almost no increase with speed. This time, the oil consumption is presented in grams per hour basis, a standard more commonly used in industry. This representation is an absolute representation of the speed and load effects on oil consumption, and does not give information about the oil consumption every cycle as in the other results. Nevertheless, the calculation to get the result in per cycle basis was carried and a very similar trend to the one presented was found.

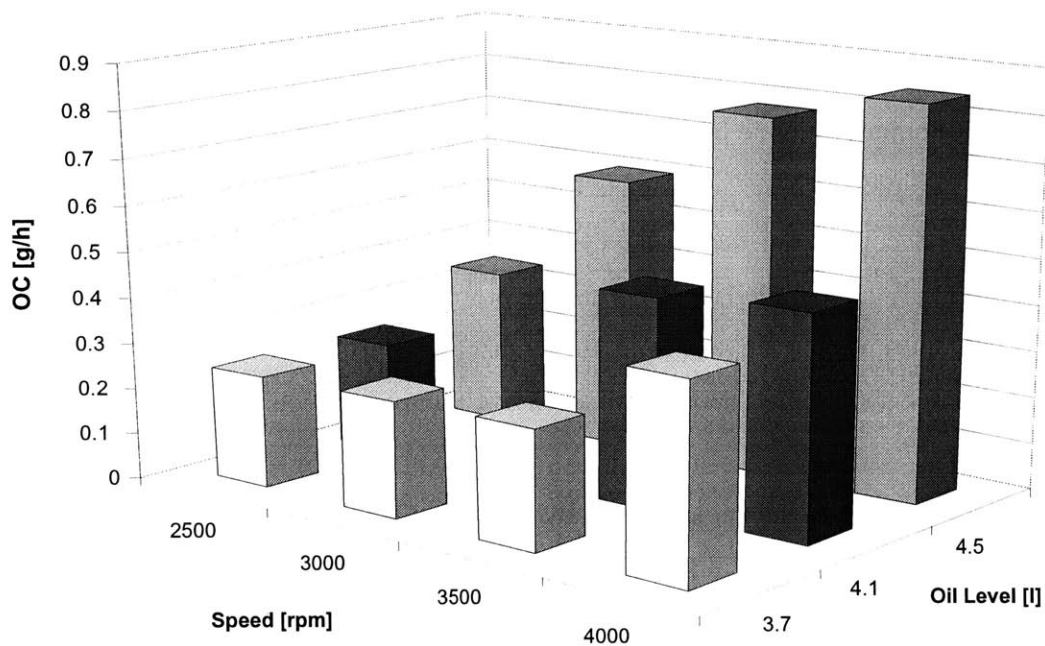


Figure 3-15 PCV blowby consumption at 100% load as a function of oil level and engine speed

Oil consumption again had been decreased due to the isolation of most of the oil entrain in the engine crankcase. There was less oil stirring as the oil level decreases, thus lowering the oil entrainment in the crankcase. The effect of increase liner temperature did not have a great effect on the low-level oil case either, suggesting that the oil evaporation limits the oil entrainment. Again, the increase in temperature did not entrain more oil to the flow, since the blowby flow almost did not change with speed. These results

suggested that a lot of the oil entrainment came from the interaction of the moving components in the oil sump.

3.4.2.1 Ring-pack Oil Entrainment

The blowby gases that flow through the ring-pack influence the oil distribution in the piston lands. As these blowby gases flow through the ring-pack, they entrain oil in the liquid and vapor form by different driving forces: oil evaporation and oil atomization into micron size particles by locally high-speed velocity gases. The engine operating condition affects these driving forces, changing the oil entrainment into the blowby gas flow. For high loads, as the engine thermal loading and the blowby flow increases, these two oil entrainment mechanisms are enhanced. However, as shown in Figure 3-16, the oil loading for 3500 rpm did not increase with load for the lower oil levels. This phenomenon was true for all the speeds investigated. Assuming that most of the oil entrained in the crankcase was minimized, it looks like the oil entrainment was limited by the oil evaporation rate, which is a function of the distillation curve and not by the oil mass transfer by the atomization of the oil film, since the blowby flow did not increase the oil consumption.

On the contrary, the increase in speed did not either increase the oil loading for the highest load cases, although the engine thermal loading was increased. Figure 3-17 shows the oil entrainment for 100% and different speeds, and did not show an increase in oil loading but for 4000 rpm. This high-speed engine extreme thermal condition had evaporated an extra amount of oil. Thus, the oil entrainment in the blowby gas flow through the ring pack was mostly limited by the evaporation rate of the oil, although it also entrained oil through the atomization of the oil film as stated in Section 3.3.1.

It also has to be noted, that some of the oil that was evaporated in the power cylinder could condensate while flowing through the crankcase due to the relatively lower temperatures. More detail discussion follows in the next section.

3.4.2.2 Crankcase Oil Entrainment

The blowby gases that have flown through the ring-pack and the high-speed gases driven by the movement of the engine components in the crankcase also entrain a large portion of the oil in the flow while they are in the sump. In the crankcase, moving engine parts with significant velocities and the alternating motion of the piston may generate high-local velocities. Here the splashing of the oil by the moving parts, the leak of oil from the bearings and the spray cooling jet of the piston could entrain additional oil. The spray jet cooling is employed to reduce the high piston temperatures and to supply additional lubrication to the highly loaded major thrust side of the cylinder liner [1]. The oil is being sprayed from a nozzle at the big end of the connecting rod towards the inner side of the piston. Airborne oil in the crankcase from sources described above can reach significant velocities relative to the moving engine parts. The interaction between the airborne oil and the high-speed gases promote oil droplet breakup, forming smaller oil droplets due to the augmentation surface tension. Furthermore, collision of the oil particles with the engine moving components may also generate smaller size particles. These smaller particles are likely to be entrained in the blowby flow, since the aerodynamic drag force is larger relative to the inertia force of the particles.

Figure 3-16 shows that as the engine loading increased for 3500 rpm the oil entrainment also augmented for the high oil level. The higher velocity blowby gases, entrained more of the oil particles in the crankcase due to higher aerodynamic drag force as discussed above. For this case, it also can be noticed that as the oil level was minimized the interaction of the moving parts with the oil was minimized.

On the other hand, it is clearly shown in Figure 3-17 a strong correlation in the oil loading with speed for the high oil level. As predicted in Ertan Yilmaz study, the increase in speed increases the oil entrainment in the blowby flow that goes through the PCV system [1]. The speed enhanced the oil droplet breakup and consequent entrainment in the gas flow. This effect was minimized as the oil level is decreased, almost not having an effect for the lowest possible oil level, where the oil and moving component interaction was minimized. This was true for all the engine speed investigated. In

addition, at high engine speed, surface waves in the oil sump could be generated in the air-oil interface inducing additional oil entrainment, such as at 4000 rpm.

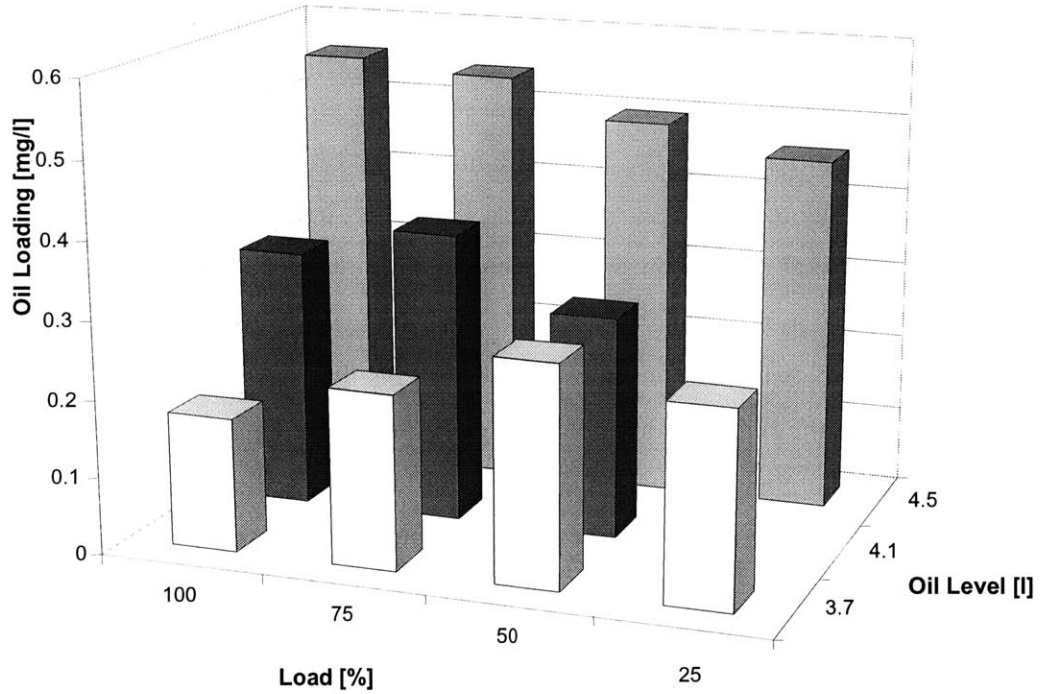


Figure 3-16 PCV blowby oil loading at 3500 rpm as a function of oil level and load

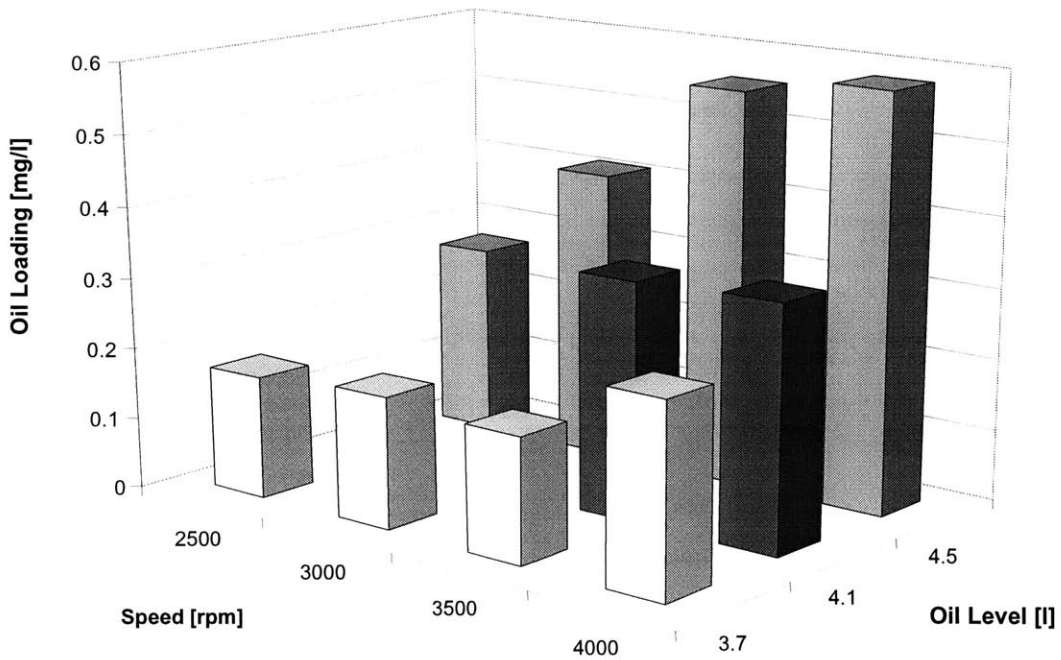


Figure 3-17 PCV blowby oil loading at 100% load as a function of oil level and speed

3.4.3 Lubrication Condition in Interring Pack for Different Oil Levels

Although results have shown that an important fraction of the oil entrained in the blowby flow comes from the crankcase, it also has to be checked that the different oil levels do not affect the engine lubrication condition. Even though the oil level had influenced the contribution of the crankcase in the blowby flow through the PCV, it did not really affect the total oil consumption as shown in Figure 3-18. For the 100% load case shown, the total oil consumption remained about the same for the different speeds apart from normal run-to-run variability in the engine oil consumption and the small difference in the blowby oil consumption. This means that the lubricating condition and oil distribution in the ring pack are not greatly affected to the extent of the changes in the blowby oil consumption by the oil level, not affecting the dominating oil transports (inertia and evaporation) present in the power cylinder. The total oil consumption also did not change much for the different load conditions at a constant speed either.

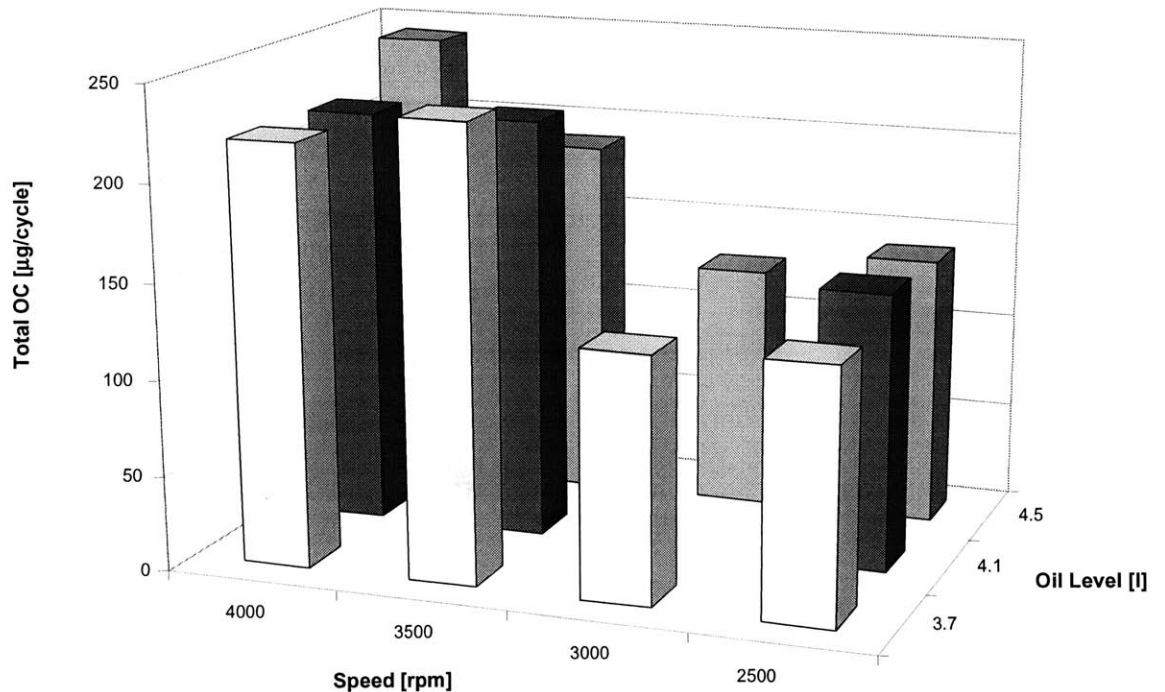


Figure 3-18 Total oil consumption for 100% load as a function of oil level and engine speed

Nevertheless, the Laser Induced Fluorescence (LIF) measurements were also carried as a check that the lubrication distribution in the liner was about the same. The oil supply rates along the piston-ring-liner system to the top land are likely to remain unchanged for all oil levels, which was also supported by the LIF measurements of the piston lands as shown in Figure 3-19.

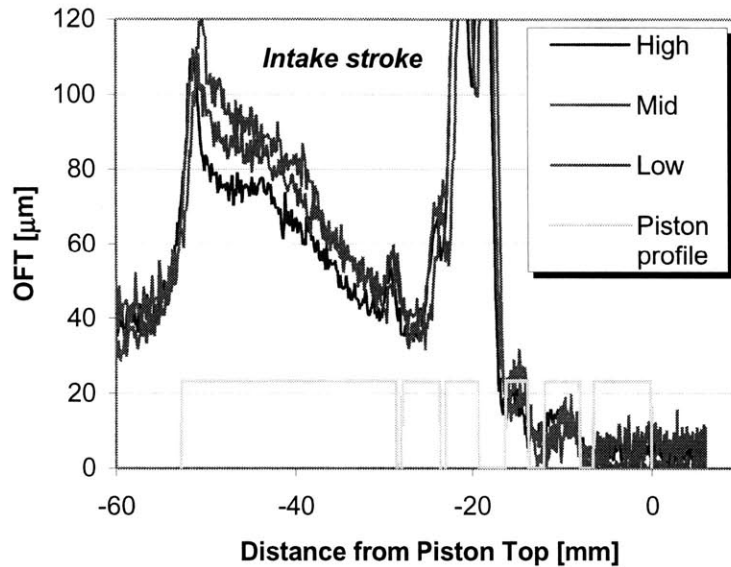


Figure 3-19 Oil Film Thickness (OFT) distribution at different oil levels for 3500 rpm and 75% Load

Average oil film thickness was also calculated to see the trends of oil film thickness with the oil level in the crankcase. The average oil film on each piston land was quantified by integrating the oil film thickness trace along each land, dividing this oil volume by the corresponding land's length for each stroke, and averaging the obtained value for the oil film on each land over all engine strokes.

Figure 3-20 and 3-21 shows the average oil film thickness for the top crown and second lands for 2500 rpm. The results showed that the oil film thickness varies with condition and oil level for both the top and second lands. Nevertheless, the difference was small to the extent it affected the blowby oil consumption, not the total oil consumption when changing the oil level not affecting the oil distribution and the consequent oil entrainment much. One thing to note is that the oil film thickness for the load of 75% and oil levels of 3.7 and 4.1 liters showed quite different results. However, there can be

seen how the lower oil film in the top crown has been removed to the second land. Thus, they represent a similar lubrication condition. The difference comes from the time when the data is acquired, which affects the results as stated in Section 2.3.2.1.

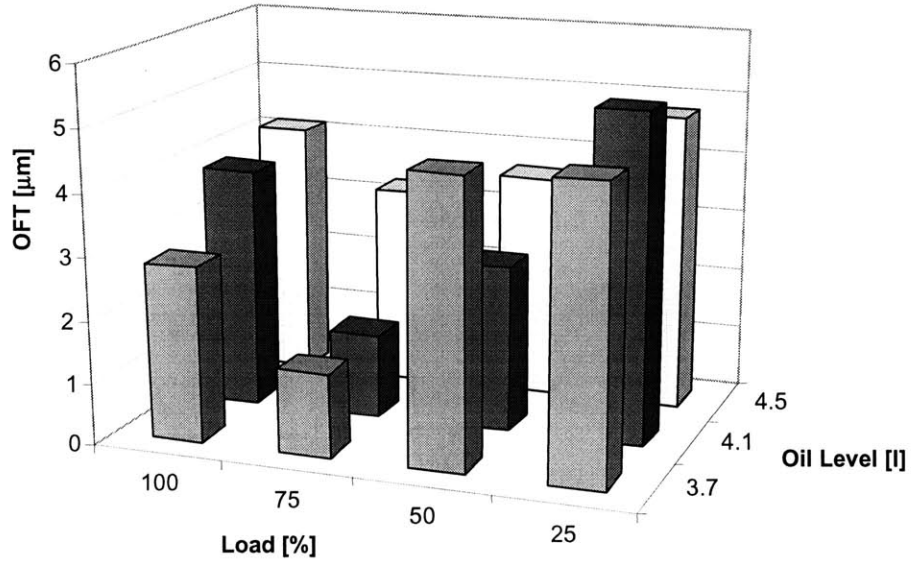


Figure 3-20 Top crown land average oil film thickness for 2500 rpm

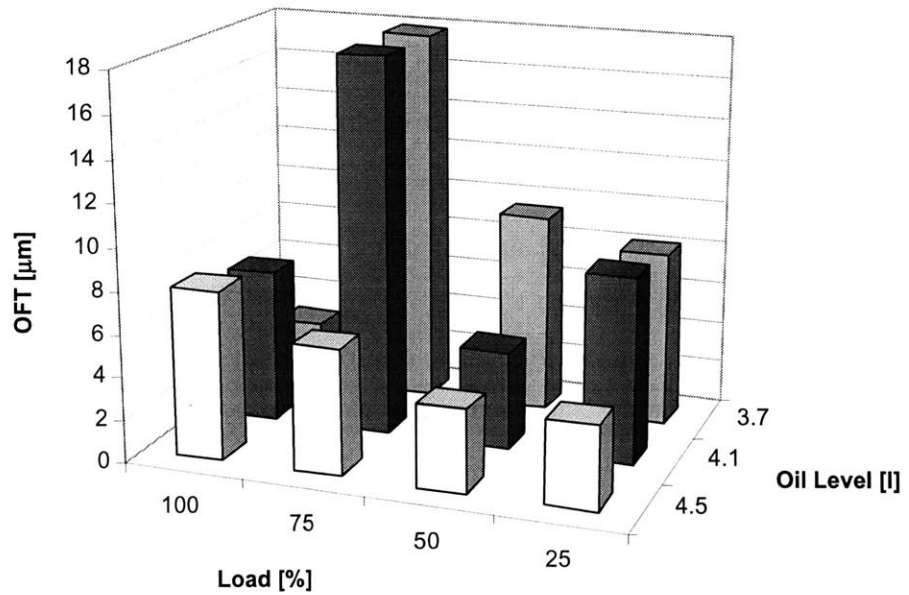


Figure 3-21 Second land average oil film thickness for 2500 rpm

CHAPTER 4: PCV System Blowby Lube Characteristics

The PCV blowby oil consumption contributes to the total oil consumption although results have shown that is not one of the main contributors for most of the engine operating conditions. In Chapter 3, the blowby oil transport has been described, and the sources of oil in the flow gases have been identified. The PCV blowby flow is composed of the blowby gases that flow through the ring-pack, which entrain oil by oil film atomization in the ring gaps and oil evaporation under high gas and component temperatures. Furthermore, these gases that flow through the power cylinder are mixed with the high speed velocity gases induced by the alternating movement of the engine components in the crankcase, which also entrain oil by particle atomization and some local oil evaporation. As mentioned in the previous chapter, it is believed that most of the larger particles are believed to come from the crankcase, while the smaller particles are from the atomization of the oil by the high speed gas flows under the small clearances in the ring gap.

The PCV blowby consumption is limited by the flow magnitude, the oil entrainment in the flow and the separator performance. After characterizing the blowby flow and oil entrainment, it is of great interest to understand the characteristics of the oil in the blowby, in either vapor or liquid form. In this chapter, the effect of the liner temperature in the oil evaporation and entrainment in the flow are studied by carrying some experiments at different thermal conditions. In addition, by using the gravimetric method (See Chapter 2.3.1.3.3) and different pore size filters, a study of the smallest size oil particles mass distribution has been obtained. All of these oil characteristics in the blowby will affect its consumption and contribute to the total engine oil consumption.

4.1 Blowby Oil Particle Size Distribution

Previous experimental studies have assessed the performance of different oil separators for different engine operating conditions [4][5][6][7]. For these studies, not only the separation efficiency curve of the separator was found, but also the particle size

mass distribution for the oil particles was obtained. Figure 4-1 shows the typical average separator efficiency curve for most of the modern automotive engines. The parameter R is the cumulative droplets size mass distribution. It is obvious that the separation efficiency for the fine particles ($< 4 \mu\text{m}$) is very inefficient. The larger droplets that are separated do not make a large percentage of the oil mass present in the blowby. However, the smaller particles that are present in the blowby in a greater frequency can add up to a higher oil mass percentage, thus influencing the blowby oil consumption. Moreover, it has to be noted that if the oil present in the flow is in vapor form, most of the widely used separators will not separate it from the flow. Thus, it is important to study the impact of oil evaporation, as the engine power and size are decreased leading to higher thermal loading.

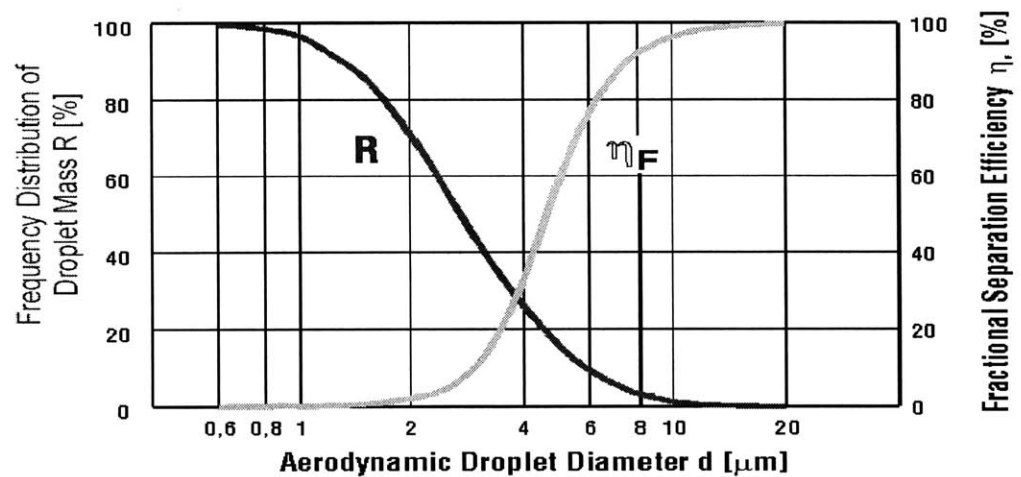


Figure 4-1 Typical droplet size distribution and separation efficiency [5]

As briefly discussed in Chapter 3, the engine operating conditions, such as the speed and load, affect the particle size atomization (shown in Figure 3-3) and thus influencing blowby oil consumption. The speed and load conditions also affect the pressure variation of the blowby gas flow, which yield the pressure drop available for separation. Normally, to increase the separator efficiency, the pressure drop across the separator needs to be increased. However, there is a limit of increasing the separator efficiency by increasing the pressure drop. In order to prevent the blowby gases to be vented from the crankcase, it is necessary to provide a pressure below atmospheric at the crankcase. Specially at the

low speed range of the spark ignition engine, the pressure in the induction port will not be sufficient to guarantee a pressure below ambient in the crankcase if the pressure loss is very high [5].

4.1.1 Oil Separators

As the gases flow through the separator, oil droplets are removed from the main gas flow and returned to the engine sump. There exist different separator types based on the varying separation principles: diffusion separators, inertial separators and electric separators [5][7]. The diffusion separator's principle relies on the aerosol hitting a layer of fine fibers or wires and the liquid particles hitting the obstacles, thus leaving the gas cleaned after the filter. The inertial separators rely on the skillful guidance of the flow in the separator in order to remove the oil particles by making them impact with obstacles. The electrical separators charge the particles or droplets by spray electrodes. Then the ionized aerosol moves in the electrical field towards the precipitation electrode and separated there.

The test engine for this study was equipped with an inertial baffle separator. A schematic illustrating the principle of a baffle separator is shown in Figure 4-2 along with different types of inertial separators. This separator type has prevailed in the automotive industry, driven mainly by an acceptable separation efficiency of small droplets ($< 10 \mu\text{m}$) at a reasonable pressure drop. In addition, the limited space in modern engines, combined with economic factors, contributed to the popularity of the baffle separator in passenger car engines.

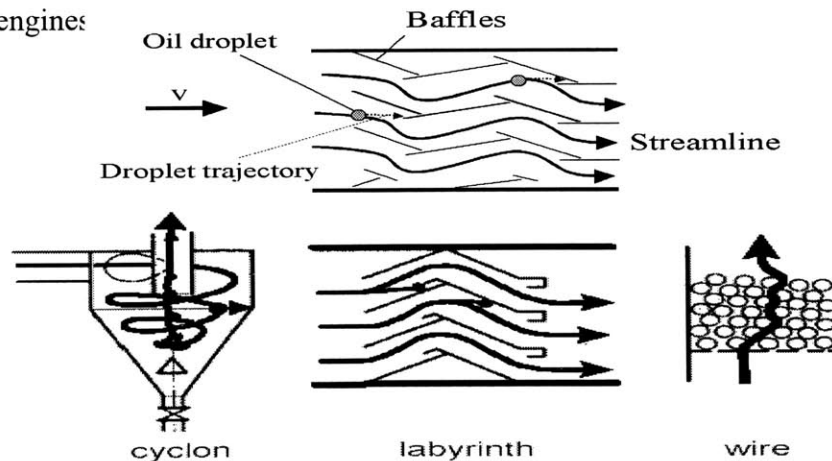


Figure 4-2 Illustration of several inertial separators [5]

The separation principle is based on inertial movements of the disperse phase, relative to the carrier gas streamline. The movement of small droplets (order of 10 μm) in a gas stream is governed by inertia forces and aerodynamic drag. When the exerted aerodynamic drag on the droplet is not able to overcome the inertial forces, the droplets divert from the flow streamline and impact on the baffles. Subsequently, the separated oil drains off from drainage holes to the oil sump. However, not all particles can be efficiently separated from the carrier gas; droplet sizes smaller than a certain diameter may follow the gas flow. This is because inertia forces are proportional to the droplet diameter to the cube (and the droplet velocity), and aerodynamic drag to the droplet diameter (for Reynolds numbers smaller than 0.5). As a result, with decreasing droplet size, the aerodynamic drag becomes significantly greater than droplet inertia and causes the droplet to follow the gas flow. Therefore, it can be assumed that the probability for droplets to divert from the streamline and impact on a baffle plate increases with their diameter and their velocity.

Therefore, oil separators play a critical role in the blowby oil consumption since their performance influences the percentage contribution to total oil consumption. However, this study did not go to see the effects of different separator types, and the engine was run with the stock baffle separator.

4.1.2 Particle Size Mass Distribution Measurements

The test engine was run at two different speeds (2500 rpm and 3500 rpm) and different loads, in order to see the impact of the operating conditions in the oil particle size mass distribution. The gravimetric analysis of the PCV blowby flow with different pore size filters shows the mass distribution of oil particles in that range. The pore sizes used are of 0.3 and 0.5 μm and depending on the running conditions there should be a percentage difference between the oil collected by these filters. Previous studies have shown that the 0.3 μm pore size collect more than 95% of the oil mass in the blowby flow [5][6]. Most of the actual oil separators do not have the capability to filter the small particles, which can contribute to the blowby oil consumption.

Figure 4-3 shows the results for the oil consumption measured by the gravimetric analysis for 3500 rpm at standard thermal conditions ($T_{\text{coolant}}=81.5\pm 1.5\text{ }^{\circ}\text{C}$). For the smaller pore size filter, the oil consumption increased as the load is increased. Previous studies have showed how the engine load increases the concentration of the smallest particles in the blowby flow [1]. Meanwhile for the larger pore size filter, it did not really change that much. The load increased the mass percentage of the oil particles between the two rated sizes. The larger magnitude of blowby that flows through the ring gaps and groove seemed to increase the atomization of the oil film into this micron scale oil particles. These small oil particles are believed to come from the power cylinder since the gas passages are much smaller than in the crankcase. In addition the test engine has a spray jet to cool the piston and supply additional lubrication for the highly loaded thrust side. This jet sprays oil with a nozzle, combined with the higher speed flow might entrain more of the smaller particles into the blowby.

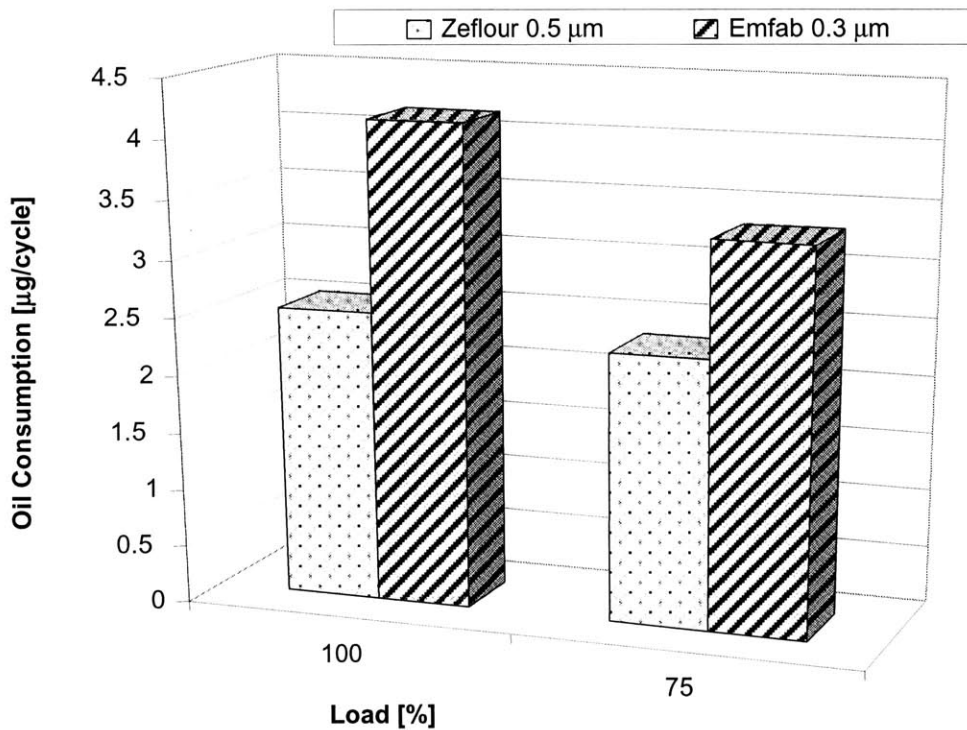


Figure 4-3 Oil consumption for the two different pore size paper filters

Results in Figure 4-4 show the percentage oil mass of particles between 0.3 and 0.5 µm over the oil mass collected with the smallest pore size, which was calculated by

taking the difference of the oil collected with the two different filters. The speed affected the creation of high gas velocities in the crankcase and enhanced the droplet breakup into small droplets due to the more violent interaction of the engine parts with the oil in the sump. This phenomenon, as the speed was increased, augmented the concentration of the smaller size oil particles. The increase in flow pulsations might also affected the separation efficiency, as the small particle pass by the separator. Furthermore, the faster movement of the reciprocating parts also enhanced the entrainment from the oil jet nozzle and oil in the sump. Thus, the figure correlates to the oil consumption increase in the PCV blowby consumption map shown in Section 3.3.1 and explains the increase in the oil consumption. Nevertheless, it also has to be taken into account the thermal loading effect in the oil consumption map, since at higher speeds the oil evaporation is enhanced. However, the oil in evaporated form was not collected in the gravimetric method and thus has no impact in these results. In summary, the increase in the PCV blowby consumption came due to the increase of the atomization of smaller size particles and the increase in the evaporated oil. However, as seen in Section 3.4.2 the oil evaporation did not seem to increase for the lower oil level, meaning that its impact should not increase severely.

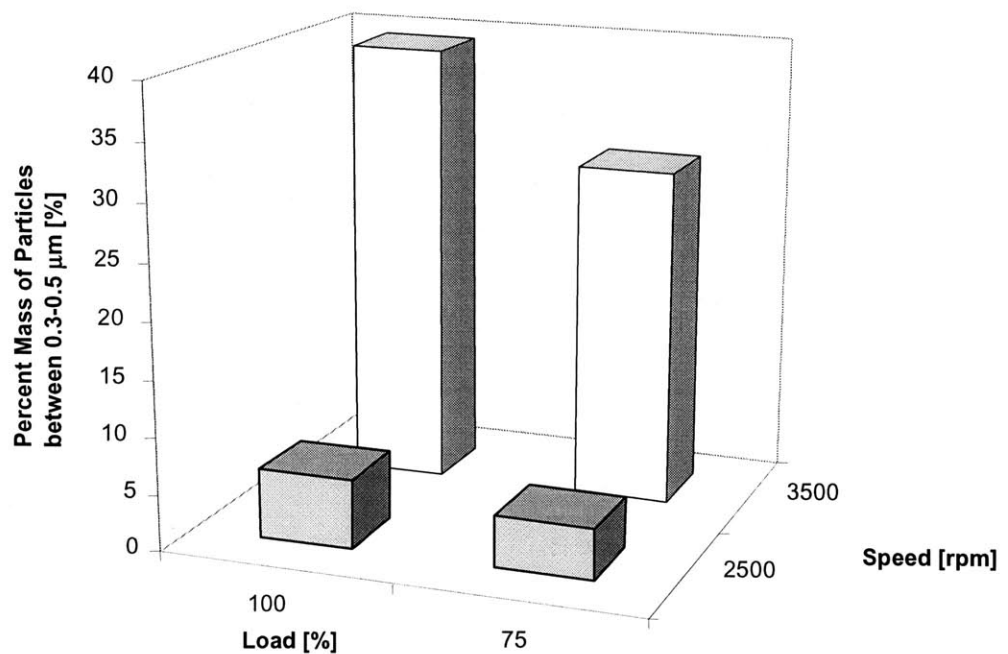


Figure 4-4 Percent oil mass of total PCV blowby oil for different engine operating conditions

There was a strong correlation between engine speed and oil entrainment in the PCV blowby gases, which also was seen in Figure 4-4. The results showed that the mass percentage of the particles in the range between 0.3 and 0.5 μm increased as the engine speed was increased. The concentration of the small particles ($<0.5 \mu\text{m}$) was enhanced due to the droplet breakup enhancement by the higher blowby flows and more violent interaction with the engine moving parts. This in turn increased the total PCV blowby oil consumption. These oil particles entrained in the gas flow, go through the separators. The particles that are larger were separated because the exerted aerodynamic drag force did not overcome the inertial forces, thus impacting the baffles [2]. Therefore, as the gas speeds were larger and the droplet sizes were smaller, particle passed by the separators and contributed to the PCV blowby oil consumption. For current oil separators, the efficiency is almost zero for the small particles ($<4\mu\text{m}$). Therefore, as the automotive engine speeds are increased and the droplet breakup into smaller particles is enhanced, the PCV consumption can increase.

Moreover, increasing engine speed might also affect the oil separator's efficiency. Oil separator efficiency and pressure drop both depend on gas flow characteristic and the size and velocity of the entrained droplets. Increasing engine speed has little impact on the average gas flow rate (per unit time), but it increases the frequency of flow pulsations. The impact of speed on blowby pulsation amplitude and on separator efficiency, however, is unknown. The understanding of the impact of engine speed on the separation efficiency requires detailed analysis of gas flow through the separator, which is beyond the scope of this work.

4.2 Effect of Cylinder Liner Temperature

In addition to the particle size effect on the separation efficiency and consequently in the total engine oil consumption, the oil in vapor form can contribute significantly in the oil consumption. In order to study the evaporation effect, the test engine was run at different coolant outlet temperatures, which affect the liner thermal conditions. The liner temperature increase enhances the evaporation. However, the increase in the temperatures also modifies the oil transport modes, increasing the engine total oil consumption

drastically as shown in previous studies [1][2]. Nevertheless, the scope of this study was to investigate the lube properties in the PCV blowby oil transport and does not look into the total engine consumption. It also must be recognized that viscosity affects the flow of the oil to the upper regions of the piston-ring-liner system and therefore affects oil consumption. The HTHS (High Temperature High Shear) viscosity is believed to influence ring and piston liner lubrication, and thus govern the oil transport on the liner. All these properties for the oil are shown in Table 2-2. Since the change in temperature influences the oil viscosity (See Appendix C), then the change in liner temperature will therefore have effects on oil transport. However, even though some of the oil transports to the different regions are changed, the limiting factor in the blowby oil consumption is believed to be the oil evaporation.

4.2.1 Different Cylinder Liner Temperature Measurements

The increased temperature in the cylinder liner influences the evaporation of the oil. Total oil consumption previous results showed how the oil evaporation dominates as the liner temperature was increased [1][2]. Figure 4-5 shows the total oil consumption for 3500 rpm and two oils with different volatilities from previous study of Ertan Yilmaz in the Sloan Automotive Lab. In addition, the increase in liner temperature can have a great impact in oil viscosity and in components thermal expansion, and possibly affecting the blowby flow and oil entrainment greatly.

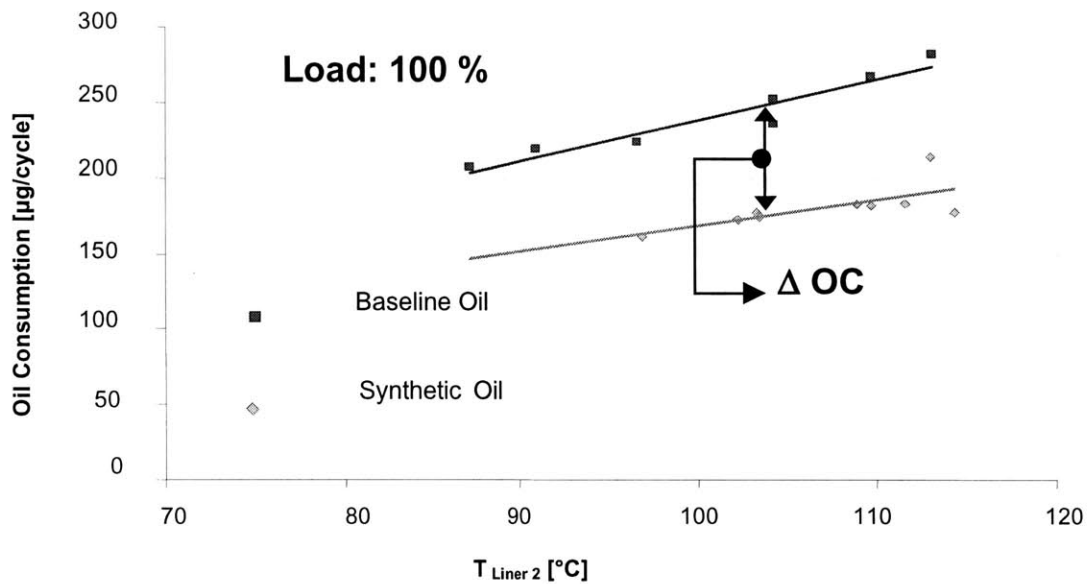


Figure 4-5 Total engine oil consumption for different liner temperatures

Figure 4-6 show the trend on PCV blowby oil consumption as the coolant outlet temperature was increased for 2500 rpm. For all the loads but 100% case, the oil consumption increased by a factor of around two. This was mainly due to the increase in oil evaporation, although for the 100% case the engine lower oil viscosity and the thermal expansion, which affected the blowby greatly, reduced the oil entrainment and consumption.

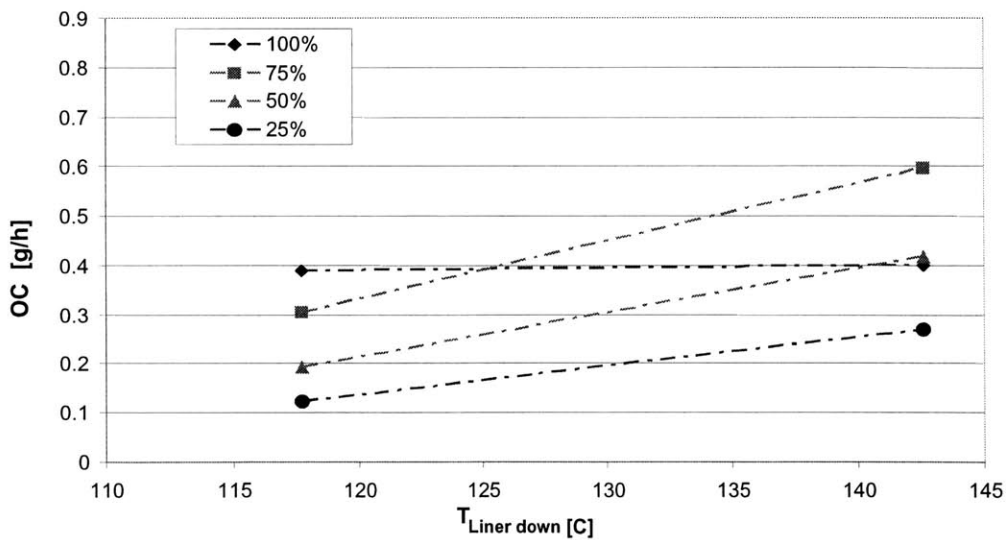


Figure 4-6 Temperature effect on oil consumption for 2500 rpm

4.2.1.1 Liner Temperature Effect on Blowby Flow

There was almost no increase in oil consumption for the highest load. Therefore, by taking the measurements of the blowby flow we can get the information to explain this. The increase in temperature lead to the thermal expansion of the piston and rings, consequently decreasing in the blowby flow by about 2 l/min for 2500 rpm as shown in Figure 4-7. Although the larger decrease in flow happened to the 100% case, it occurred to all of the loads in some manner. This decrease limits the effect of increase in evaporation that lead to higher oil loading in the flow. The thermal expansion of the various components in the power cylinder restricted and influenced the flow paths through the ring gaps and grooves. Therefore, for the highest load, this flow restriction could limit its oil consumption, inhibiting the oil consumption increase.

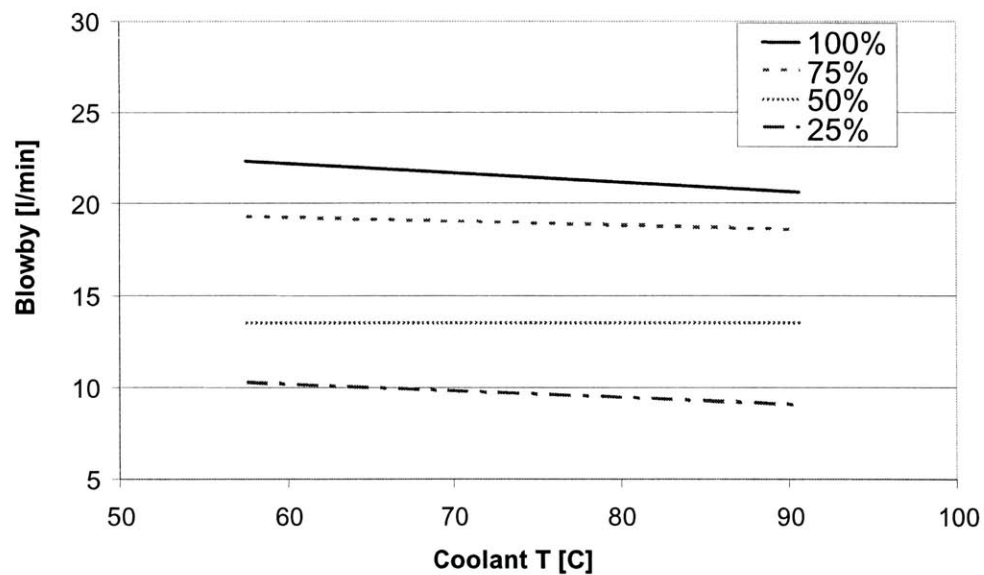


Figure 4-7 Temperature effect on blowby flow for 2500 rpm

4.2.1.2 Liner Temperature Effect on the Oil Concentration

The oil (vapor and liquid) concentration in the blowby increased due to the higher evaporation for high liner temperatures. On the other hand, the higher flow at lower temperatures was believed to promote the oil film atomization into few micrometers

particles. Therefore, the oil loading varied with the engine operating condition due to the oil transport mechanism change. Figure 4-8 shows the oil mass concentration for 100 % and 75 % load cases for 2500 rpm. The oil concentration was greater for the 75% case at the highest liner temperature. The change in the evaporation rate of the light end species of oil was more important at this operating condition while the flow was not reduced as dramatically as in the 100 % load case. In addition, the change in oil viscosity changed the oil film thickness distribution, thus affecting the oil entrainment in the flow. The lower oil viscosity promoted the oil consumption via mechanical throw off to the combustion chamber. Therefore, even if the blowby flow magnitude was greater for the higher load, there was not an increase in the atomization of oil particles due to the variation in the oil film distribution.

Consequently, the oil entrainment driving mechanisms varied for different operating conditions as shown in Figure 4-8. However, for the higher liner temperatures, the increase in evaporation and component thermal expansion controlled the oil entrainment mechanism and consumption. Although higher liner temperatures increased the oil evaporation, they also affected the oil viscosity, which influenced the mechanical oil transport. In addition, the component thermal expansion affected and modified the blowby flow through the ring-pack influencing the oil entrainment mechanism. Since oil consumption through the PCV system depends in the blowby flow and oil entrainment, the trend varied from condition to condition with increasing liner temperature depending which was the controlling factor, the evaporation or flow characteristics.

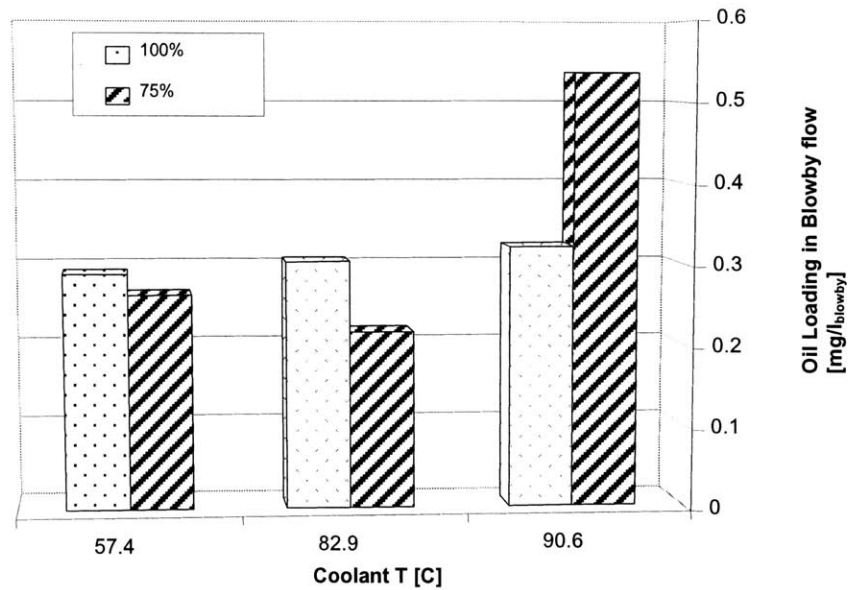


Figure 4-8 Temperature effect on oil loading for 2500 rpm

4.2.2 Liner Temperature Effect on the Oil Evaporation

For the production engine, higher speeds have higher liner temperature for any load. Evaporation seemed to be more dominant for the higher speeds, and as shown in Figure 4-9 for the 3500 rpm case, the oil consumption for all the loads at the lower coolant temperature was much higher than compare to the 2500 rpm (See Figure 4-6). Moreover, the oil consumption tended to converge to approximately 0.55 g/h for both speeds. However, the change in the oil consumption with temperature was more saddle for the 3500 rpm case. The very high liner temperature did not evaporate a large portion of the next light end species in the distillation curve. As it happened in the lower speed, the restriction of the blowby flow also controlled the blowby oil consumption, one because the blowby flow was reduced and second because the oil loading stayed almost unchanged. In addition, the higher temperatures at this speed reduced the oil viscosity, which governs different oil transport methods to the top regions and affects the oil entrainment by atomization into the blowby gases [2].

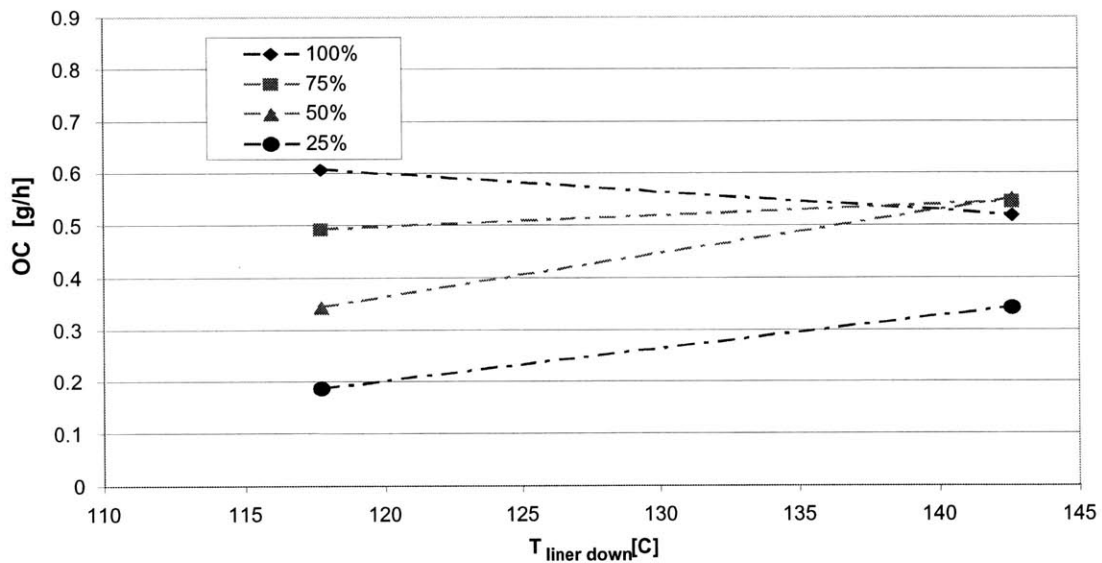


Figure 4-9 Temperature effect on oil consumption for 3500 rpm

The change in liner temperature had a great effect on the PCV blowby oil consumption at the low loads for both the high and low speed conditions. For high load conditions, which have hotter thermal conditions, the increase in liner temperature did not bring higher blowby oil consumption. For these cases, even though the liner temperature was increased, the blowby flow was modified and restricted and the high temperatures did not evaporate the next light end oil species of the distillation curve. The other effect on increasing the liner temperatures was the decrease in the oil's viscosity.

Since the PCV blowby consumption is both a function of oil loading and blowby flow, the decrease in the flow can limit the absolute oil consumption. Figure 4-10 shows the increase in oil consumption from the colder coolant outlet operating condition to the hotter coolant condition. The effect of increase liner temperature was more appreciated at the lower loads and speeds. This was due to the non-linear behavior of the distillation of oil with temperature and the flow restriction with the increasing liner temperatures. In general, the dependence of oil vapor pressure on temperature is described by an exponential relationship [2]. The reducing effects in the blowby flow magnitude and

change in oil transport due to the lower oil viscosity explain the decrease in oil consumption for the highest load condition, where the liner temperatures are much higher.

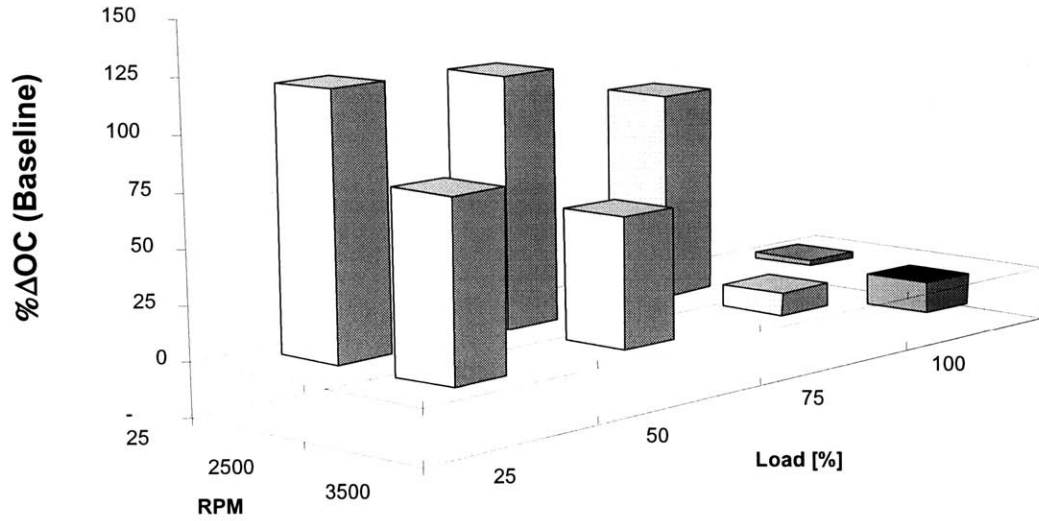


Figure 4-10 Oil consumption percent change from the coldest coolant outlet temperature [$T_{\text{coolant}} = 56 \text{ }^{\circ}\text{C}$] to the higher coolant temperature [$T_{\text{coolant}} = 91 \text{ }^{\circ}\text{C}$]

CHAPTER 5: Conclusions

For this work, the Positive Crankcase Ventilation (PCV) blowby contribution to oil consumption in a production spark ignition engine was analyzed and quantified for different engine operating conditions. The study also examined the oil entrainment sources and lubricant characteristics in the blowby flow that affect the separation efficiency of separators and the PCV blowby consumption.

On a two liter, four-cylinder production spark ignition engine, a diagnostic system was implemented to measure engine total and blowby oil consumption and in-cylinder parameters that affect the oil transport mechanisms. A sulfur-based oil consumption method was used to measure real-time blowby and total oil consumption along with a gravimetric method in order to check these results. A blowby flow meter was used to measure total blowby flow out of the engine in the PCV system. Several measurement probes were implemented to gain information on the in-cylinder parameters. The Laser Induced Fluorescence (LIF) technique was used to study the oil distribution in the piston-ring-pack. Two pressure transducers were positioned along the cylinder liner to measure inter-ring land pressures. An additional pressure transducer mounted on the cylinder head provided cylinder pressure traces. Two temperature probes along the cylinder liner provided liner temperatures.

Blowby oil consumption along with total oil consumption, blowby flow and in-cylinder parameters were measured in order to quantify and describe the PCV blowby oil transport mechanism. Steady state measurements were taken at different operating conditions in order to see the effect on the blowby oil consumption. Both the PCV blowby oil consumption and blowby flow (in volume per cycle units) magnitude increased with load and speed. The total oil consumption measurements also showed the same trend as the PCV blowby oil consumption. Nevertheless, the PCV blowby contribution to the total oil consumption varies from condition to condition, having a maximum contribution of around 7% for the results measured directly from the PCV line. The gravimetric method showed similar results as the direct method results. However, the blowby percent contribution to the total engine oil consumption was calculated to be higher for the difference method's highest loads. This difference happened because the

engine was run at two different operating conditions: with the PCV line connected and disconnected. The downstream vacuum was lower when the PCV line was connected. This vacuum pressure modified the position of a valve placed along the line, and which was used to match the blowby flow produced with what it flowed out of the engine. At the highest load condition, the difference in the PCV valve operation was the greatest, thus affecting the blowby oil consumption results, and augmenting the percent contribution result.

The blowby oil entrainment sources were investigated by running the engine at different oil levels in the crankcase. The blowby oil sources are believed to be the power cylinder and the crankcase. The oil entrainment in the crankcase comes from the splashing of the oil with the engine moving parts and the light oil species that evaporated under the high temperatures. Running the engine at the lowest level possible under safe operating conditions minimized the contribution from the crankcase oil entrainment. Results show that between 40-70% of the oil consumption was reduced from the PCV blowby when the engine was at the lowest level. Results also show that the contribution from the power cylinder reaches a limit, even if the thermal conditions or the blowby increase with load or speed. This oil consumption bound seemed to be limited by the oil evaporation rate rather the increase in blowby flow that enhanced the oil atomization, as shown by the trend in oil consumption versus the load for all the speeds run. In-cylinder parameters, such as inter-ring pressure traces and oil film thickness were measured and showed that the lubricating conditions did not change with the investigated operating conditions tested.

Oil characteristics in the blowby flow were also investigated. The size distribution of oil droplets were estimated using different pore size filters. The proportion of oil droplets in the range from 0.3- 0.5 μm (small droplets) increased as the engine speed was increased. This increase was believed to come from the oil droplet enhancement due to the higher speed engine components that splashed the oil in the sump. The load increase also augmented the percentage oil mass between the two particle sizes. This raise comes with the increase in oil entrainment of small particles due to the higher blowby flows that boost the oil droplet breakup from the oil film in the power cylinder.

The engine was run at different liner temperatures, by controlling the coolant outlet temperature. The blowby oil consumption increased for the lowest loads with the increase in the liner temperature. This increase came from the increase in oil evaporation. The oil evaporation was limited by the increase in components temperatures. However, for the 100% case the blowby oil consumption did not increase with temperature, and even decreased at the highest speed investigated (3500 rpm). The oil properties such as the viscosity and engine component thermal expansion were also affected by the increase in the engine thermal conditions. The lower viscosity and the increase in the component thermal expansion, which reduced the blowby flow by about 10%, affects the oil transport mechanism and the entrainment in the blowby flow. Thus increase in the evaporation, without the great effect in the change in oil properties and thermal expansion, could greatly influence the blowby oil consumption. Nevertheless, the increase in liner temperature modified the rest of oil transport mechanisms, in most of the cases reducing the percent contribution of the PCV blowby consumption.

This study is an important advancement in understanding the blowby oil transport mechanism. It has described and characterized the oil entrainment sources and some of the oil characteristics that affect the blowby oil consumption for the test engine equipped with a standard baffle separator. This study has made a great contribution to developing new engine cylinder ring-pack designs and providing guidelines to developing new analytical tools for new engine developments.

(This page was intentionally left blank)

Nomenclature

P.C.V.	Positive Crankcase Ventilation
O.C.	Oil Consumption
O.F.T.	Oil Film Thickness
L.I.F.	Laser Induced Fluorescence
O.C.R.	Oil Control Ring
T.C.	Thermocouple
D.A.S.	Data Acquisition System
PTFE	Polytetrafluoroethylene
F.L.	Focal Length
λ	Lambda, ratio of actual air to fuel ratio to stoichiometric air to fuel ratio
$\dot{m}_{blowbyOC}$	PCV blowby oil consumption in g/h
\dot{Q}_{blowby}	PCV blowby flow in l/h
ρ_{blowby}	Blowby gases density in g/l
P_{atm}	Atmospheric pressure
T_{blowby}	Blowby temperature
R	Universal gas constant (Section 2.3.1.5)
$\psi_{s,blowby}$	Dry Sulfur concentration in blowby in wt. %
$\frac{M_s}{M_{blowby}}$	Sulfur and blowby molecular weight ratio
$\psi_{s,oil}$	Sulfur concentration in oil in wt. %
$\dot{m}_{OC,w/PCV}$	Total oil consumption with PCV line connected to the engine intake
$\dot{m}_{OC,w/outPCV}$	Total oil consumption with PCV line disconnected to the atmosphere
$\dot{m}_{inertia}$	Oil mass consumption by mechanical throw-off
\dot{m}_{evap}	Oil mass consumption by evaporation

\dot{m}_{blowby}	Oil mass consumption by blowby transport
$m_{collected}$	Mass collected for gravimetric analysis
t_{sample}	Sampling time
T.D.C	Top Dead Center
ΔOC	Change in oil consumption
r.p.m.	Revolution per minute
C.A.	Crank Angle
T	Temperature
R	Cumulative droplets size mass distribution (for Section 4.1)
η_F	Separator efficiency

References

- [1] Yilmaz, Ertan: “Sources and Characteristics of Oil Consumption in a Spark Ignition Engine”, PhD Thesis, Department of Mechanical Engineering, MIT, September, 2003
- [2] Yilmaz, E., Tian T., Wong V. W., Heywood, J. B.: “An Experimental and Theoretical Study of the Contribution of Oil Evaporation to Oil Consumption”, SAE paper 2002-01-2684, 2002
- [3] Yilmaz, E., Thirouard, B., Tian, T., Wong, V. W., Heywood, J. B., and Lee, N.: “Analysis of Oil Consumption Behavior During Ramp Transients in a Production Spark Ignition Engine”, SAE paper 2001-01-3544, 2001
- [4] Froelund, K.: “Real-Time Steady State Measurement of PCV-Contribution to Oil Consumption on Ford 4.6 L SI –Engine”, SAE paper 2000-01-2876, 2000
- [5] Koch F., Haubner F. G., Orłowski K.: “Lubrication and Ventilation System of Modern Engines – Measurement, Calculations and Analysis” SAE paper 2002-01-1315, 2002
- [6] Bischof O. F., Tuomenoja H.: “The Measurement of Blow-by Gas Particles” MTZ 7-8, 2003
- [7] Harmut L., Trautmann P.: “Measurement and Separation of Oil Mist Aerosol from the Crankcase Exhaust of Internal Combustion Engines”, MTZ 6-12,2000
- [8] Froelund, K.: “ Real-Time Steady State Oil Consumption Measurement on Commercial SI-Engine”, SAE paper 1999-01-3461, 1999
- [9] Hill S. H., Sytsma S. S.: “A System Approach to Oil Consumption” SAE paper 910743, 1991
- [10] Krause W., Spies K. H., Bell L. E., Ebert F.: “Oil Separation in Crankcase Ventilation – New Concepts Through System Analysis Through System Analysis and Measurements” SAE paper 950939, 1995
- [11] Koch F., Hardt T., Haubner F. G.: “Oil Aeration in Combustion Engines – Analysis and Optimization”, SAE paper 2001-01-1074, 2001
- [12] Tamai, Goro; “Experimental Study of Engine Oil Film Thickness Dependence on Liner Location, Oil Properties and Operating Conditions”, MS Thesis, Department of Mechanical Engineering, MIT, August, 1995
- [13] Heywood, J.B., Internal Combustion Engine Fundamentals, McGraw, 1988

- [14] Pulkrabek, W.W., *Engineering Fundamentals of the Internal Combustion Engine*, Prentice Hall, 1997
- [15] Ranganathan, G., Mohanram, P.V., “Tribological Studies for the Design Input Parameters on Small Displacement – 4 Stroke Petrol Engines – A View from Engine Oil Conservation”, SAE paper 2002-02-1728, 2002
- [16] Shayler P.J., Winborn L.D., Scarisbrick A.: “Fuel Transport to the Crankcase, Oil Dilution and HC Return with Breather Flow During the Cold Operation of a SI Engine”, SAE paper 2000-01-1235, 2000
- [17] Antek, *Antek R6000 SE Sulfur Analyzer*, Antek Industrial Instruments L.P.
- [18] Ebner H. W., Jaschek A. O.: “The Importance of Blow-By Measurements, Measuring Equipment Required and Implementation”, SAE paper 981081, 1998
- [19] Toyota, *Emission Sub Systems- Positive Crankcase Ventilation System*, Toyota Motor Sales, U.S.A.
- [20] Thirouard, Benoist : “Characterization and Modeling of the Fundamental Aspects of Oil transport in the Piston-Ring Pack of Internal Combustion Engines,” Ph.D. Thesis, Department of Mechanical Engineering, MIT, May 2001.
- [21] Thirouard, B., Tian, T., and Hart, D. P.: “Investigation of Oil Transport Mechanisms in the Piston Ring Pack of a Single Cylinder Diesel Engine, Using Two Dimensional Laser Induced Fluorescence”, SAE paper 982658, 1998.
- [22] Conze, M., “Fired and Non-Fired Engine: A Comparative Study of Crankcase Emission on Dynamometer Test Rigs”, *AutoTechnology* 6/2001, 2001
- [23] Crane M.E., Ariga S., Boulard R., Lindamood B.: “A Non-Intrusive Method of Measuring PCV Blowby Constituents”, SAE paper 941947, 1994
- [24] Tian T., Noordzij B., Wong V. W., Heywood J. B.: “Modeling Piston-Ring Dynamics, Blowby, and Ring-Twist Effects”, ASME paper ICE-Vol. 27-2, 1996
- [25] De Petris, C., Giglio, V., Police, G.: “Some Insights on Mechanisms of Oil Consumption”, SAE paper 961216, 1996
- [26] Thirouard, B., Tiant, T. “Oil Transport in the Piston Ring Pack (Part 1): Identification and Characterization of the Main Oil Transport Routes and Mechanism”, SAE paper 2003-01-1952, 2003
- [27] Thirouard, B., Tiant, T. “Oil Transport in the Piston Ring Pack (Part 2): Identification and Characterization of the Main Oil Transport Routes and Mechanism”, SAE paper 2003-01-1952, 2003

- [28] Froelund, K. Schramm, J., Noordzij, B. Tian, T., Wong, V.W. :“An Investigation of the Cylinder Wall Oil Film Development During Warm-Up of an SI-Engine Using Laser Induced Fluorescence”, SAE paper 971699, 1997
- [29] Ellermann, J., Rohrle, M.D., Schelling, H. “Oil Consumption and Blowby of Truck Diesel Engines – Test Bench Results”, SAE paper 810937, 1981
- [30] Furuhashi, S., Hiruma, M., Yoshida, H., “An Increase of Engine Oil Consumption at High Temperature of Piston and Cylinder”, SAE paper 810976, 1981
- [31] Bailey, B. K., and Ariga, S.: “On-Line Diesel Engine Oil Consumption Measurement”, SAE paper 902113, 1990.
- [32] Noordzij, B. L.: “Measurement and Analysis of Piston Inter-Ring pressure and Oil Film Thickness and their Effects on Engine Oil Consumption”, MS Thesis, Department of Mechanical Engineering, MIT, June 1996

(This page was intentionally left blank)

Appendix

Appendix A: Sample of Results Acquired and Calculations

Speed [rpm]	Load [%]	Blowby OC [$\mu\text{g}/\text{cycle}$]	Blowby OC [g/h]	Blowby [l/min]	Blowby [cm^3/cycle]	Oil Concentration [mg/l]	Oil Concentration [$\mu\text{g}/\text{cm}^3$]	T _{cool}	T _{down}	T _{up}
2500	100	4.589	0.343	21.205	16.968	0.269	0.270	82.94	101.01	128.27
2500	75	2.752	0.205	18.194	14.555	0.188	0.189	82.16	98.45	120.30
2500	50	1.925779	0.143	15.211	12.168	0.157	0.158	81.31	95.66	112.95
2500	25	1.211	0.090	11.266	9.012	0.133	0.134	79.94	92.53	104.47
3000	100	6.677	0.600	24.316	16.210	0.411	0.411	83.28	103.17	134.22
3000	75	4.944	0.445	21.368	14.245	0.347	0.347	82.63	101.28	125.48
3000	50	3.645	0.328	15.887	10.591	0.345	0.344	81.37	97.83	117.38
3000	25	2.728	0.246	10.933	7.289	0.375	0.374	81.05	94.91	108.87
3500	100	7.392	0.778	23.269	13.296	0.557	0.556	83.48	104.79	136.33
3500	75	5.979	0.628	19.304	11.031	0.542	0.542	83.13	103.28	129.43
3500	50	4.458	0.469	15.503	9.030	0.494	0.493	82.55	99.52	120.24
3500	25	2.663	0.280	10.175	5.814	0.459	0.458	81.82	96.26	111.34
4000	100	6.935	0.421	24.165	12.082	0.582	0.573	84.29	106.70	137.88
4000	75	6.322	0.844	21.718	10.859	0.585	0.582	84.14	105.72	132.42
4000	50	1.798	0.763	16.412	8.206	0.220	0.219	83.72	103.20	125.01
4000	25	1.218	0.146	11.376	5.688	0.215	0.214	83.05	99.738	116.52

Table A-1. Direct method data for the high level case

Speed [rpm]	Load [%]	Blowby OC [$\mu\text{g}/\text{cycle}$]	Blowby OC [g/h]	Blowby [l/min]	Blowby [cm^3/cycle]	Oil Concentration [mg/l]	Oil Concentration [$\mu\text{g}/\text{cm}^3$]	T _{cool}	T _{down}	T _{up}
2500	100	3.299	0.245	23.864	19.091	0.171	0.173	82.94	101.01	128.27
2500	75	2.734	0.204	18.647	14.918	0.182	0.183	82.16	98.45	120.30
2500	50	1.779	0.132	15.176	12.141	0.145	0.147	81.31	95.66	112.95
3500	100	1.085	0.457	22.816	13.038	0.120	0.121	79.94	92.53	104.47
3500	75	2.827	0.407	18.098	10.342	0.184	0.185	81.40	102.44	133.31
3500	50	2.568	0.233	13.581	7.761	0.200	0.201	81.46	101.11	125.24
4000	100	1.792	0.481	23.521	11.760	0.185	0.186	80.85	98.23	118.18
4000	75	1.231	0.407	19.356	9.678	0.169	0.169	79.89	95.78	109.44
4000	50	2.474	0.301	14.350	7.175	0.174	0.175	81.02	106.33	138.00

Table A-2. Direct method data for the medium level case

Speed [rpm]	Load [%]	Blowby OC [$\mu\text{g}/\text{cycle}$]	Blowby OC [g/h]	Blowby [l/min]	Blowby [cm^3/cycle]	Oil Concentration [mg/l]	Oil Concentration [$\mu\text{g}/\text{cm}^3$]	T _{cool}	T _{down}	T _{up}
2500	100	3.299	0.245	23.864	19.091	0.171	0.173	82.94	101.01	128.27
2500	75	2.734	0.204	18.647	14.918	0.182	0.183	82.16	98.45	120.30
2500	50	1.779	0.132	15.176	12.141	0.145	0.147	81.31	95.66	112.95
2500	25	1.085	0.081	11.200	8.960	0.120	0.121	79.94	92.53	104.47
3000	100	2.827	0.252	22.880	15.253	0.184	0.185	81.40	102.44	133.31
3000	75	2.568	0.229	19.130	12.753	0.200	0.201	81.46	101.11	125.24
3000	50	1.792	0.160	14.429	9.619	0.185	0.186	80.85	98.23	118.18
3000	25	1.231	0.110	10.896	7.264	0.169	0.169	79.89	95.78	109.44
3500	100	2.474	0.258	24.764	14.151	0.174	0.175	81.02	106.33	138.00
3500	75	2.442	0.255	18.785	10.734	0.226	0.228	80.71	104.65	130.26
3500	50	2.433	0.254	14.817	8.467	0.286	0.287	80.25	101.23	122.37
3500	25	1.395	0.146	9.616	5.495	0.253	0.254	79.71	97.27	113.21
4000	100	3.552	0.421	26.609	13.305	0.264	0.267	81.62	109.63	140.02
4000	75	2.390	0.285	20.721	10.360	0.229	0.231	81.20	107.30	133.41
4000	50	2.372	0.283	14.950	7.475	0.315	0.317	83.13	103.92	125.93
4000	25	1.438	0.171	11.130	5.565	0.255	0.258	81.91	99.30	116.32

Table A-3. Direct method data for the low level case

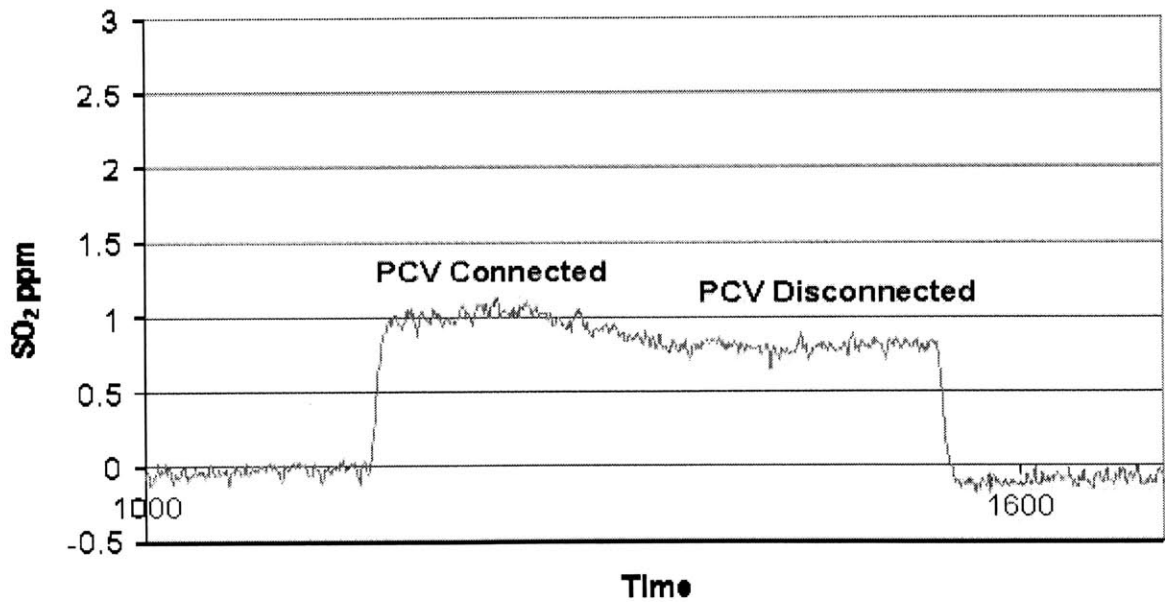


Figure A-1 Sample of sulfur concentration output for DAS with the difference method for 100% and 3500 rpm

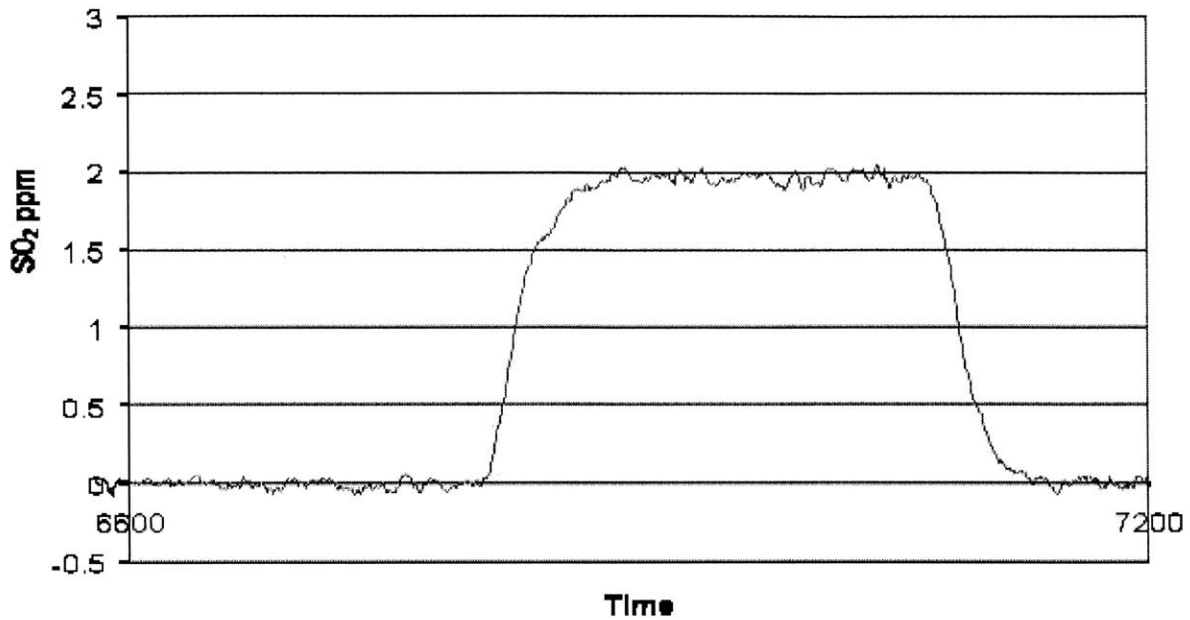


Figure A-2 Sample of sulfur concentration output for DAS with the direct method for 100% and 3500 rpm

Running condition	Mass Filter Before [mg]	Mass Filter After [mg]	T _{blowby}	Sample Time [min]	Mass Flow [mg/min]	Oil Concentration [mg/l]	Blow by [l/min]	OC [g/h]
2500rpm 100%	87.6	89.5	29.3	4	0.483	0.293	21.57	0.386
2500rpm 75%	88.8	91.8	29.4	6	0.503	0.253	18.13	0.288
2500rpm 50%	89.6	91.5	29.3	6	0.323	0.154	14.61	0.129
2500rpm 25%	88.1	89.5	29.2	6	0.248	0.114	9.38	0.062
3000rpm 100%	89.3	92.1	37.9	5	0.560	0.268	21.69	0.349
3000rpm 75%	90.0	93.9	38.1	7	0.557	0.267	20.44	0.327
3000rpm 50%	91.0	94.9	38.2	9	0.433	0.207	15.50	0.193
3000rpm 25%	91.8	95.1	37.8	9	0.367	0.175	9.55	0.101
3500rpm 100%	90.7	94.2	38.6	5	0.700	0.335	25.87	0.436
3500 rpm 75%	91.9	96.5	38.8	7	0.657	0.314	19.39	0.348
3500 rpm 50%	91.9	96.7	38.9	9	0.533	0.255	15.03	0.243
3500 rpm 25%	92.9	96.9	38.6	9	0.444	0.213	9.12	0.153
4000 rpm 100%	90.8	96.0	39.0	5	1.040	0.498	27.17	0.811
4000 rpm 75%	91.8	99.7	39.1	7	1.129	0.540	21.71	0.704
4000 rpm 50%	89.9	98.3	39.1	9	0.933	0.447	15.24	0.408
4000 rpm 25%	90.1	97.2	39.2	9	0.789	0.377	9.51	0.215

Table A-4. Gravimetric method data for the low level case

Running condition	Mass Filter Before [mg]	Mass Filter After [mg]	T _{blowby}	Sample Time [min]	Mass Flow [mg/min]	Oil Concentration [mg/l]	Blow by [l/min]	OC [g/h]
2500rpm 100%	89.3	91.9	18.1	4.000	0.650	0.311	19.789	0.369
2500rpm 75%	87.6	92.9	18.3	6.000	0.700	0.335	18.462	0.371
2500rpm 50%	89.3	91.9	18.2	6.083	0.427	0.204	13.000	0.160
3500rpm 100%	87.9	90	20.5	5.000	0.420	0.201	22.003	0.265
3500rpm 75%	89.3	93.5	20.1	7.000	0.600	0.287	17.441	0.300
3500rpm 50%	90.3	93.6	19.6	9.000	0.367	0.175	11.802	0.124
4000rpm 100%	89.7	92.1	24.1	5.000	0.480	0.230	22.522	0.310
4000rpm 75%	88.3	92.5	24.5	7.000	0.600	0.287	18.757	0.323
4000rpm 50%	88.8	91.5	21.8	9.000	0.300	0.144	12.141	0.105

Table A-5. Gravimetric method data for the medium level case

Running condition	Mass Filter Before [mg]	Mass Filter After [mg]	T _{blowby}	Sample Time [min]	Mass Flow [mg/min]	Oil Concentration [mg/l]	Blow by [l/min]	OC [g/h]
2500rpm 100%	87.6	89.5	29.3	4	0.483	0.231	21.57	0.299
2500rpm 75%	88.8	91.8	29.4	6	0.503	0.241	18.13	0.262
2500rpm 50%	89.6	91.5	29.3	6	0.323	0.155	14.61	0.136
2500rpm 25%	88.1	89.5	29.2	6	0.248	0.119	9.38	0.067
3000rpm 100%	89.7	91.7	29.6	5	0.414	0.198	22.16	0.263
3000rpm 75%	88.1	91.0	29.9	7	0.419	0.200	18.50	0.222
3000rpm 50%	89	92.3	30.1	9	0.368	0.176	14.57	0.154
3000rpm 25%	87.6	90.0	30	9	0.277	0.132	9.86	0.078
3500rpm 100%	89.7	92.0	29.6	5	0.462	0.221	22.79	0.302
3500 rpm 75%	88.2	91.1	29.7	7	0.416	0.199	19.07	0.228
3500 rpm 50%	88.9	92.3	29.9	9	0.388	0.186	13.70	0.153
3500 rpm 25%	88.7	90.8	29.9	9	0.348	0.166	8.08	0.081
4000 rpm 100%	90	93.5	30.4	5	0.704	0.337	24.05	0.486
4000 rpm 75%	89.3	93.8	30.8	7	0.797	0.381	19.11	0.437
4000 rpm 50%	88.4	93.9	31.1	9	0.613	0.293	14.27	0.251
4000 rpm 25%	90.5	94.7	31.2	9	0.471	0.225	9.08	0.123

Table A-6. Gravimetric method data for the low level case

Total oil consumption formula:

An oil consumption formula is derived using the measured sulfur dioxide concentration in the exhaust, the airflow rate, the air/fuel ratio, and the mass fractions of sulfur in the oil and fuel. In this section, the basic assumption and essential relations of the oil consumption formula will be described:

The consumed sulfur mass from the oil can be calculated from mass conservation,

$$\dot{m}_{S,Oil} = \dot{m}_{S,Wet\ Exhaust} - \dot{m}_{S,Fuel} - \dot{m}_{S,Air} \quad (1)$$

where $\dot{m}_{S,Oil}$, $\dot{m}_{S,Fuel}$, $\dot{m}_{S,Wet\ Exhaust}$, $\dot{m}_{S,Air}$ are mass flow rates of the sulfur in oil, fuel, wet exhaust gas, and air respectively. The sulfur content of air is negligible (in the order of 10 ppb), therefore

$$\dot{m}_{S,Air} = 0 \quad (1)$$

With

$$\dot{m}_{S,Oil} = \dot{m}_{Oil} * \xi_{S,Oil} \quad (2)$$

$$\dot{m}_{S,Fuel} = \dot{m}_{Fuel} * \xi_{S,Fuel} \quad (3)$$

$$\dot{m}_{S,Wet\ Exhaust} = \dot{m}_{Wet\ Exhaust} * \xi_{S,Wet\ Exhaust} \quad (4)$$

where $\xi_{S,Oil}$, $\xi_{S,Fuel}$, $\xi_{S,Wet\ Exhaust}$ are the mass fractions of sulfur in oil, fuel, and exhaust respectively. Substituting equations (2), (3), (4), (5) into (1):

$$\dot{m}_{Oil} = \frac{1}{\xi_{S,Oil}} \left[\dot{m}_{Wet\ Exhaust} * \xi_{S,Wet\ Exhaust} - \dot{m}_{Fuel} * \xi_{S,Fuel} \right] \quad (5)$$

From mass conservation and

$$\frac{\dot{m}_{Air}}{\dot{m}_{Fuel}} = L = \lambda * L_{St} \quad (6)$$

where L is the air/fuel ratio, and L_{St} is the stoichiometric air/fuel ratio, it follows that

$$\dot{m}_{Wet\ Exhaust} = \dot{m}_{Air} + \dot{m}_{Fuel} + \dot{m}_{Oil} \approx \dot{m}_{Air} \left(1 + \frac{1}{L_{St} * \lambda} \right) \quad (7)$$

The mass fraction of sulfur in the exhaust can be written as

$$\xi_{S, Wet Exhaust} = \psi_{S, Wet Exhaust} * \frac{M_S}{M_{Wet Exhaust}} \quad (8)$$

Where $M_{Wet Exhaust}$ is the molecular weight of wet exhaust, M_S is the molecular weight of sulfur (32g/mol), and $\psi_{S, Wet Exhaust}$ is the molar fraction of sulfur in wet exhaust. With

$$\psi_{SO_2, Wet Exhaust} = \psi_{S, Wet Exhaust} \quad (9)$$

where $\psi_{SO_2, Wet Exhaust}$ is the molar fraction of sulfur dioxide in wet exhaust. The molar fraction of sulfur dioxide in the wet exhaust may be written as

$$\psi_{SO_2, Wet Exhaust} = \psi_{SO_2, Dry Exhaust} * \left(1 - \frac{\dot{n}_{H_2O}}{\dot{n}_{Wet Exhaust}} \right) \quad (10)$$

where $\psi_{SO_2, Dry Exhaust}$ is the molar fraction of sulfur dioxide in dry exhaust, and \dot{n}_{H_2O} and $\dot{n}_{Wet Exhaust}$ are the moles of water and wet exhaust respectively. Substituting (8), (9), (10), (11) into (6) results in the final form of the oil consumption formula:

$$\dot{m}_{Oil} = \frac{\dot{m}_{Air}}{\xi_{S, Oil}} * \frac{1}{\lambda * L_{St}} \left(\psi_{SO_2, Dry} * \frac{M_S}{M_{Wet Exhaust}} * [1 + \lambda * L_{St}] * \left(1 - \frac{\dot{n}_{H_2O}}{\dot{n}_{Wet Exhaust}} \right) - \xi_{S, Fuel} \right) \quad (11)$$

Speed (rpm)	Load (%)	Blowby OC (µg/cycle)	Blowby OC (g/h)	Blowby (l/min)	Blowby (cm ³ /cycle)	Oil Concentration
2500	100	8.299	1.245	22.971	18.377	0.903
2500	75	2.001	0.300	18.894	15.115	0.265
2500	50	0.835	0.125	15.078	12.062	0.138
2500	25	46.981	3.504	9.827	7.861	5.943
3000	100	17.910	1.616	22.461	14.974	1.199
3000	75	4.071	0.394	16.594	11.063	0.396
3000	50	1.963	0.185	13.442	8.961	0.230
3000	25	1.825	0.179	8.777	5.851	0.340
3500	100	16.503	1.741	21.249	12.142	1.366
3500	75	11.943	1.272	18.591	10.623	1.140
3500	50	4.209	0.448	14.117	8.067	0.529
3500	25	0.000	0.000	8.030	4.588	0.000
4000	100	11.985	1.495	22.086	11.043	1.128
4000	75	6.235	0.710	19.490	9.745	0.607
4000	50	0.454	0.049	15.449	7.725	0.053
4000	25	6.531	0.774	9.005	4.503	1.432

Table A-7. Difference method data for high level

Speed (rpm)	Load (%)	Blowby OC (µg/cycle)	Blowby OC (g/h)	Blowby (l/min)	Blowby (cm ³ /cycle)	Oil Concentration
2500	100	5.588	0.413	22.498	17.998	0.306
2500	75	-0.513	-0.046	16.121	12.897	-0.048
2500	50	0.518	0.037	13.312	10.649	0.046
3500	100	8.260	0.855	21.897	12.512	0.650
3500	75	2.555	0.274	16.487	9.421	0.277
3500	50	0.694	0.027	11.977	6.844	0.038
4000	100	4.077	0.515	22.668	11.334	0.379
4000	75	4.730	0.578	17.592	8.796	0.548
4000	50	0.322	0.023	12.283	6.141	0.032

Table A-8. Difference method data for medium level

Speed (rpm)	Load (%)	Blowby OC (µg/cycle)	Blowby OC (g/h)	Blowby (l/min)	Blowby (cm3/cycle)	Oil Concentration
2500	100	14.831	1.126	22.661	18.129	0.828
2500	75	0.000	0.000	18.285	14.628	0.000
2500	50	5.068	0.383	13.035	10.428	0.490
2500	25	4.016	0.293	6.779	5.423	0.719
3000	100	10.867	0.963	23.693	15.795	0.678
3000	75	0.000	0.000	16.865	11.243	0.000
3000	50	7.203	0.643	12.461	8.307	0.860
3000	25	3.796	0.344	8.646	5.764	0.664
3500	100	13.886	1.437	20.927	11.958	1.145
3500	75	4.691	0.490	18.013	10.293	0.453
3500	50	1.822	0.178	13.449	7.685	0.221
3500	25	5.332	0.556	8.305	4.745	1.116
4000	100	5.141	0.591	28.522	14.261	0.345
4000	75	7.832	0.965	20.179	10.089	0.797
4000	50	7.796	0.926	14.686	7.343	1.051
4000	25	13.306	1.588	9.259	4.629	2.858

Table A-9. Difference method data for low level

Appendix B: Common Reference Numbers

Converting $\mu\text{g}/\text{cycle}$ to g/h :

- at 2500 rpm $\Rightarrow 1 \mu\text{g}/\text{cycle} = 0.075 \text{ g}/\text{h}$
- at 3000 rpm $\Rightarrow 1 \mu\text{g}/\text{cycle} = 0.090 \text{ g}/\text{h}$
- at 3500 rpm $\Rightarrow 1 \mu\text{g}/\text{cycle} = 0.105 \text{ g}/\text{h}$
- at 4000 rpm $\Rightarrow 1 \mu\text{g}/\text{cycle} = 0.120 \text{ g}/\text{h}$

Typical Numbers with the SI 4-cylinder 2.01 L engine:

- Total Oil Consumption
 - Full Load and 2500 rpm $\Rightarrow 10 \text{ g}/\text{h}$
 - Low Load and 2500 rpm $\Rightarrow 4 \text{ g}/\text{h}$
 - Full Load and 4000 rpm $\Rightarrow 30 \text{ g}/\text{h}$
 - Low Load and 4000 rpm $\Rightarrow 17 \text{ g}/\text{h}$
- Blowby Oil Consumption
 - Full Load and 2500 rpm $\Rightarrow 0.4 \text{ g}/\text{h}$ (direct) & $1 \text{ g}/\text{h}$ (differential)
 - Low Load and 2500 rpm $\Rightarrow 0.15 \text{ g}/\text{h}$ & $0 \text{ g}/\text{h}$ (differential)
 - Full Load and 4000 rpm $\Rightarrow 1 \text{ g}/\text{h}$ & $1.7 \text{ g}/\text{h}$ (differential)
 - Low Load and 4000 rpm $\Rightarrow 0.3 \text{ g}/\text{h}$ & $0.7 \text{ g}/\text{h}$ (differential)

Blowby flow magnitude, and restriction study:

- Engine operating conditions & blowby flow (0.24 mm Top ring gap)
 - Full Load and 2500 rpm $\Rightarrow 969 \text{ mbar}$ & $5.4 \text{ l}/\text{min}$ per cylinder
 - Low Load and 2500 rpm $\Rightarrow 402 \text{ mbar}$ & $2.2 \text{ l}/\text{min}$ per cylinder
 - Full Load and 4000 rpm $\Rightarrow 940 \text{ mbar}$ & $6 \text{ l}/\text{min}$ per cylinder
 - Low Load and 4000 rpm $\Rightarrow 420 \text{ mbar}$ & $2 \text{ l}/\text{min}$ per cylinder
- Engine operating conditions & blowby flow (0.48 mm Top ring gap)
 - Full Load and 2500 rpm $\Rightarrow 960 \text{ mbar}$ & $7.1 \text{ l}/\text{min}$ per cylinder
 - Low Load and 2500 rpm $\Rightarrow 408 \text{ mbar}$ & $3.0 \text{ l}/\text{min}$ per cylinder
 - Half Load and 4000 rpm $\Rightarrow 680 \text{ mbar}$ & $6.6 \text{ l}/\text{min}$ per cylinder

* Note: Day to day variation on the intake pressure is less than 1%, and the torque was controlled to be the same every run.

Appendix C: Experimental Configurations

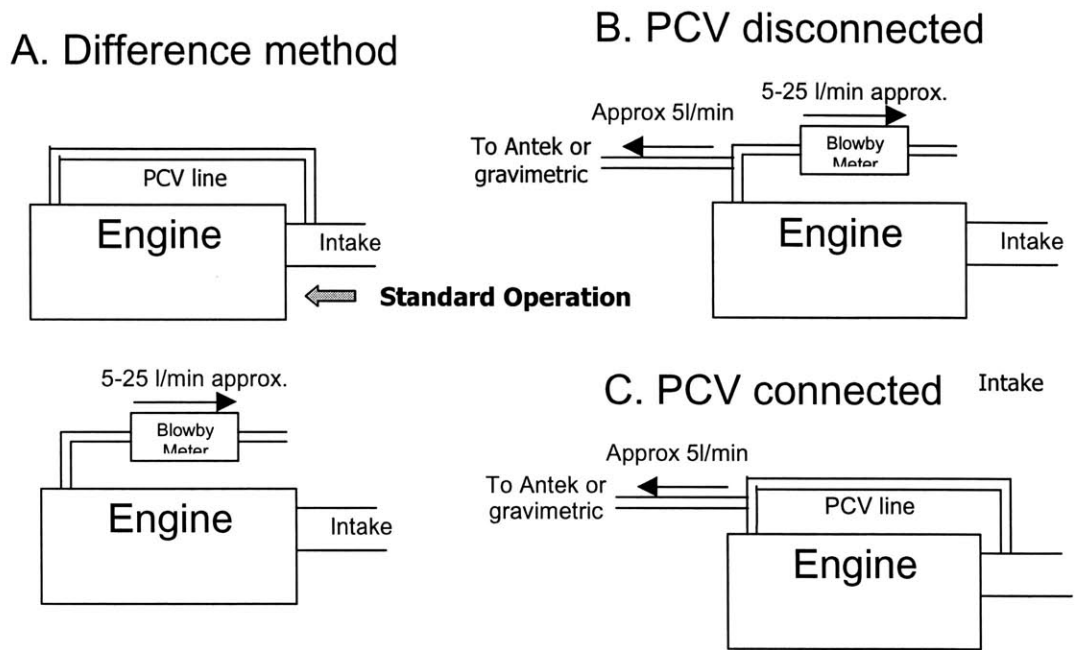


Figure C-1 Different operating configuration used in the different diagnostics methods. Configuration A is for the differential method, while the configuration B & C are used for both the direct and gravimetric methods

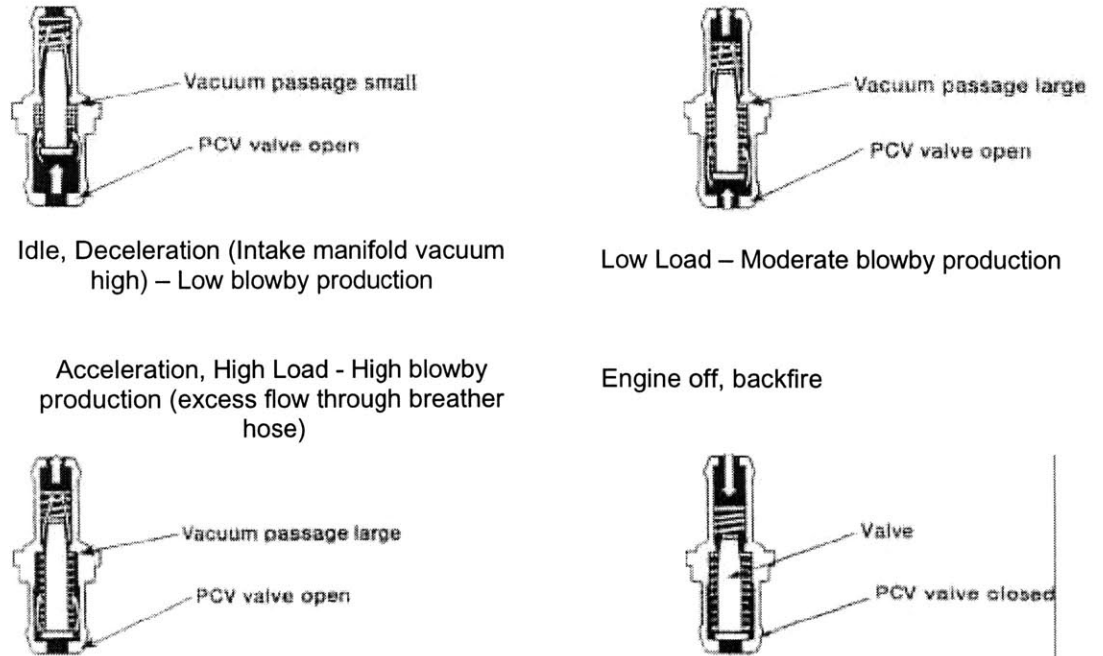


Figure C-2 PCV valve conditions for different loads

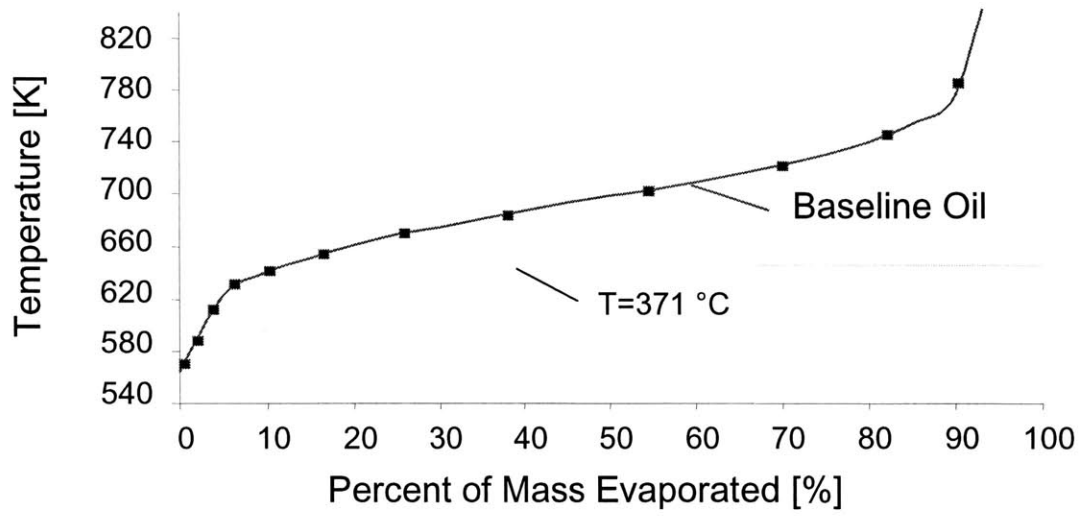


Figure C-3 Baseline oil distillation curve

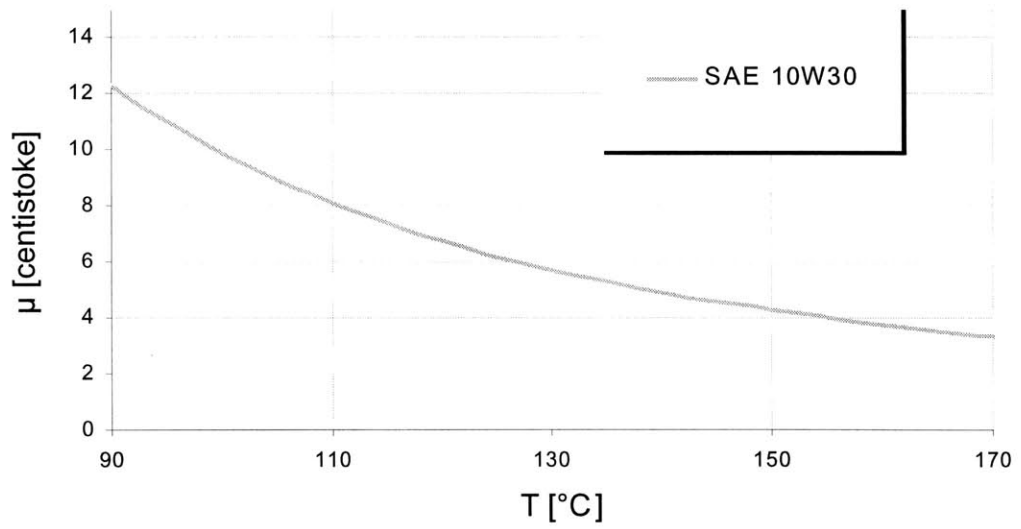


Figure C-4 Baseline oil viscosity curve against temperature

Appendix D: Other Significant Blowby Results and Plots

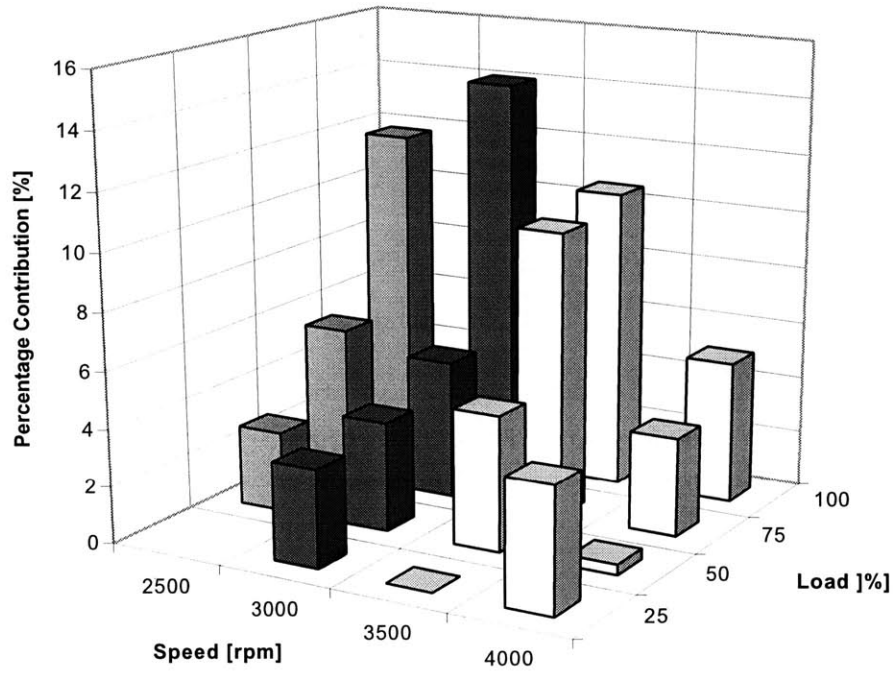


Figure D-1 Percent blowby OC contribution to total OC with the difference method at high oil level

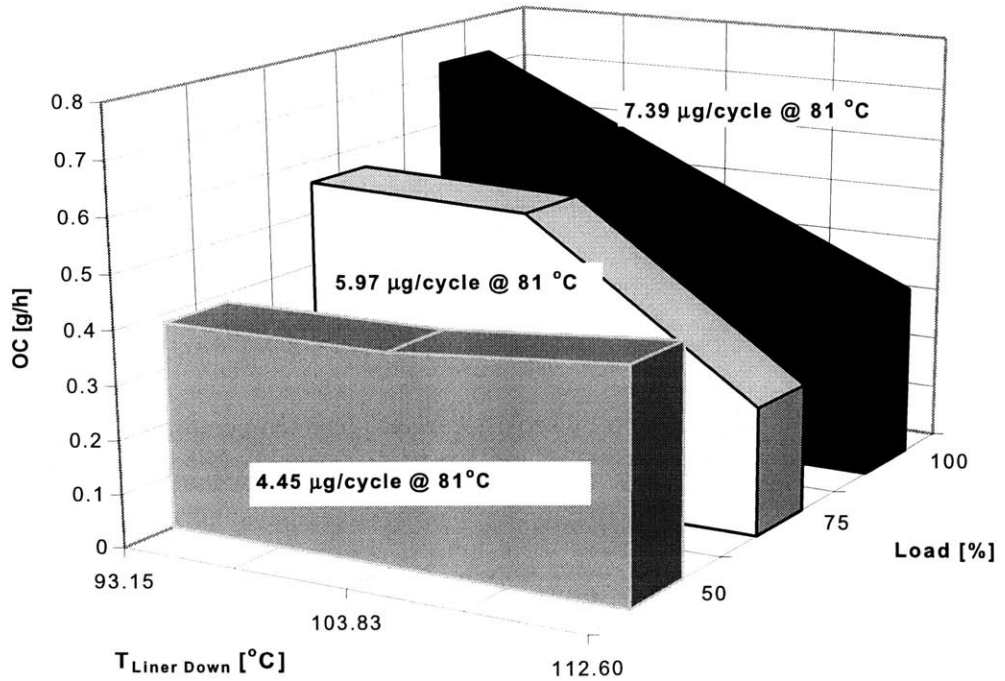


Figure D-2 Blowby OC for different lower liner temperatures for 3500 rpm and different loads

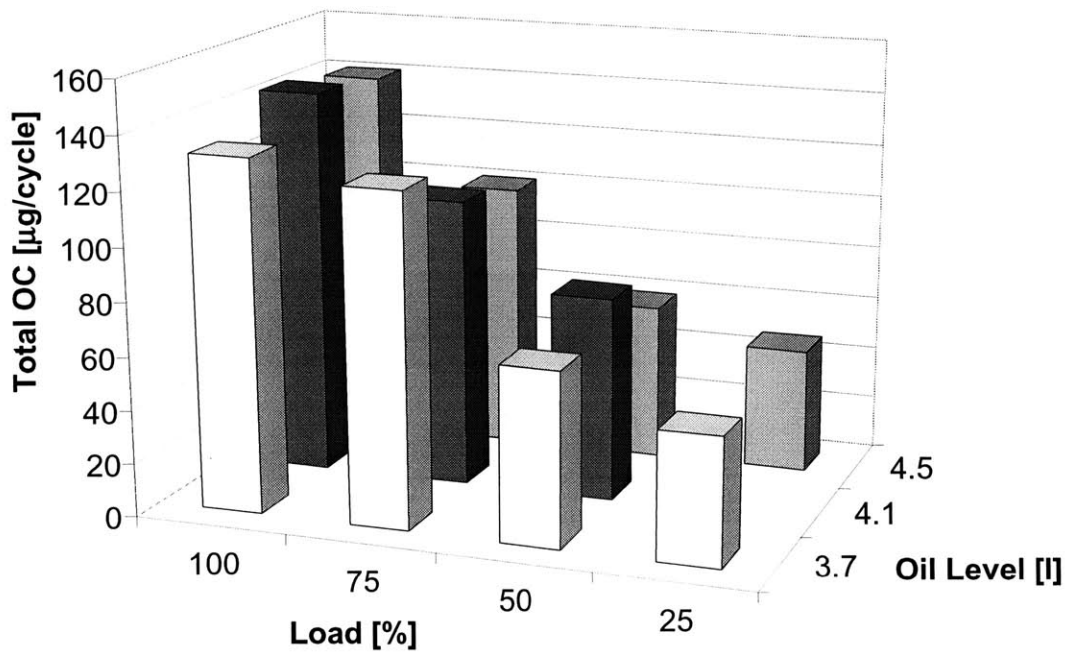


Figure D-3 Total OC for different loads for 2500 rpm and different oil levels